Functional analysis of a posttranslational modification of plant α-tubulin

Zur Erlangung des akademischen Grades eines

DOKTORS DER NATURWISSENSCHAFTEN

(Dr. rer. nat.)

Fakultät für Chemie und Biowissenschaften

Karlsruher Institut für Technologie (KIT) - Universitätsbereich

vorgelegte

DISSERTATION

von

Aleksandra Zimmermann geb. Jovanović

aus

Subotica

Dekan: Prof. Dr. S. Bräse

Referent: Prof. Dr. P. Nick

Korreferent: Prof. Dr. R. Fischer

Tag der mündlichen Prüfung: 11.02.2011

Die vorliegende Dissertation wurde am Botanischen Institut des Karlsruher Instituts für Technologie (KIT) am Lehrstuhl I für Molekulare Zellbiologie im Zeitraum von April 2006 bis Dezember 2010 angefertigt.

Mein besonderer Dank gilt Herrn Prof. Dr. Peter Nick für die hervorragende Betreuung und Unterstützung während meiner Doktorarbeit und für die Möglichkeit, dieses interessante Thema zu bearbeiten.

Herrn Prof. Dr. Reinhard Fischer danke ich für die Übernahme des Korreferats.

For protein analysis by MALDI TOF, I would like to thank Dimitri Heinz, Laboratoire de Spectrométrie de Masse Bio-Organique, Université Louis Pasteur, Strasbourg, France.

Für die gute Betreuung, Zusammenarbeit und das Erlernen neuer Techniken während meines Auslandsaufenthalts in Prag von Februar bis Mai 2008 möchte ich mich bei Prof. Dr. Zdeněk Opatrný, Dr. Kateřiná Schwarzerová und Janá Kobrlová bedanken.

Für die kompetente Hilfestellung bei Fragen und Problemen bedanke ich mich herzlich bei Dr. Petra Hohenberger, Dr. Michael Riemann und Dr. Jan Maisch.

Für die exzellente technische Unterstützung bedanke ich mich bei Sarah Rocke, Markus Riese, Franziska Bühler, Juliane Draksler, Anna Görnhardt und Olivia Huber, außerdem bei Frau Angelika Piernitzki und den Mitarbeitern des Botanischen Gartens für die hervorragende Anzucht und Pflege meiner Reispflanzen.

Dr. Kai Eggenberger danke ich herzlich für die vielen Stunden, die er mit Korrekturlesen meiner Arbeit verbracht hat und Steffen Durst für die tolle Zusammenarbeit vor, während und nach seiner Diplomarbeit.

Den Mitarbeitern des Instituts danke ich für die schöne Atmosphäre, die tolle Unterstützung und die schöne Zeit, ganz besonders meinen Dachgeschoss-Mitbewohnern Dr. Maurice Ouko, Dr. Kai Eggenberger, Dr. Stephan Schröder, Steffen Durst, Isabel Molina, Jan Klotz, Natalie Schneider und Holger Ludwig.

Mein Studium und damit diese Arbeit wurden mir erst durch die Unterstützung durch meine Eltern ermöglicht, ihnen und meiner Schwester Kristina danke ich, vor allem für die letzten Monate, von ganzem Herzen. Bei meinem Ehemann Matthias bedanke ich mich ganz besonders, da er immer an mich geglaubt hat und mich unterstützt hat wo es nur ging.

Hiermit erkläre ich, dass ich die vorliegende Dissertation, abgesehen von der Benutzung der angegebenen Hilfsmittel, selbstständig verfasst habe.

Alle Stellen, die gemäß Wortlaut oder Inhalt aus anderen Arbeiten entnommen sind, wurden durch Angabe der Quelle als Entlehnungen kenntlich gemacht.

Diese Dissertation liegt in gleicher oder ähnlicher Form keiner anderen Prüfungsbehörde vor.

Gernsbach, den 10. Januar 2011

.....

(Aleksandra Zimmermann)

Abbreviations

This list gives the declarations of the abbreviations used in the thesis at hand. Not listed here are SI-units, chemical symbols, nucleotides and the one and three letter code of amino acids.

2,4-D	dichlorophenoxyacetic acid
ADP	adenosine-5'-diphosphate
APS	ammonium peroxydisulfate
A.t.	*Agrobacterium tumefaciens*
ATP	adenosine-5'-triphosphate
BCIP	5-bromo-4-chloro-3-indolylphosphate-p-tuloidine
BSA	bovine serum albumine
BY-2	*Nicotiana tabacum* L. cv. Bright Yellow 2
CBB	Coomassie Brilliant Blue
CHAPS	3-[(3-cholamidopropyl)dimethylammonio]-2-hydroxy-1-propanesulfonate
CLSM	confocal laser scanning microscopy
cMT	cortical microtubule
detyr-tub	detyrosinated α-tubulin
DIC	differential interference contrast
DMSO	dimethyl sulfoxide
dNTP	deoxynucleotide triphosphate
E. coli	*Escherichia coli*
EGTA	ethylene glycol tetraacetic acid
EPC	ethyl-N-phenylcarbamate
FITC	fluorescein isothiocyanate

FRAP	fluorescence recovery after photobleaching
GDA	geldanamycin
GFP	green fluorescent protein
GTP	guanosine-5'-triphosphate
Hoechst 33258	2′-(4-Hydroxyphenyl)-5-(4-methyl-1-piperazinyl)-2,5′-bi-(1H-benzimidazole) trihydrochloride
Hsp90	heat shock protein 90
KOD	*Thermococcus kodakaraensis* DNA polymerase
LB	lysogeny broth
MAP	microtubule associated protein
MES	4-Morpholineethanesulfonic acid
MF	actin microfilament
MI	mitotic index
MS	Murashige and Skoog
MT	microtubule
MTOC	microtubule organising centre
NBT	nitrobluetetrazolium
NO	nitric oxide
NOS	nitric oxide synthase
NO_2Tyr	3-Nitro-L-tyrosine
NR	nitrate reductase
NT	3-Nitro-L-tyrosine
NtHsp90	Hsp90 from *Nicotiana tabacum*
OD_{600}	optical density at 600 nm
OsHsp90	Hsp90 from *Oryza sativa*
PAGE	polyacrylamide gel electrophoresis

PCR	polymerase chain reaction
PFA	paraformaldehyde
PIPES	1,4-Piperazinediethanesulfonic acid
PLD	phospholipase D
PMSF	phenylmethylsulfonyl fluoride
PPB	preprophase band
PVDF	polyvinylindene fluoride
PVP	polyvinylpyrrolidone
RFP	red fluorescent protein
rpm	revolutions per minute
RT	room temperature
RT-PCR	reverse transcription polymerase chain reaction
SDS	sodiumdodecylsulfate
SE	standard error
SOC	super optimal broth (SOB) plus glucose
TBST	tris buffered saline supplemented with triton
TCA	trichloacetic acid
TCP	tubulin-tyrosine carboxypeptidase
TE	tris-EDTA buffer
TEMED	tetramethylethylenediamine
Tris	tris(hydroxymethyl)-aminomethane
TRITC	tetramethylrodamine isothiocyanate
TTC	tubulin-tyrosine carboxypeptidase
TTCP	tubulin-tyrosine carboxypeptidase
TTL	tubulin-tyrosine ligase
tyr-tub	tyrosinated α-tubulin

v/v	volume per volume
w/v	weight per volume
WB	washing buffer
WT	wild type

Zusammenfassung

Die posttranslationale Modifikation von Proteinen stellt für Zellen eine Möglichkeit dar, ein und dasselbe Protein verschiedenartig zu markieren und damit Interaktionspartnern ein Signal zu setzen. Eine dieser posttranslationalen Modifikation ist die Detyrosinierung von α-Tubulin, bei der das C-terminale Tyrosin enzymatisch abgespalten (durch TTL) und wieder angeheftet werden kann (durch TTC, noch nicht identifiziertes Protein).

Diese Detyrosinierung geht einher mit einer erhöhten Stabilität des Mikrotubulus, sie ist jedoch nicht deren Ursache. Die vorliegende Dissertation beschäftigt sich mit der Frage nach der biologischen Funktion der Detyrosinierung (in den beiden Modellorganismen Reis und Tabak).

Um Detyrosinierung untersuchen zu können, werden vier Strategien gewählt. Die ersten Drei unterdrücken das Signal der Detyrosinierung (durch Veränderung des Substrats von TTC, durch Inhibition der TTC und durch Überexpression der TTL), die Vierte untersucht einen möglichen Empfänger des Signals (Hsp90).

Durch die Veränderung des Substrats der TTC konnte die natürliche Verteilung von tyrosiniertem und detyrosiniertem α-Tubulin verschoben werden, außerdem konnte gezeigt werden, dass Detyrosinierung eine wichtige Rolle im einwandfreien Ablauf der Zellteilung hat. Diese Ergebnisse konnten durch Inhibition der TTC bestätigt werden.

Die Ergebnisse der Überexpression von TTL wiesen darauf hin, dass diese mutmaßliche Ligase Eigenschaften bzw. Funktionen der noch unbekannten TTC aufweist, was auf ein Aufsehen erregendes Ergebnis hinweist, nämlich die Identifikation einer bis dato unbekannten TTC.

Durch Untersuchungen von Hsp90 konnte gezeigt werden, dass dieses Protein *in vitro* an Mikrotubuli bindet und *in vivo* mit Mikrotubuli kolokalisiert. Des Weiteren konnte Hsp90 eine wichtige Rolle in der Plastizität von Mikrotubuli zugewiesen werden.

Table of contents

1 Introduction

Microtubules (MTs) are present in all eukaryotic cells, they are responsible for various tasks such as cytoplasmic organisation, vesicle transport, cell division, cell elongation, and cell shape. They are, besides intermediary filaments and actin microfilaments, a component of the cytoskeleton.

The term cytoskeleton could lead to a wrong impression; even though microscopic images of the microtubular array (e.g. obtained by electron microscopy) remind of a rigid and inflexible meshwork, cytoskeletal components can be flexible and dynamic, and are subject to constant polymerisation and depolymerisation.

1.1 The plant cytoskeleton – an overview

In contrast to the animal cytoskeleton which has additional intermediary filaments, the plant cytoskeleton is made up of two components: MTs and actin microfilaments, both of them are characterised as fibres and networks made of proteins.

The actin cytoskeleton plays an important role in cell growth and morphology; more precisely it regulates cytoplasmic streaming and vesicle trafficking, both crucial for exocytosis. Actin microfilaments (filamentous actin, F-actin) are composed of globular actin (G-actin), which is a highly conserved monomeric protein with a molecular size of approximately 42 kDa. G-actin can polymerise head-to-tail to dimers and further to protofilaments by hydrolysing adenosine-5'-triphosphate (ATP) to adenosine-5'-diphosphate (ADP). Two of these protofilaments form a helical actin microfilament by twisting around each other (resembling a double-rowed pearl necklace; see Figure 1.1).

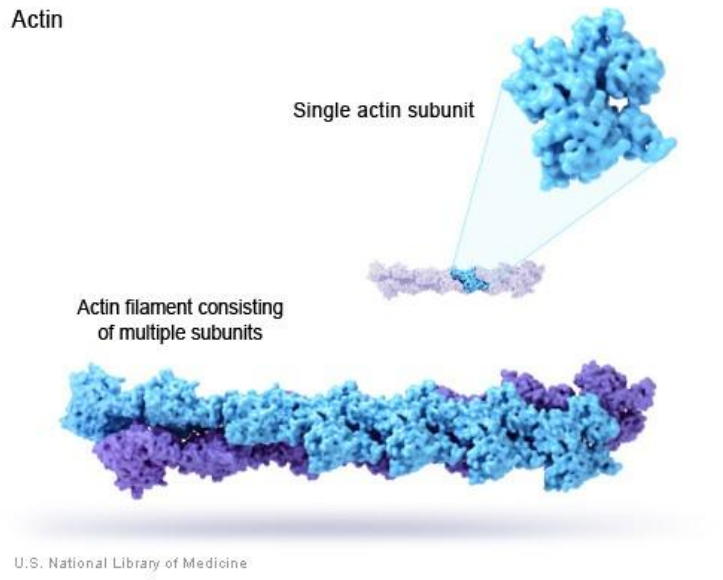

Figure 1.1: Schematic diagram of the actin microfilament assembly. The double-row filament which has a diameter of approx. 7 nm and various lengths and is built up of multiple G-actin subunits (image ©: Genetics Home Reference, U.S. National Library of Medicine, http://ghr.nlm.nih.gov).

Actin microfilaments (as well as MTs) may undergo treadmilling: by head-to-tail polymerisation of the monomers, polarity of the microfilament is predetermined. It is reflected in the treadmilling process through polymerisation at the plus-end and depolymerisation at the minus-end (Holmes et al., 1990; Hussey et al., 2006). Actin microfilaments feature different structural characteristics depending on their appearance, for example they feature a mesh like structure in root hair and the apical region of pollen tubes where they regulate tip growth, whereas they have a bundled structure in the subapical region (Higaki et al., 2007; Hepler et al., 2001).

The other cytoskeletal components are MTs. The National Library of Medicine gives the following definition: “Slender, cylindrical filaments found in the cytoskeleton of plant and animal cells. They are composed of the protein tubulin.” (Definition from: Unified Medical Language System at the National Library of Medicine, http://ghr.nlm.nih.gov). MTs play a crucial role in cytoplasmic organisation, cell shape, division and elongation, and in response to environmental influences.

MTs are hollow tubes with a diameter of approx. 24 nm, consisting of 13 protofilaments (Figure 1.2) which in turn consist of head-to-tail dimerised soluble α- and β-tubulin, each monomer having a molecular weight of about 50 kDa (Goddard et al., 1994). Although characterised by their dynamics, MTs attain a certain persistency by their helical constitution (Sept et al., 2003).

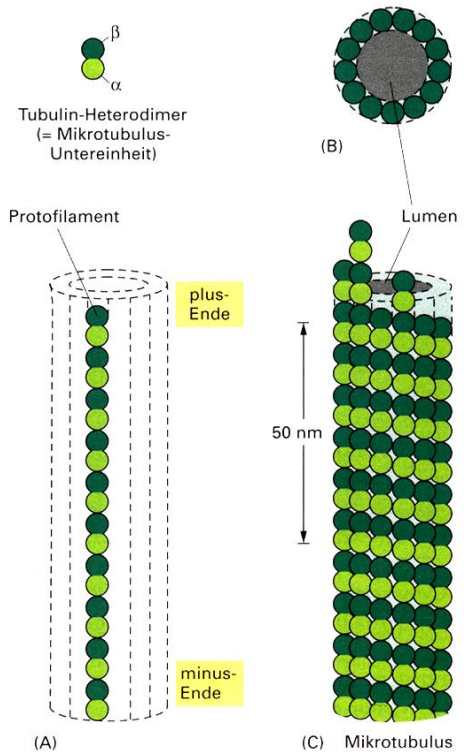

Figure 1.2: Schematic diagram of MT assembly. **[A]** α/β-tubulin heterodimer (subunits of MTs) and the orientation of heterodimers in a protofilament featuring a plus- and minus-end. **[B]** Transversal view of a MT which consists of 13 protofilaments. Based on head-to-tail polymerisation of heterodimers, MTs show structural polarity: plus-end reveals β-tubulin, minus-end reveals α-tubulin only. **[C]** Side view of a MT, helical structure as apparent assembly (source: Alberts et al., 2005).

MTs feature high dynamics: fluorescence recovery after photobleaching (FRAP) studies revealed half-life times of plant cortical microtubules of about a minute only (Himmelspach et al., 1999). These dynamics are characterised by constant assembly and disassembly, regeneration and disappearance.

Dynamics of the MT cytoskeleton is carried out mainly by polymerisation and depolymerisation of α/β-tubulin heterodimers. Two main processes play the key roles: treadmilling and dynamic instability. The treadmilling process is controlled by GTP binding and hydrolysis: β-tubulin of soluble tubulin dimers is connected

with GTP and added to the plus-end of a protofilament. GTP is hydrolysed to GDP shortly after incorporation, and the GDP bound heterodimers are removed from the MT at the minus-end (Wilson et al., 1999). Dynamic instability on the other hand is characterised by conditions of polymerisation and depolymerisation, depending on the ratio of polymerisation and hydrolysis of GTP (Chrétien et al., 1995).

The binding of GTP to tubulin has direct influence on stability of MTs: tubulin dimers bound to GTP have a higher affinity to each other than if bound to GDP, which as a consequence gives stability to the region of GTP-tubulin. This stabilised area of tubulin polymerisation at the plus-end of a MT is called “GTP-cap”. In contrast to this, GDP bound tubulin dimers have lower affinity to each other, which makes the MT shrink and depolymerise at the minus-end (Alberts et al., 2005).

In plant MTs (in contrast to animal MTs) polymerisation and depolymerisation are not so strictly related to plus- and minus-end; dynamic assembly and disassembly can occur at both ends of a MT. Growing and shrinking seems to take place mainly at the plus-end, whereas the minus-end generally reveals less dynamics. MT growth and movement therefore results from dynamic instability with favoured polymerisation at the plus-end and slow, periodical appearance of depolymerisation at the minus-end (Shaw et al., 2003).

1.1.1 Cortical microtubules

Plant cells feature a special kind of microtubular structure called cortical MTs (cMTs, first described by Ledbetter and Porter, 1963) which can be found mainly in tissue with elongating cells. cMTs are associated with the plasma membrane and predominantly organised in a parallel array perpendicular to the growth axis (see Figure 1.3F). Orientation of cellulose fibres in elongating cells continuously displayed parallel orientation to cMTs, but it was not until 2006 that proof was given for a model in which the cMTs are functionally associated with cellulose synthase complexes. Movement of cellulose synthases and hence orientation of cellulose microfibrils is controlled by cMTs (Paredez et al., 2006).

Growth in the vertical direction to cMTs is due to the inside turgor pressure of the cell (as water uptake is the driving force of cell expansion or growth): as the cMTs (and therefore cellulose microfibrils) function like a restrictive belt or corset, expansion is only possible in the vertical direction to cMTs (Taiz and Zeiger, 2000).

The system of cMTs is very susceptible to stimuli like red and blue light, phytohormones, change of gravity direction and injury (Nick, 1998; Himmelspach et al., 1999). As a response, rapid reorientation of cMTs can be examined. An interesting observation regarding the reorientation of cMTs is described in the work of Chan and colleagues (Chan et al., 2007). In effort to explain upcoming layers of cellulose with different orientation they monitored domains of cMTs resembling patches all over the cell surface. MTs in one domain were oriented in a parallel array while MT-orientation of the single domains could differ. Reorientation occurred by migration of the whole domains themselves. Clockwise and counter clockwise rotation of MT arrays within the domains was observed; domains collided and were also able to replace one another.

1.1.2 Microtubules and plant cell division

In plant cells, MTs show different and, when compared to animal cells unknown appearance, either in interphase or mitosis (Wasteneys, 2002). As already mentioned, interphasic cMTs are related to development of the plant cell wall.

In late G2 phase, the first sign of oncoming mitosis appears: the preprophase band (PPB, see Figure 1.3A; first described by Picket-Heaps and Northcote, 1966). The PPB is an arrangement of MT bundles and F-actin (Palevitz, 1987), generally encircling the midplane of the mothercell, predicting the future cell plate attachment site, although disappearing long before the new cell wall forms. The PPB is connected to the nucleus by the phragmosome, consisting of bundles of MTs and F-actin.

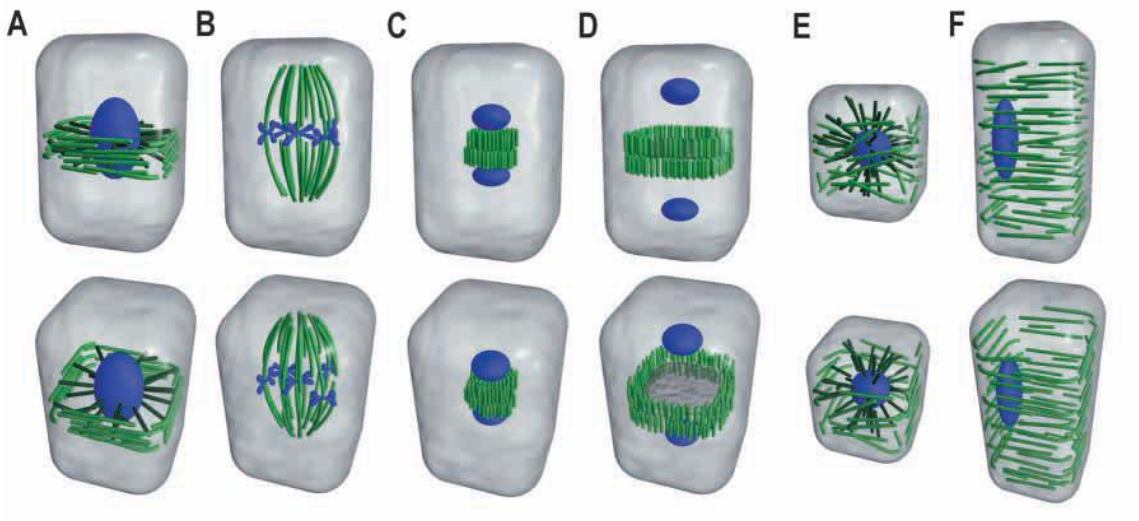

Figure 1.3: Schematic diagram of MT arrays (in green) in different stages of the cell cycle, blue colour represents nucleus and chromosomes. **[A]** A PPB is located at the future division plane, linked to the nucleus by the phragmosome. **[B]** Mitotic spindle in anaphase of the cell cycle. **[C]** In telophase, the phragmoplast forms as a concentrated cylinder of microtubules between daughter nuclei. **[D]** The cytokinetic phragmoplast expands centrifugally, leading the cell plate towards attachment sites previously established by the PPB. **[E]** Once cytokinesis is complete, microtubules extend from the nucleus toward the cell cortex. **[F]** Plant cells in interphase with cMTs arranged in a parallel array. Direction of cell expansion is perpendicular to the orientation of cMTs (image source: Wasteneys, 2002).

In prophase, the first phase of mitosis, MTs concentrate in the nuclear area of the cell, the nuclear envelope breaks down and MTs, emerging from the MT organising centres (MTOCs), migrate to the chromosomes. MTs are connected to the MTOCs with their minus-end (Goddard et al., 1994). Nuclear envelope breakdown and dissolution of the PPB coincide with mitotic spindle formation (Wasteneys, 2002).

During metaphase the mitotic spindle is completely developed (Figure 1.3B), spindle fibres stick to chromosomes and accomplish chromosome migration towards the diametrical poles. Plant spindle poles are typically broad, as they lack centrosomes (which can be found in spindle poles of animal cells).

At the transition of anaphase and telophase the phragmoplast, which is another plant specific MT formation, appears between the condensing chromatin of the daughter nuclei (Figure 1.3C). Like the PPB it doesn't consist of MTs only, but of actin as well. The phragmoplast is, similar to the mitotic spindle, a bipolar formation, with the plus-ends of MTs meeting at midplane. In contrast to animal cell division, the cell plane develops from within the cell and grows centrifugally.

Golgi vesicles, delivering cell wall components (Nebenführ et al., 2000) are directed towards the newly developing cell wall. The double ring of a phragmoplast is self-organised and grows by increase of the radius towards the cell wall of the mother cell, as formation of the middle cell plane proceeds (Figure 1.3D).

Entering interphase, MTs are arranged in a radial organisation for a short time, spanning the cell from nucleus to cell periphery (Figure 1.3E). Soon after this, MTs are often arranged in a parallel orientation throughout the cell periphery as cMTs (Figure 1.3F).

1.2 Posttranslational modifications of proteins

Plant tubulins, as well as all eukaryotic tubulins, undergo various posttranslational modifications, such as acetylation, glutamylation, phosphorylation and cyclic detyrosination/tyrosination (Hammond et al., 2008; Banerjee, 2002). These posttranslational modifications are considered as mechanisms to define functionally different subpopulations of one protein without the need to synthesise the respective proteins *de novo*. Although several posttranslational modifications have been known for years, their precise function has remained unclear.

One of the best investigated posttranslational modifications is the reversible tubulin tyrosination cycle, which was first described in 1973 (Barra et al., 1973) and which is unique for α-tubulin (MacRae, 1997). Most of the eukaryotic α-tubulin genes encode a C-terminal tyrosine, which can be removed by a specific and as yet not identified tubulin-tyrosine carboxypeptidase (TTC, also referred to as TCP or TTCP), preferring polymers rather than α/β-tubulin heterodimers (Ersfeld et al., 1993). Thus, TTC is creating detyrosinated α-tubulin (detyr-tub), which is hence exposing a C-terminal glutamic acid (therefore often designated as Glu-tubulin). After depolymerisation of the MT, the α-subunit of the soluble α/β-tubulin heterodimers can be (re-) tyrosinated by an ATP-dependent tubulin-tyrosine ligase (TTL, first isolated and cloned from

porcine brain by Ersfeld et al., 1993), creating the initial tyrosinated α-tubulin (tyr-tub). TTL prefers the α-tubulin of soluble α/β-tubulin heterodimers as substrate and has a lower affinity for assembled microtubules (for review see Westermann and Weber, 2003).

The degree of tubulin detyrosination is correlated with the stability of MTs, the higher the degree of detyrosination, the more stable the MT. However, *in vitro* studies showed that detyrosination is neither the cause of increased MT lifetime nor of increased MT length (Skoufias and Wilson, 1998), but rather the consequence of stability and therefore a biochemical signal for it. The real cause of increased stability of MTs is still unknown, although it is assumed that microtubule associated proteins (MAPs) play an important role (Infante et al., 2000). Possible targets for this signal are the kinesin motors, which preferentially bind to detyrosinated MTs; in case of an experiment with recombinant kinesin this was ~2,8-fold increased affinity for detyrosinated over tyrosinated MTs (Liao and Gundersen, 1998). In animal cells, a proper balance between tyrosinated and detyrosinated α-tubulin is thought to be used as a cell cycle checkpoint to monitor abnormalities (Idriss, 2004).

Database research (e.g. with http://www.expasy.org) revealed three different TTL-like sequences in rice, whereas one of them will be focused upon here. This protein, named TTL Swiss-Prot accession Q10QY4) consists of 870 amino acids and has a molecular weight of 98,8 kDa.

1.3 Microtubule associated proteins

Microtubule associated proteins (MAPs) are defined as proteins that demonstrate binding to MTs *in vivo* (Morejohn et al., 1994; Nick et al., 1995). Both animal and plant cells possess MAPs with distinct functions, for example vesicle transport driven by motor proteins like kinesins (Alberts et al., 2005), and axonal MT bundling and stabilisation accomplished by Tau (Samsonov et al., 2004).

Kinesins and dyneins are both motor proteins that play an important role in intracellular transport. Usually, kinesins move towards the plus-end of MTs and dyneins towards the minus-end. Dyneins are involved in movement of spermatozoids in moss, fern and *Ginkgo* and are absent in higher plants. Since higher plants need motor protein migration towards the minus-end of MTs as well, kinesins inherit the functional role of dyneins, as could be shown for kinesin-14 motor proteins (Cross, 2010).

Another group of MAPs are the heat shock proteins (Hsps). Hsps are molecular chaperons, essential for correct protein folding, in both animal and plant cells. Their name derives from the observation that synthesis of Hsps in animal cells is strongly induced after heat shock, although synthesis of Hsps is generally stress inducible, as they play an important role in abiotic stress response in plants (Agueli et al., 2001).

Hsps are subdivided into five families, according to their approximate molecular weight and function, which are Hsp100, Hsp90, Hsp70, Hsp60 (chaperonins) and small Hsps (sHsps, α-crystallins; Liang and MacRae, 1997; Zou et al., 2009). Sometimes Hsps act cooperatively, for instance Hsp70 and its cofactor Hsp40. As a complex these two are believed to regulate MT dynamics (Chuong et al., 2004).

Hsp90 is a highly conserved molecular chaperone, important for protein stability and folding. In cells of *Tetrahymena*, one member of the Hsp90 familiy (Hsp82) and three members of the Hsp70 family (Hsp72, 73, and 78) were identified in a protein complex with a molecular weight of 700 kDa (Williams and Nelsen, 1997). Furthermore, Hsp73 and Hsp82 were found to associate with mature MTs in cilia and cortex of *Tetrahymena.*

To pick up posttranslational modifications again, in human cells binding of the two isoforms Hsp90α and Hsp90β and their substrate proteins to MTs depends on the percentage of tubulin acetylation, providing a mechanism by which the stability of MTs could regulate cell signalling (Giustiniani et al., 2009).

1.4 The scope of this work

The general question stated at the beginning of this study was: What is the function of α-tubulin detyrosination in plant cells? Of course, a general solution and answer to this question cannot be presented in this work, as detyrosination is an expansive field and divided in many puzzle-like pieces. But in order to unravel some secrets of detyrosination, this work approaches the problem from different directions, which will be described in the following.

Database research (for example with UniProtKB http://www.uniprot.org) shows that the C-terminal tyrosine of α-tubulin is quite highly conserved and can be found in many organisms, such as human, mouse, rat, pig, *Tetrahymena thermophile*, *Arabidopsis thaliana*, *Oryza sativa*, *Aspergillus nidulans* etc., although exceptions exist (e.g. *Sacharomyces cerevisiae*).

This common conservation and the fact that C-terminal tyrosine can be cleaved off and reattached posttranslationally (with consumption of ATP) lead to the assumption that the tubulin tyrosination cycle is of particular importance for a cell.

A number of observations showed that the level of detyrosination correlates with stability of MTs, although detyrosination is not the cause for stability but rather the consequence of a stable MT. This leads back to the fact that MTs, not the soluble α/β-tubulin heterodimers, are the favoured substrate of TTC (as already mentioned in chapter 1.2); the longer the lifetime of a MT, the higher is the possibility to become “victim” of TTC. Additionally, dynamics of MTs could not be altered by insertion of tyr-tub (Webster et al. 1990).

The question (what is the function of α-tubulin detyrosination in plant cells?) was attended with four strategies:

The first strategy was to interfere in the tubulin tyrosination cycle by blocking the detyr-signal. This was done by experiments with 3-Nitro-L-tyrosine (NO_2Tyr), a modified amino acid which creates irreversibly tyrosinated α-tubulin (for details see chapter 1.6.1). The question asked here was whether treatment with

NO_2Tyr could disturb mechanisms which are MT-controlled or where MTs are involved (e.g. cell expansion and cell division); and whether it is possible to alter tyr/detyr distribution in a cell.

The second strategy was to block the enzyme which is responsible for detyrosination (TTC) by applying the sesquiterpene parthenolide, an inhibitor of TTC (see chapter 1.6.2). Could tyr/detyr distribution be altered with this approach, and is the result similar to treatment with NO_2Tyr (because in theory it should be the same, as both approaches block the detyrosination signal, the first one by altering the substrate, the second one by blocking the enzyme)?

The third strategy of interference in the tubulin tyrosination cycle was overexpression of TTL in tobacco BY-2 cells, which was also the third approach of blocking the detyrosination signal. The questions stated here are: how is TTL distributed in the cell and can treatment with NO_2Tyr or with parthenolide bother tyr/detyr distribution in the expected way (which would be a drastic increase of tyr-tub at the cost of detyr-tub level)?

In the fourth approach, a possible acceptor of the detyr-signal was investigated: the MAP Hsp90 which belongs to the Hsp90 family. Hsp90 was identified in three different experiments: first, OsHsp90 (Hsp90 from *Oryza sativa*) was found in the same fraction with detyr-tub in an affinity chromatography experiment, indicating binding to soluble α/β-tubulin heterodimers. Secondly, the same protein was identified by a coassembly assay with taxol, indicating binding to MTs. Both experiments were performed with rice coleoptiles. Additionally, NtHsp90 (Hsp90 from a *Nicotiana tabacum* cell culture) was identified in membrane ghosts (patches of plasma membrane together with plasma membrane interacting proteins) where it bound to cMTs (experiment performed by our cooperation partners Jana Kobrlová and Kateřina Schwarzerová from the Department of Plant Physiology, Faculty of Science at the Charles University in Prague, Czech Republic). This work will discuss the question of Hsp90 interaction with MTs *in vitro* and *in vivo*, and will suggest a functional role of Hsp90 in plant cells.

1.5 Rice and tobacco as model plants

Two model plants have been used in this work: rice and tobacco.

Rice (*Oryza sativa* L.) is a model species for studies of monocotyledons (grasses and cereals) and belongs to the family of *Poaceae*. Rice is diploid and among other cereals it has one of the smallest genomes with ~430 million base pairs with estimated 50000 genes, distributed on 12 chromosomes (Sasaki and Sederoff, 2003; Yuan et al., 2001; http://www.jcvi.org). For comparison: *Arabidopsis* has a genome with 125 million base pairs and 26000 genes (Schoof and Karlowski, 2003), *Triticum aestivum* has the largest genome of agricultural crops, with 16000 million base pairs it is nearly 40-fold larger than that of rice (Gill et al., 2004). Another advantage of rice (*Oryza sativa* ssp. *japonica* var “Nipponbare”) is that the full genome sequence is known and can be obtained and worked with in the usual databases (e.g. http://rice.plantbiology.msu.edu/ or http://expasy.org/sprot/).

Working with rice is also very practicable, as caryopses of rice produce seedlings within a couple of days. Coleoptiles of young rice plants grown in photobiological darkness can be used as a model for nondividing cells with cell elongation exclusively, whereas the primary root of the plant serves as a model for cell elongation and division.

Tobacco (*Nicotiana tabacum* L.) belongs to the family of *Solanaceae*, like tomato, potato, eggplant and pepper. In contrast to rice, the tobacco cell culture BY-2 (*Nicotiana tabacum* L. cv. Bright Yellow 2) serves as a model for cycling cells. It is a well-established cell culture and currently used in many labs for research of cytokinesis, cell cycle, auxin response, protein transport etc. Doubling time of the cell line is 13 – 14 hours (Nagata and Kumagai, 1999).

The advantage of tobacco BY-2 cell culture is that it can be cultivated without much effort, a large number of cells is available after short time, and *Agrobacterium* mediated transformation is possible and effective. The genome

of tobacco consists of approximately 4500 million base pairs, but it is not yet fully sequenced (Opperman et al., 2003).

1.6 Experimental approaches

1.6.1 3-Nitro-L-tyrosine

Cellular malfunctions in animal cells, for instance in cancer cells or during infection by pathogens, are known to increase the abundance of nitric oxide (NO). NO is capable of producing 3-Nitro-L-tyrosine (nitrotyrosine, NO_2Tyr), created by nitration of tyrosine (for review see Beckman and Koppenol, 2003). NO_2Tyr is a substrate to TTL and can therefore be incorporated into detyr-tub (see Figure 1.4).

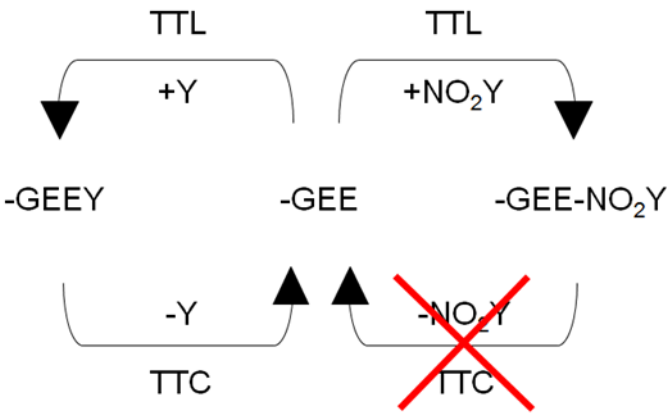

Figure 1.4: Schematic diagram of the tubulin tyrosination cycle. Left side represents the uninterrupted cycle which begins with the recently translated tyr-tub (with the most common amino acids glycine, two glutamic acids, and tyrosine) which is detyrosinated by TTC and retyrosinated by TTL. On the right side NO_2Tyr is incorporated into α-tubulin instead of tyrosine, which blocks the function of TTC and leads to irreversibly (nitro-) tyrosinated α-tubulin.

However, nitrotyrosination is an irreversible process, once nitrotyrosinated, α-tubulin cannot be detyrosinated by TTC, although opinions differ in this point (Chang et al., 2002; Bisig et al., 2002). Thus, the elevated levels of NO_2Tyr in ill-natured or stressed cells will result in elevated levels of irreversibly nitrotyrosinated α-tubulin. This leads to microtubule malfunctions and inaccurate microtubule-motor interactions, which will normally culminate in apoptosis. However, cancer cells are able to escape this cell death by phosphorylating

TTL, which suppresses the function of the ligase and therefore reduces the quantity of nitrotyrosinated α-tubulin (Idriss, 2004).

In plant cells, nitrosative stress is known to be existent, although the metabolism and sources have not been investigated as successfully as in the animal field and are still not completely understood (Corpas et al., 2007). However, NO has been identified as an important plant signalling molecule. One (enzymatic) source of NO in plants is discussed to be nitric oxide synthase (NOS), with L-arginine as a source for NO. Evidence is shown for its activity in extracts, and NOS inhibitors reduced the release of NO, however, no genes encoding NOS could be found in the *Arabidopsis* genome. As a very likely enzymatic alternative for NOS, nitrate reductase (NR) is considered to be a candidate; the production of NO by NR could be demonstrated *in vitro* and *in vivo.* Once generated, NO is able to move within a cell and also from cell to cell, due to its chemical property. As it is not expected that NO has a specific receptor, but the cell undoubtedly senses the presence of NO, there must be other target molecules or proteins. It is well known that NO can interact with amino acids (such as cysteine and tyrosine) and with thiol groups (for review see Neill et al., 2003; Planchet and Kaiser, 2006). In case of the reaction with tyrosine, NO_2Tyr is created.

Since plant homologues of TTL exist, as well as the tubulin tyrosination cycle (Wiesler et al., 2002), it can be expected that NO_2Tyr produces specific effects in plant cells. However, NO_2Tyr impact on plant cell organisation has not been investigated yet.

1.6.2 Treatment with parthenolide

One possibility to interfere in the tubulin tyrosination cycle is treatment of cells with parthenolide (Fonrose et al., 2007). Parthenolide is a sesquiterpene isolated from *Tanacetum parthenium* (feverfew, family of *Asteraceae*) and was first examined for its anticancer properties. Additionally, it is inhibiting TTC, giving hint to involvement if the tubulin tyrosination cycle in cancer development.

1.6.3 Examination of TTL in an overexpression BY-2 cell culture

The tobacco BY-2 cell culture stably overexpressing TTL together with red fluorescent protein (TTL-RFP), and transiently together with green fluorescent protein (TTL-GFP) has been investigated in this work, with the help of diploma students Steffen Durst, Natalie Schneider and Holger Ludwig (Durst, 2009; Schneider 2010; Ludwig, 2010). Doubt aroused whether TTL is a ligase or possibly catalyses other reactions, either exclusively or additionally. One experiment suggested that TTL had TTC function, which was then further explored.

In this work, accumulated data concerning the TTL overexpressing cell culture and treatment of the culture with NO_2Tyr and parthenolide is pooled and discussed, together with consideration of the role of detyrosination in plant cells.

1.6.4 Examination of Hsp90 MAPs

The tobacco BY-2 cell culture overexpressing Hsp90 together with GFP (GFP-Hsp90) has been investigated in this work. Two almost identical MAPs have been isolated from rice and tobacco. As one of them (OsHsp90) was identified in the same fraction as detyr-tub, Hsp90 was a possible candidate for detector of the detyrosination signal.

For further analysis, transiently and stably transformed tobacco BY-2 cell cultures GFP-OsHsp90 and GFP-NtHsp90 were examined concerning phenotype and MT-binding properties.

The functional role of Hsp90 in plant cells has been investigated by treatment of the transformed cell culture with geldanamycin (GDA). In animal cells, GDA binds to Hsp90 and inhibits ATPase activity by binding to the N-terminal ATP-binding domain of the chaperone. Although Hsp90 is essential for cellular viability, its inhibition with GDA features a method of inhibition of tumorgenesis (Gooljarsingh, 2006).

2 Material and methods

2.1 Standard chemicals, reagents and equipment

All standard chemicals had highest purity and were obtained from Roth (Karlsruhe, Germany), Sigma-Aldrich (parent company of Sigma, Aldrich and Fluka, Steinheim, Germany), Duchefa (Haarlem, The Netherlands), Amersham/GE Healthcare (München, Germany), unless stated otherwise.

Antibodies were obtained from Sigma-Aldrich, a prestained broad range protein marker came from New England Biolabs (NEB, Frankfurt, Germany), and material for Western blotting was purchased from Roth.

Solutions and media were assembled with ultrapure water, produced in an Ultra Clear UV plus system (SG, Barsbüttel, Germany). Deionised water was produced with a Seradest SD2800 filter (ELGA LabWater, Celle, Germany) and used for rice cultivation.

All solutions and media used for cell culture were sterilised by autoclaving (HA300 MIIC, Wolf Laboratories, York, UK), solutions containing heat sensitive chemicals like e.g. antibiotics or amino acids were sterilised by using a sterile filter with a pore size of 0,22 µm.

Laboratory equipment that played a significant role in this study is mentioned in the respective chapter, standard laboratory equipment is not listed.

2.2 Basic commodities

2.2.1 Standard media and solutions

Table 2.1: Standard media for cell culture and bacteria

Medium	Contents	Concentration
Murashige and Skoog (MS) pH 5,8	Murashige and Skoog salts	4,3 g/l
	Sucrose	30 g/l
	KH_2PO_4	0,2 g/l
	Myo-inositol	0,1 g/l
	Thiamine	1 mg/l
	Dichlorophenoxyacetic acid (2,4-D)	0,2 mg/l
MS agar	Agar-agar (*dänisch*) in MS medium	0,8 % [w/v]
Lysogeny broth - Lennox (LB) pH 7	Yeast extract	5 g/l
	Tryptone	10 g/l
	NaCl	5 g/l
LB agar	Agar-agar, Kobe I	1,5 % [w/v]
Super optimal broth with glucose (SOC) pH 7	Yeast extract	5 g/l
	Tryptone	20 g/l
	NaCl	10 mM
	KCl	2,5 mM
	$MgCl_2$	10 mM
	$MgSO_4$	10 mM
	Glucose	20 mM

Table 2.2: Standard buffers and solutions

Labelling	Contents	Concentration
Phosphate buffered saline (PBS) pH 7,2	NaCl	0,15 M
	KCl	2,7 mM
	KH_2PO_4	1,2 mM
	Na_2HPO_4	6,5 mM
Tris buffered saline supplemented with Triton (TBST) pH 7,4	Tris/HCl	20 mM
	NaCl	150 mM
	Triton X-100	1 % [v/v]
Extraction buffer pH 6,9	4-Morpholineethanesulfonic acid (MES)	25 mM
	Ethylene glycol tetraacetic acid (EGTA)	5 mM
	$MgCl_2$	5 mM
	Glycerol	1 M
	Dithiothreitol (DTT)	1 mM
	Phenylmethylsulfonyl fluoride (PMSF) (DTT and PMSF added freshly)	1 mM

2.2.2 Subsidiary proteins

Molecular weight marker

A prestained broad range molecular weight marker (P7708, New England Biolabs, München, Germany) was used to estimate the size of proteins separated by sodiumdodecylsulfate polyacrylamide gel electrophoresis (SDS-PAGE). The marker was incubated at 95 °C for 5 min prior to use and immediately loaded to the gel, 5 µl for each gel pocket.

Primary antibody TUB-1A2

TUB-1A2 is a monoclonal antibody produced in mouse which binds to the last 12 amino acids on the C-terminus of α-tubulin. Therefore it is possible to detect tyrosinated tubulin (tyr-tub) specifically. The epitope consists of the following amino acids: VEGEGEEEGEEY (Kreis 1987). The antibody was used for immunostaining and Western blotting.

Primary antibody DM1A

DM1A is a monoclonal antibody, also detecting α-tubulin and produced in mouse. The epitope consists of the amino acids 424-430 (DMAALEK, Breitling and Little, 1986) within the protein. The antibody was used for detection of detyrosinated α-tubulin (detyr-tub, for detection and specificity see Wiesler et al., 2002) in immunostaining and Western blot experiments.

Secondary antibody conjugated with alkaline phosphatase

For signal development in Western blot experiments a polyclonal secondary antibody against mouse produced in goat (anti-mouse IgA) was used. This antibody is coupled to alkaline phosphatase, causing coloration on a polyvinylindene fluoride (PVDF) membrane by phosphorylating its substrates nitrobluetetrazolium (NBT) and 5-Bromo-4-chloro-3-indolyl phosphate-p-tuloidine (BCIP).

Secondary antibody conjugated with FITC or TRITC

For immunostaining experiments polyclonal secondary antibodies against mouse produced in goat (anti-mouse IgG) were used. The antibodies were coupled with fluorescein isothiocyanate (FITC, green staining in fluorescence microscopy) or tetramethylrodamine isothiocyanate (TRITC, red staining in fluorescence microscopy).

2.3 Cultivation of plant material

2.3.1 Rice plants

Caryopses of rice (*Oryza sativa* L. ssp. japonica cv. Nihonmasari) were deposited equidistantly on foam plastic meshes, floating on 100 ml deionised water in plastic boxes, assuring that caryopses can grow under optimal aerobic conditions with adequate water supply. Seedlings were raised in photobiological darkness (plastic boxes wrapped in black cloth, stored in light-proof boxes) at 25 °C for 6 dayd (Nick et al., 1994).

Treatment of rice seedlings with agents was accomplished by adding the required amount of a stock solution directly to the culture medium.

2.3.2 Tobacco cell culture

The tobacco cell culture BY-2 (*Nicotiana tabacum* L. cv. Bright Yellow 2, Nagata et al., 1992) was cultivated in liquid MS. For subcultivation, 1 - 2 ml of stationary phase cells were weekly transferred to 100 ml Erlenmeyer flasks containing 30 ml fresh medium and cultured on a rotary shaker (KS 260 basic, IKA Labortechnik, Germany) at 150 rpm and 25 °C, in the dark. Stock BY-2 calli were kept on MS agar and subcultured every 4 - 6 weeks.

Transgenic cell lines were maintained in MS containing 25 mg/l kanamycin or 50 mg/l hygromycin (for details see Table 2.3), calli were maintained on MS agar containing antibiotics of the same sort and concentration.

2.3.3 Transgenic tobacco cell cultures

Table 2.3 gives an overview of the transgenic cell cultures (based upon tobacco BY-2) which were used in this study.

Table 2.3: Transgenic tobacco BY-2 cell lines

Labelling	Transgene	Fusion / vector	Resistance	Source
GFP-OsHsp90	Hsp90, *Oryza sativa,* Swiss-Prot accession A2YWQ1	GFP fused to N-terminus of the protein of interest, vector pK7WGF2,0	Kanamycin	This work
GFP-NtHsp90	Hsp90, *Nicotiana tabacum,* Swiss-Prot accession Q14TB1	GFP fused to N-terminus of the protein of interest, pDrive cloning vector (Qiagen)	Hygromycin	J. Kobrlová, Charles University, Prague, Czech Republic
TTL-RFP	TTL, *Oryza sativa,* Swiss-Prot accession Q10QY4	RFP fused to N-terminus of the protein of interest, vector pH7WGR2,0	Hygromycin	This work, construct by P. Hohenberger, (Durst, 2009; Schneider 2010; Ludwig 2010)
Free GFP	GFP only	GFP in pDrive cloning vector	Kanamycin	K. Schwarzerová, Charles University, Prague, Czech Republic

2.4 Treatment and quantification of responses in rice and tobacco

2.4.1 Quantification of responses to 3-Nitro-L-tyrosine in rice

For treatment with 3-Nitro-L-tyrosine (NO_2Tyr), the modified amino acid was added to deionised water to the respective concentration at the time of sowing and caryopses incubated for 6 d (for growth measurements and determination of mitotic index), or NO_2Tyr was added after 6 d and seedlings further incubated for 1 h (for determination of the mitotic index). Controls were either treated without NO_2Tyr or with tyrosine (Tyr) in the corresponding concentrations.

For growth measurement, the length of treated and untreated coleoptiles and roots was determined. A minimum of 18 seedlings was analysed for growth

measurement of coleoptiles and roots, for comparison of root growth after treatment with Tyr or NO_2Tyr, at least 11 roots were evaluated.

To determine the mitotic index (MI), root tips were fixed for 1 h in 3,7 % [w/v] paraformaldehyde (PFA) in PBS, washed 3 x with PBS and minced into small pieces. DNA was stained with 2′-(4-Hydroxyphenyl)-5-(4-methyl-1-piperazinyl)-2,5′-bi(1H-benzimidazole) trihydrochloride (Hoechst 33258) in a final concentration of 1 µg/ml. For each concentration of NO_2Tyr, 3 independent sets of experiments with 300 cells each were evaluated; for comparison of Tyr and NO_2Tyr, 5 independent sets of experiments with 240 cells each were evaluated. Observation under a fluorescence microscope is described in chapter 2.8.

2.4.2 Quantification of responses to 3-Nitro-L-tyrosine in BY-2 cells

To test the response to NO_2Tyr, a sterile stock solution of NO_2Tyr was diluted directly to the medium to yield the desired concentration.

Total growth of the BY-2 culture was quantified by measuring the sedimented cell volume in a sample of 15 ml at day 4 after subcultivation, in at least 4 independent experimental sets.

To assess mitotic index, NO_2Tyr was added to fresh medium at the time of subcultivation and incubated for 3 d, when the time point of exponential growth is reached. Cells were then fixed in Carnoy fixative (3 parts pure ethanol, 1 part acetic acid, complemented by 0,5 % [w/v] Triton X-100, Campanoni et al., 2003), stained with Hoechst 33258 at a final concentration of 1 µg/ml and observed under the fluorescence microscope (see chapter 2.8). For each concentration of NO_2Tyr, 7 independent sets of experiments with 300 cells each were evaluated; for comparison of Tyr and NO_2Tyr, 5 independent sets of experiments with 260 cells each were evaluated.

For measurement of cell length, cell wall orientation and protein extraction followed by Western blot analysis, NO_2Tyr was added 3 d after subcultivation and further incubated for 24 h. Cells were examined by differential interference contrast under the fluorescence microscope (chapter 2.8).

Cell length was defined as the distance between the midpoints of the two cross walls of a cell. For each concentration, 3 independent experimental sets with 500 cells each were analysed.

To quantify the orientation of cross walls, the two angles between cross wall and side wall were measured and the ratio between the larger over the smaller angle was calculated as shown in Figure 2.1; 2 independent experimental sets with 150 cross wall ratios each were evaluated. For symmetric cross walls, this ratio is 1, for asymmetric orientations, this ratio deviates from 1.

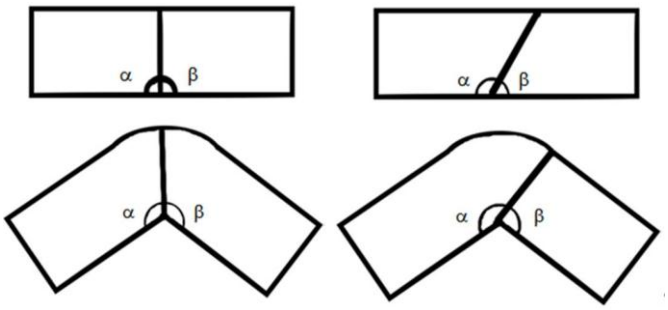

Figure 2.1: Determination of symmetry in cross wall orientation in BY-2 cell files. The two cell files on the left, a straight and a curved one, show symmetric cross walls with two equal angles α and β. The two cell files on the right demonstrate asymmetric cross wall orientation in a straight and a curved cell file (image source: M. Zimmermann).

To test whether NO_2Tyr has a direct influence on MTs, NO_2Tyr was administered in combination with oryzalin in another set of experiments (at least 3) by measuring the sedimented cell volume.

Controls were either treated without NO_2Tyr or with the equivalent concentrations of Tyr.

2.5 Biochemical methods and analysis

2.5.1 Soluble protein extraction

Extraction of soluble proteins from rice

For biochemical analysis, rice coleoptiles were harvested 6 d after sowing, under green light to avoid light dependent reorientation of cortical microtubules

(cMTs), which can occur in a very short time (half time of plant cMTs is about 1 min, for detailed information see Himmelspach et al., 1999). Coleoptiles were cut off by a razor blade or scalpel and transferred into liquid nitrogen immediately. The following steps could be performed under normal light conditions.

The plant material was ground to a powder in liquid nitrogen to avoid thawing and thereby denaturation of proteins. The powder was transferred to 2-ml centrifuge tubes and mixed with the same volume of cold extraction buffer. Cell wall debris and other insoluble remains were removed by centrifugation at 13000 g for 5 min (Heraeus Instruments, Biofuge pico, Osterode, Germany, rotor PP 1/96 #3324), followed by ultracentrifugation of the supernatant in a Beckman TL-100 ultracentrifuge (Beckman, California, USA, rotor TLA 100.2) at 4 °C and 100000 g for 15 min. The obtained supernatant contained the soluble proteins including tubulin (Nick et al., 1995). This soluble protein extract was the starting material for affinity chromatography.

Extraction of soluble proteins from tobacco BY-2 cells

Protein extracts were prepared from 4 d old BY-2 cells, either untreated or after pre-treatment with NO_2Tyr for 24 h. After sedimentation in 15-ml test tubes for 10 min and 1500 g in a Hettich centrifuge (Hettich Centrifuge Typ 1300, Tuttlingen, Germany), cells were homogenised in one volume of cold extraction buffer by using a glass potter (on ice).

Insoluble tissue debris was removed by centrifugation for 5 min at 13000 g, followed by ultracentrifugation at 20 °C and 100000 g for 15 min. In this experiment, all steps were carried out at room temperature to avoid depolymerisation of microtubules and to collect only the soluble proteins including soluble tubulin heterodimers.

Protein precipitation by trichloracetic acid (TCA)

Table 2.4: Solutions required for TCA precipitation

Labelling	Contents	Concentration
Solution A	Sodium desoxycholate Sodium azide	1,5 % [w/v] 1 % [w/v]
Solution B	TCA	72 % [w/v]
Acetone, -20 °C	Acetone	80 % [v/v]

The soluble protein extract was transferred to a 2-ml centrifuge tube, mixed with 1 % [v/v] solution A by using a vortex blender and incubated for 15 min at RT. After incubation, 10 % [v/v] of solution B was added, thoroughly mixed again and centrifuged at 13000 g for 30 min. The supernatant was discarded, the sediment was washed with 1 ml acetone and centrifuged at 13000 g for 30 min. The supernatant was removed again, the sediment contained the precipitated proteins and was left to air-dry (Bensadoun and Weinstein, 1976).

2.5.2 Coassembly of microtubule associated proteins (MAPs) with taxol

Table 2.5: Solutions required for MAP coassembly with taxol

Labelling	Contents	Concentration
Extraction buffer with GTP	See Table 2.2 Guanosine-5'-triphosphate (GTP)	 1 mM (added freshly)
Taxol stock	Paclitaxel in methanol	500 µM
Sucrose solution	Sucrose in extraction buffer	10 % [w/v]

A soluble protein extract was made from rice coleoptiles as described above, using extraction buffer with GTP. After centrifugation and ultracentrifugation, the supernatant was filtered through a sterile filter with a pore size of 0,22 µm to get rid of absolutely all cell wall fragments, insoluble debris etc. The pH of the filtrate was adjusted to 6,9.

For polymerisation of MTs from soluble tubulin dimers, the filtrate was supplemented with 20 µM taxol and 0,15 M KCl, and incubated at 27 °C for 1 h.

Ultracentrifuge tubes half filled with prewarmed (27 °C) sucrose solution were overlaid with the sample and centrifuged at 27 °C and 60000 g for 1 h. The supernatant was discarded; the sediment contained MTs and coassembled MAPs.

The sediment was collected in 100-500 µl extraction buffer with GTP, including 20 µM taxol and 0,7 M KCl. The high salt concentration released MAPs from the MTs. To separate the MAPs, the sample was centrifuged at 100000 g and 4 °C for 30 min. The sediment contained MAPs, tubulin was left in the supernatant (Vantard et al., 1991).

2.5.3 SDS-PAGE and Western blot analysis

Protein samples were separated using discontinuous SDS-polyacrylamide gels (Laemmli, 1970). To control loading of the SDS-polyacrylamide gels and the concentration of the proteins, one parallel set of lanes was visualised by staining with Coomassie Brilliant Blue (CBB). The other gels were used for Western blotting and treated with the accordant antibodies (TUB-1A2 for detection of tyr-tub, DM1A for detection of detyr-tub).

Sodiumdodecylsulfate polyacryamide gel electrophoresis (SDS-PAGE)

Table 2.6: Solutions required for SDS-PAGE

Labelling	Contents	Concentration
Sample buffer	1 M Tris/HCl pH 6,8	5 % [v/v]
	Glycerol	10 % [v/v]
	SDS	2 % [w/v]
	Bromphenolblue	0,1 % [w/v]
	1 M DTT (added freshly)	10 % [v/v]
Electrophoresis buffer	Glycine	186 mM
	Tris	25 mM
	SDS	3,5 mM

The precipitated protein samples were dissolved in 200 µl sample buffer, and denatured by incubation at 95 °C for 10 min. 5 µl of the prestained protein marker and 20 µl of each sample were loaded to a standard 10 % SDS-polyacrylamide mini-gel.

Table 2.7: Composition of a 10 % SDS-polyacrylamide gel, adequate for 3 gels

Component	Separation gel	Stacking gel
Acrylamide mix (37,5:1 acrylamide:bisacrylamide)	6,7 ml	1,7 ml
S-buffer (1,5 M Tris/HCl, pH 8,8)	5 ml	-
C-buffer (0,5 M Tris/HCl, pH 6,8)	-	2,5 ml
H_2O	8 ml	3,3 ml
10 % SDS	200 µl	100 µl
10 % ammonium peroxydisulfate (APS)	80 µl	80 µl
Tetramethylethylenediamine (TEMED)	10 µl	10 µl

The gels were run for 90 min at a constant current of 25 mA for each gel, using an Atto mini PAGE system (Atto, Tokyo, Japan). Both anode and cathode tank were filled with electrophoresis buffer.

Coomassie Brilliant Blue (CBB) staining

Table 2.8: Solutions required for Coomassie Brilliant Blue (CBB) staining

Labelling	Contents	Concentration
Coomassie Brilliant Blue (CBB)	Coomassie Brilliant Blue R250	0,04 % [w/v]
	Methanol	40 % [v/v]
	Acetic acid	10 % [v/v]
Destainer	Ethanol	30 % [v/v]
	Acetic acid	10 % [v/v]

For CBB staining, one gel was released from the stacking gel after electrophoresis and transferred immediately to the CBB staining solution and incubated for 1 h, shaking. After the staining step, CBB was removed and replaced by destainer. The destainer was exchanged from time to time until the protein bands were clearly visible. For long time storage, the gel was embedded between two layers of afore watered cellophane foil, spanned onto a plastic frame and dried for two days.

Western blotting and signal development

Table 2.9: Solutions required for Western blotting and signal development with alkaline phosphatase

Labelling	Contents	Concentration
Transfer buffer	Glycine Tris Methanol	1,4 % [w/v] 1,2 % [w/v] 20 % [v/v]
TBST	See Table 2.2	
Milk buffer	Low fat milk powder in TBST	3 % [w/v]
Primary antibody	TUB-1A2 or DM1A in TBST	0,25 % [v/v]
Secondary antibody	IgA (alkaline phosphatase) in milk buffer	0,04 % [v/v]
Staining solution pH 9,7	Tris/HCl NaCl	0,1 M 0,1 M
Magnesium stock	$MgCl_2 \cdot 6H_2O$	0,5 M
NBT	NBT in 75 %Dimethylformamide	75 mg/ml
BCIP	BCIP in 100 %Dimethylformamide	50 mg/ml

Proteins were transferred to a polyvinylidene fluoride (PVDF) membrane by semi-dry Western blotting. For this purpose, the stacking gel of the accordant SDS-gel was removed, the PVDF membrane and two layers of blotting paper (thickness 1,5 mm, both membrane and filter paper from Roth, Karlsruhe, Germany) were cut exactly the same size as the separation gel. Before blot assembly, the PVDF membrane had to be activated in methanol for 30 s and the filter paper soaked in transfer buffer. Beginning from the anode, the blot was prepared as follows: one layer of filter paper, activated PVDF membrane, stacking gel, one layer of filter paper, covered by the cathode. The blot was run at a constant current of 100 mA per gel, using a Semi-Dry Transfer System (Trans-Blot SD cell, Bio-Rad, München, Germany).

After protein transfer, the unspecific binding sites of the membrane were blocked by incubation in milk buffer for 1 h (all incubation steps took place at RT and on a shaker, if not stated otherwise). The milk buffer was washed away by rinsing twice in TBST, followed by incubation with the primary antibody, either

for 1 h at RT or overnight at 4 °C. The primary antibody was removed by washing 3 times for 15 min with TBST. Subsequently, the blot was incubated with the secondary antibody, again either for 1 h at RT or overnight at 4 °C. The secondary antibody was washed away by rinsing twice for 1 min in milk buffer and twice for 5 min in TBST.

As prerequisite for signal development, the membrane was incubated 15 min in freshly prepared staining solution containing 10 % [v/v] magnesium stock. Signal development was achieved by incubation of the blot in 5 ml of developer (66 µl NBT and 33 µl BCIP in staining solution containing 10 % [v/v] magnesium stock) in the dark, until signals appeared. The staining reaction was stopped by rinsing the membrane in water. The membranes were air-dried prior to scanning.

2.5.4 Ethyl-N-phenylcarbamate (EPC) affinity chromatography

For the separation of tyr-tub and detyr-tub, affinity chromatography using EPC-sepharose (Nick et al., 1995) is required. The main principle is that detyr-tub has a higher affinity to EPC-sepharose than tyr-tub and therefore needs higher concentrations of salt in the accordant buffer to be washed off the column.

Preparation of EPC-sepharose is accomplished in successive steps, which are:

- Production of carboxy-EPC
- Production of aminoethyl-sepharose
- Coupling of carboxy-EPC to aminoethyl-sepharose

Production of carboxy-EPC

20 g of 3-Aminobenzoic acid were dissolved in 250 ml 1 M NaOH. The pH was adjusted to 7,0. Stirring constantly, 25 g ethychlorocarbonate were added dropwise. N-Carboxyl-EPC precipitated and could be separated from the solution by filtration. N-Carboxyl-EPC was subsequently dissolved in 250 ml

pure ethanol and was filtered again. The filtrate was stored under the fume hood until the whole liquid evaporated and crystals formed.

Production of aminoethyl-sepharose

15 g CNBr-activated sepharose 4B (GE Healthcare, München, Germany) were soaked in 50 ml 1 M HCl, diluted in 75 ml binding buffer (100 mM $NaHCO_3$, 0,5 M NaCl, 100 mM ethylenediamine, pH 8,3), and incubated overnight at 4 °C under permanent shaking. Washing steps were carried out at room temperature (RT), using a separating column equipped with a sintered glass filter. The aminoethyl-sepharose was washed approximately 2 h with 500 ml washing buffer (WB; 100 mM Tris/HCl, pH 8), then 3 times with alternating cycles of 500 ml salt-WB (0,5 M NaCl in WB) and 500 ml acid-WB (100 mM sodium acetate, 0,5 M NaCl in WB, pH 2; Cuatrecasas, 1970).

Coupling of carboxy-EPC to aminoethyl-sepharose

1 g N-Carboxyl-EPC was soaked in 50 ml pure ethanol and mixed with 50 ml soaked aminoethyl-sepharose. After filtration, 150 mg carbodiimide (synonym: cyanamide, Sigma-Aldrich, Steinheim, Germany) was added to the filtrate. Binding occurred at RT for 3 d on an overhead rotor. The resulting EPC-sepharose was washed with water first, followed by pure ethanol and 1 M NaCl. EPC-sepharose was stored at 4 °C in 3 M KCl, containing 0,1 % sodium azide to suppress microbial growth (Mizuno et al., 1985).

EPC affinity chromatography

All steps of the affinity chromatography were performed in a cold room at 5 °C, and accomplished according to Wiesler et al. (2002).

EPC-sepharose was loaded onto a separating column and washed 3 times with 100 ml extraction buffer using a mild vacuum, to remove the salt used for storage. To allow binding of the proteins to the matrix, 1 part of soluble protein extract was mixed with 1 part of washed EPC-sepharose and incubated on a rotary shaker for 1 h. After this, the mixture was loaded onto a fresh separating

column. Using the vacuum pump again, first the flow through was collected, followed by the proteins which were separated in fractions using increasing concentrations of KCl in extraction buffer. Based on a stock solution of 3 M KCl in extraction buffer, the following concentration gradient was produced:

0,05 M, 0,1 M, 0,15 M, 0,2 M, 0,25 M, 0,3 M, 0,4 M, 0,5 M, 1 M, 3 M.

After collecting the protein fractions in test tubes, the fractions were concentrated by TCA precipitation and analysed by SDS-PAGE.

2.6 Molecular biological methods

For stable and transient transformation of the BY-2 cell culture and subsequent analysis of the proteins of interest, plasmids including these proteins together with a fluorescent labelling had to be constructed. For this purpose, the Gateway® cloning technology (Invitrogen, Karlsruhe, Germany) was utilised.

To obtain cDNA of OsHsp90, RNA from rice coleoptiles was isolated, followed by reverse transcription. For sequence details see appendix.

2.6.1 Primers

All primers used in this study and their applications are listed in Table 2.10. Primers were obtained from Sigma (Steinheim, Germany), and suspended in Tris-EDTA buffer (TE, 1 mM EDTA, 10 mM Tris/HCl, pH 8) to a concentration of 100 µM as a stock solution, the working solution had a concentration of 20 µM, diluted in water. Sequencing was carried out by GATC (Konstanz, Germany), either with the below stated primers or with standard sequencing primers such as M13. The so received sequences were aligned against the original gene sequence, using the Basic Local Alignment Search Tool (BLAST) from NCBI (http://blast.ncbi.nlm.nih.gov/Blast.cgi).

Table 2.10: List of primers for OsHsp90 cloning

Name	Sequence 5' to 3'	Application
*att*B1-OsHsp90	GGGGACAAGTTTGTACAAAAAAGCAGGCTTCATG GCCTCGGAGACGGAGACGTTC	Gateway® cloning
*att*B2-OsHsp90	GGGGACCACTTTGTACAAGAAAGCTGGGTCTTA GTCGACCTCCTCCATCTTGCTC	Gateway® cloning RT-PCR
OsHsp90-500-F	CAGCTTGGGAGGGGTACTAAG	Sequencing

2.6.2 Cloning of plasmids

The cloning of plasmids and all associated steps were accomplished according to the instructions given in the Gateway® manual (see www.invitrogen.com). The main principle and background of the Gateway® system is demonstrated in Figure 2.2.

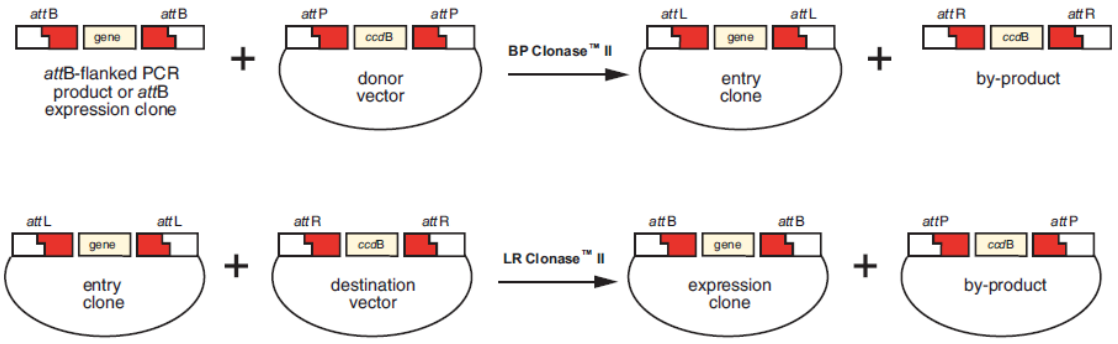

Figure 2.2: Schematic illustration of the steps to be taken to create the desired expression clone. Top row: Mode of action of BP Clonase™ II and production of the entry clone from *att*B-flanked PCR product and donor vector. Bottom row: Mode of actionof LR Clonase™ II and production of the expression clone from entry clone and destination vector. Image origin: www.invitrogen.com

Isolation of total RNA from rice

For isolation of total RNA, 100 mg of rice coleoptiles were frozen in liquid nitrogen and pulverised by a TissueLyser (Qiagen, Hilden, Germany). Using an RNeasy Plant Mini Kit (Qiagen), the sample was treated as described in the operating manual. RNA was either used immediately for reverse transcription or stored at -70 °C until usage.

Reverse transcription

Reverse transcription polymerase chain reaction (RT-PCR) was performed with total RNA with the objective of obtaining the cDNA of OsHsp82. The RT-PCR was set up as shown in Table 2.11 (deoxynucleotide triphosphates dNTPs were purchased from NEB, final concentration of the dNTP-mix was 10 mM each in TE buffer, SuperScript II Reverse Transcriptase and the appropriate buffer were purchased from Invitrogen).

Table 2.11: Experimental setup for RT-PCR

Components	Procedure
1 µl Primer *att*B2-OsHsp90 1 µg RNA 1 µl dNTP-mix 7 µl H_2O	
	→ incubate 5 min at 65 °C → place immediately on ice
4 µl first strand buffer 5x 2 µl 0,1 M DTT	
	→ incubate 2 min at 42 °C
1 µl SuperScript II	
	→ incubate 50 min at 42 °C → incubate 15 min at 72 °C

Flanking with *att*B-sequences

In the next step, the cDNA had to be equipped with *att*B flanking sequences. Table 2.12 gives an overview of the required ingredients for the following PCR (*Thermococcus kodakaraensis* KOD DNA polymerase and the appropriate buffer were purchased from Toyobo, Tokyo, Japan), which is described in Table 2.13.

Table 2.12: Composition of the PCR reaction mix

Components
1 µl dNTP-mix
1 µl *att*B1-OsHsp90
1 µl *att*B2-OsHsp90
4 µl cDNA OsHsp90
5 µl buffer 10x
0,5 µl KOD
37,5 µl H_2O

Table 2.13: Setup for PCR program for attB-flanking

PCR step	Temperature [°C]	Time [s]	Cycles
Denaturation	94	120	1
Denaturation	94	30	
Annealing	60	30	30
Elongation	72	60	
Final Elongation	72	120	1

Purification of PCR products from agarose gels

Table 2.14: Solutions required for agarose gel electrophoresis

Labelling	Contents	Concentration
TAE buffer	Tris/HCl	40 mM
	EDTA	1 mM
Agarose gel	Agarose in TAE buffer	1 % [w/v]
	SYBR Safe ™ (Invitrogen)	0,005 % [v/v]
Loading dye 5x	Glycerol	50 % [v/v]
	Bromphenol blue	0,05 % [w/v]
	Xylene cyanol	0,05 % [w/v]

The *att*B-flanked PCR products and a size marker (e.g. 2-Log DNA Ladder from NEB) were mixed with the loading dye and separated by a 1 % [w/v] agarose gel in an electrophoresis chamber at constant 100 V for approximately 45 min. Gels were analysed on a Safe Imager ™ Blue-Light Transilluminator (Invitrogen).

After identification of the correct signals, the bands of interest were excised of the gel and purified by NucleoSpin® Extract II Kit (Machery-Nagel, Düren, Germany), as stated in the protocol.

BP- and LR-reaction

The BP- and LR-reaction were performed as recommended by the Gateway® manual.

Table 2.15: Reaction mix for the BP-reaction

Components	Procedure
1 µl pDONR® Vektor (150 ng/µl) 15-150 ng *att*B-flanked PCR product to 8 µl TE buffer 2 µl BP-clonase II enzyme mix	→ incubate 18 h at 25 °C
1 µl Proteinase K (2 µg/µl)	→ incubate 10 min at 37 °C

After performance of the BP-reaction, chemically competent One Shot® TOP10 *E. coli* cells (Invitrogen) were transformed by heat shock, following the procedure described by Sambrook and Russell (2001).

Transformed cells were plated on LB agar containing 50 µg/ml zeocin for selection, and incubated at 37 °C overnight. Positive colonies were picked and transferred to test tubes filled with 2 ml LB containing 50 µg/ml zeocin, and incubated at 37 °C overnight, shaking.

Entry clones were isolated using a QIAprep Spin Miniprep Kit (Qiagen), as stated in the protocol.

Before proceeding to LR-reaction, the sequences were controlled by digestion with restriction enzymes (NEB). For this purpose, 1 µg DNA, 0,2 µl PstI (equates 2 Units, alternative restriction enzyme HindIII), 1,5 µl of the appropriate buffer and H_2O to 15 µl were mixed well and incubated for 1 h. After digestion, the samples were analysed on an agarose gel. Samples with positive

result were sent to sequencing (GATC, Konstanz, Germany) before proceeding with LR-reaction.

LR-reaction was carried out according to BP-reaction, only base products were entry clone and destination vector. The so obtained expression clones could be selected on LB agar containing 50 µg/ml spectinomycin.

In this work pK7WGF2 was used as a destination vector for OsHsp90. pK7WGF2 is a low copy vector and suitable for stable transformation in plants. GFP is fused to the N-terminus of the protein of interest. Selection markers are spectinomycin in *E. coli* and kanamycin in plants.

2.7 Cell biological methods

2.7.1 Stable transformation of BY-2

Stable transformation was performed as described in Nocarova and Fischer (2009), with some modifications.

Production of chemically competent *Agrobacterium tumefaciens*

Stable transformation of tobacco BY-2 cell culture was mediated by *Agrobacterium tumefaciens* LBA4404 (*A.t.*). For this purpose, chemically competent *A.t.* had to be produced by the following procedure:

10 ml of a pre-culture of *A.t.* in LB medium with 50 µg/ml rifampicin and 300 µg/ml streptomycin were cultivated for 2 d at 28 °C, shaking. 5 ml of the pre-culture were transferred to 100 ml LB medium with the same antibiotics and incubated shaking until an optical density OD_{600} = 0,5 – 0,6. All following steps were performed on ice or at 4 °C for centrifugation steps. The cells were harvested by centrifugation at 5000 rpm for 5 min and resuspended in 20 ml cold and sterile 0,15 M $CaCl_2$. After another centrifugation with the same conditions, cells were resuspended in 2 ml cold and sterile 20 mM $CaCl_2$. Aliquots of 200 µl were made and stored at -70 °C after shock-freezing in liquid nitrogen.

Transformation of chemically competent *Agrobacterium tumefaciens*

Chemically competent *A.t.* cells were transformed by heat shock, using the following protocol:

Table 2.16: Transformation of chemically competent cells

Components	Procedure
Competent *A.t.*	
	→ thaw on ice
1 µg DNA (binary vector)	
	→ mix carefully → incubate 5 min 37 °C → incubate 30 min on ice
1 ml LB	
	→ add to cells → incubate 2 – 4 h at 28 °C on a shaker

Transformed cells were plated on LB agar containing 50 µg/ml rifampicin, 300 µg/ml streptomycin, and 50 µg/ml spectinomycin for selection, and incubated at 28 °C for 3 d. For the following co-cultivation, a single colony of *A.t.* was picked and transferred to an Erlenmeyer flask filled with 10 ml of LB with the antibiotics named above, and incubated overnight at 28 °C, shaking.

Co-cultivation of *Agrobacterium tumefaciens* and BY-2

Required reagents and material:

- One flask (30 ml) of 3 d old BY-2 cells
- Nalgene filtration device (Nalgene, Roskilde, Germany)
- 30 ml fresh MS medium
- 20 mM acetosyringone stock solution
- 10 ml *A.t.* cell suspension grown overnight

The BY-2 cells were filtered through a Nalgene filter device and resuspended in fresh MS medium to get the original volume. 1 µl of the acetosyringone stock solution was added per 1 ml BY-2 cell suspension. This suspension was pushed 20 x through a 10 ml tip to induce small injuries and increase the transformation rate. 2 ml of BY-2 cells and 150 µl of the *A.t.* culture were

transferred to a Petri dish (6 cm in diameter). For each variant, a minimum of 5 Petri dishes were prepared. Controls were carried out without *A.t.* The co-cultivation was incubated at 28 °C for 3 d in the dark without shaking.

Selection

Required reagents and material:

- Nalgene filtration device
- 1 l sucrose solution (3 % [w/v]) containing 70 µg/ml cefotaxime
- 30 ml fresh MS medium containing 70 µg/ml cefotaxime
- Fresh MS agar plates (6 cm in diameter) containing 70 µg/ml cefotaxime and kanamycin (100 µg/ml)

After co-cultivation, the content of the Petri dishes was suspended in a small amount of sucrose solution and poured into a Nalgene filtration device. 100 ml of sucrose solution were added to resuspend cells thoroughly. After removing the sucrose solution by filtration, cells were washed with 3 x 200 ml sucrose solution. BY-2 cells were then resuspended in a small amount of MS medium (approx. 5 ml) to obtain a very dense cell suspension. This cell suspension was poured on MS agar, care was taken to obtain a moderately thin but continuous layer of cells. Petri dishes were then incubated (unsealed) in a plastic box together with an uncovered Petri dish containing H_2O to avoid drought. The plastic box was kept closed and incubated at 28 °C, for several weeks.

Establishing a liquid culture from transformed BY-2

After 2 – 4 weeks, first colonies of transformed BY-2 cells appeared. At a diameter of approximately 2 mm the calli were transferred to fresh MS agar with the aforementioned antibiotics, a fraction of the callus was checked for fluorescence. When a diameter of 1 cm was reached, the callus was transferred to 10 ml MS medium containing antibiotics and incubated on a shaker. After reaching high density (normally after 6 – 10 d), the cell suspension was subcultured. A small amount of the callus was kept on MS agar as a resource.

2.7.2 Transient transformation of BY-2

Transient transformation of BY-2 was achieved by biolistics, using a Helios Gene Gun System, tubing prep station and tubing cutter from Bio-Rad (Bio-Rad Laboratories GmbH, München Germany; the instruction manual of the Helios Gene Gun System was followed). For transformation, gold particles were coated with the plasmid of interest and shot onto the cell culture by a nitrogen gas pulse. In this work, the plasmids used for stable transformation of Hsp90 were used for transient transformation, too.

Gold coating

Required reagents and material:

- 50 mg gold (size 0,6 µm, quantity enough for 3 samples)
- 100 % water free ethanol (incubated with Sigma M-9882 beads), stored in an exsiccator
- 50 % glycerol
- Fresh 0,05 M spermidine free base
- 1 M $CaCl_2$
- Plasmid DNA (1 µg/µl) in 10 mM Tris pH 8
- 0,05 mg/ml polyvinylpyrrolidone (PVP) in ethanol, stored in an exsiccator

Gold was weighed in a 2-ml centrifuge tube, resuspended in 1 ml ethanol and incubated for 15 min at RT. The gold was sedimented at 5000 rpm for 30 s, the ethanol was discarded. Subsequently, the gold was thoroughly washed 3 x with water (7000 rpm for 30 – 60 s), resuspended in 600 µl glycerol, and divided into 3 samples of 200 µl each. The following steps apply for one sample, the rest could be stored at 4 °C for several weeks, if sterility is ensured.

To remove glycerol, the gold was washed 2 x with water as described above, and resuspended in 100 µl spermidine by 2 vortex steps of 2 s each, and sonication for 30 s (no aggregates allowed).

10 – 50 µg plasmid DNA (maximum volume 50 µl) was added to the gold (for two plasmids the total concentration was also 10 – 50 µg and a volume of 50 µl altogether). The solution was thoroughly mixed on a vortex blender for 5 s. Drop by drop, 100 µl $CaCl_2$ was added and vortexed in between. After incubation of 10 min at RT, the gold was sedimented by centrifugation at 5000 rpm for 30 s, the supernatant was discarded. Gold was washed 3 x with 500 µl ethanol (at 5000 rpm for 5 s), and resuspended in 1,8 ml PVP. This could be stored at -20 °C for 2 months, if tube was sealed.

Cartridge coating

Required reagents and material:

- GoldCoat tubing
- Tubing prep station
- Nitrogen gas
- Syringe
- Previously prepared gold solution

GoldCoat tubing was cut to the required length (approximately 75 cm), placed in the tubing prep station and pre-dried for 15 min with 0,3 – 0,4 l/min nitrogen. The syringe was placed on the tube to be able to soak the solution into the tube; bubbles had to be avoided. The tube was placed in the tubing prep station without removing the syringe. The next 5 min, every 30 s the tube was rotated a little bit to let the gold stick to the inner wall. This step was repeated, if necessary. Afterwards, the solution was removed slowly and carefully, without washing away the gold coating. The tube was turned through 180 °, the syringe was removed, and after waiting another 5 s, the tube was rotated for 30 s. The gold coating was dried for 5 min at 0,3 – 0,4 l/min nitrogen (if the gold was not dry yet, this step was repeated). The tube was removed from the tubing prep station and cut into pieces with the tubing cutter. The cartridges could be stored in a 50-ml test tube (containing silica gel) at 4 °C for several months.

Transient transformation

Required reagents and material:

- 2 - 3 d old BY-2 cell culture
- Nalgene filtration device
- MS agar in 6 cm Petri dishes
- 6 cm filter paper (fitting into Petri dishes)
- Helios Gene Gun
- 2 - 3 cartridges
- Nitrogen gas

5 ml of BY-2 cells were pipetted onto the filter paper, the spare medium was removed carefully by the filtration device, and the filter paper was placed onto MS agar. After arranging the Helios Gene Gun as required, the gold of two cartridges was shot on the cells. The nitrogen pressure was kept at 300 - 350 psi, each cartridge was used 3 times, the Petri dishes were turned after every shot for a little bit.

After shooting, the cells were incubated at 28 °C for 18 h and observed under the microscope.

2.7.3 Visualisation of microtubules in BY-2

Table 2.17: Solutions required for visualisation of microtubules

Labelling	Contents	Concentration
Microtubule staining buffer (MSB) pH 6,9	1,4-Piperazinediethanesulfonic acid (PIPES) EGTA $MgSO_4$	50 mM 2 mM 2 mM
Fixative I	PFA in MSB	3,7 % [w/v]
Fixative II	Triton X-100 in Fixative I	0,1 % [v/v]
PBS	See Table 2.2	
Digestion solution	Macerocyme in MSB Pectolyase in MSB	1 % [w/v] 0,1 % [w/v]
Blocking solution	Bovine serum albumin (BSA) in PBS	0,5 % [w/v]
Primary antibody	TUB-1A2 or DM1A in PBS	0,1 % [v/v]
Secondary antibody	FITC or TRITC conjugated antibody (IgG)	0,5 % [v/v]

For visualisation of MTs by indirect immunofluorescence, the method described in Nick et al. (2000) was used as a background. Cells were transferred to a staining chamber which was made from a cut 2-ml centrifuge tube, sealed with a mesh with 70 µm pore size (Franz Eckert GmbH, Waldkirch, Germany). Fixation of cells was accomplished by incubating 30 min in Fixative I, followed by 30 min in Fixative II. Samples were washed 3 x 10 min with MSB. Cell walls were permeabilised by incubating 7 min in digestion solution. After another washing step (3 x 10 min with MSB), cells were incubated in blocking solution for 30 min. The primary antibody was incubated for 45 min at RT or overnight at 4 °C, and removed by washing 3 x 10 min with PBS. The secondary antibody could also be incubated for either 45 min at RT or overnight at 4 °C, and was removed by washing 2 x 10 min with PBS.

2.7.4 Visualisation of DNA in BY-2

In addition to MT staining and stable and transient transformation in tobacco BY-2, the DNA was stained by using the fluorescent dye Hoechst 33258, which binds to the AT base pairs. For this purpose, a stock solution of Hoechst 33258

(0,5 mg/ml, in water) was prepared and added to the samples in a final concentration of 1 µg/ml. The samples were treated prior to microscopy.

2.8 Microscopy and image analysis

The samples were investigated either with an AxioImager Z1 microscope (Zeiss, Jena, Germany) or with a Leica TCS NT confocal laser scanning microscope (Leica Microsysteme Vertrieb GmbH, Wetzlar, Germany).

The Zeiss AxioImager Z1 was equipped with an ApoTome microscope slider used for optical sectioning, and a cooled digital CCD camera (AxioCam MRm). For measuring cell length or cell wall angles in BY-2, samples were observed in the differential interference contrast (DIC) using a 20x objective (Plan-Apochromat 20x/0.75) and the MosaiX imaging software (Zeiss). For detection of Hoechst stained DNA, samples were observed using the filter set 49 (excitation at 365 nm, beam splitter at 395 nm, and emission at 445 nm) using a 40x objective (EC Plan-Neofluar 40x/0.75 M27) for BY-2 and a 63x oil-immersion objective (Plan-Apochromat 63x/1.40 Oil DIC M27) for rice cells. Green fluorescence (from GFP or FITC) was studied by using filter set 38 HE (excitation at 470 nm, beam splitter at 495 nm, and emission at 525 nm). Red fluorescence (from RFP or TRITC) was examined with filter set 43 HE (excitation at 550 nm, beam splitter at 570 nm, and emission at 605 nm). Images were processed and analysed using the AxioVision software 4.7 (Zeiss).

The Leica TCS NT was used for BY-2 cells only, using a 63x water immersion objective (HCX PL APO ibd.BL 63,0x1,2 W). Green fluorescence (from GFP) was observed by using a He/Ne laser (excitation at 488 nm, emission at 500-560 nm). Red fluorescence (from TRITC or MitoTracker) was examined by usage of an Ar/Kr laser (excitation at 543 nm, emission 600-700 nm). Images were processed and analysed using the Leica Lite software (Leica).

3 Results

The following experiments presented in this chapter were done for the purpose of getting a deeper insight into cellular function of the tubulin tyrosination cycle. Four strategies have been followed:

- ➔ Suppression of the detyrosination signal by applying the modified amino acid NO_2Tyr as an alternative substrate for TTL, and thus creating irreversibly tyrosinated α-tubulin
- ➔ Suppression of the detyrosination signal by applying parthenolide and thus inhibiting TTC, the enzyme which is responsible for detyrosination
- ➔ Suppression of the detyrosination signal by overexpression of TTL, the enzyme which is responsible for retyrosination of the α/β-tubulin heterodimers
- ➔ Examination of a possible acceptor (MAP Hsp90) of the detyrosination signal

The following chapters deal with these four approaches and present the results of the respective experiments.

3.1 Suppression of the detyrosination signal by treatment with NO_2Tyr

By applying NO_2Tyr to rice seedlings or tobacco BY-2 cell culture, one has the ability to incorporate the modified amino acid to the C-terminus of α-tubulin and hence create irreversibly tyrosinated α-tubulin. The detyrosination signal is being suppressed and cannot be read any more.

3.1.1 NO_2Tyr inhibits plant mitosis in a dose-dependent manner

In order to identify targets for NO_2Tyr in plant cells, the growth response of rice coleoptiles (consisting of non-cycling cells that grow exclusively by cell expansion), rice seedling primary roots (consisting of cycling cells that

subsequently expand) and tobacco BY-2 cells (with strong cycling activity) to the modified amino acid was investigated by dose-response studies.

To measure growth inhibition of rice seedlings, NO_2Tyr was administered to caryopses at the time of sowing; rice coleoptiles and roots were measured after 6 d. NO_2Tyr was found to inhibit root growth strongly with a threshold of around 10 µM (Figure 3.1).

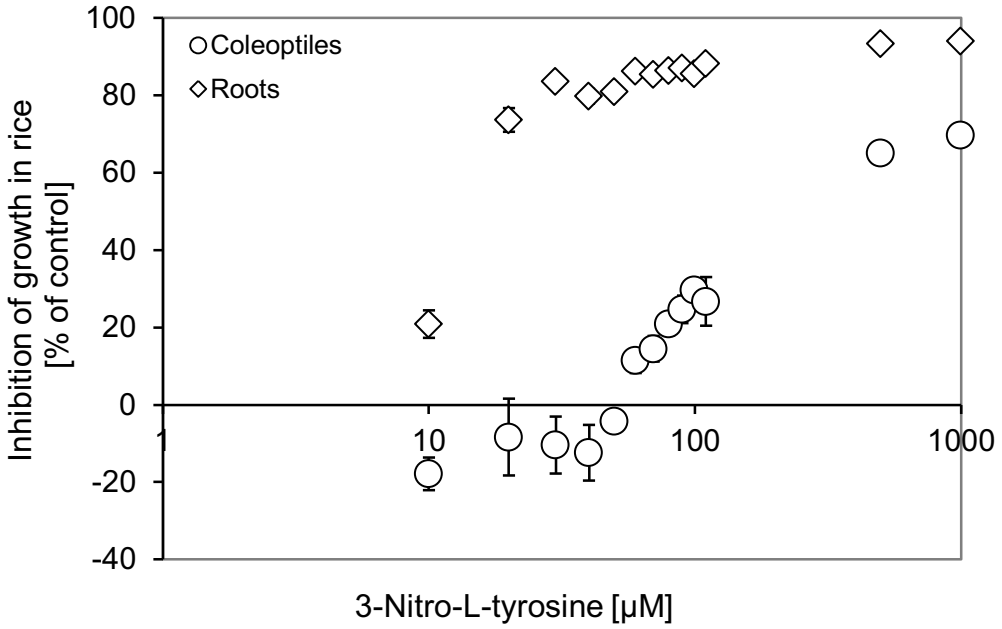

Figure 3.1: Quantification of the inhibitory effects of NO_2Tyr to 6 d old rice seedlings. Inhibition (given as % of control) of coleoptile (white circles) and root (white diamonds) growth in rice seedlings (n≥18, error bar=standard error SE).

Already at 20 µM NO_2Tyr root growth was reduced by about 70 % as compared to control seedlings. At these concentrations, coleoptile growth was still unaffected, inhibition became detectable from 60 µM NO_2Tyr, reaching a plateau (of 60 % inhibition as compared to control seedlings) only at high concentrations of at least 500 µM NO_2Tyr. Thus, the dose-response curve for coleoptile growth over NO_2Tyr was shifted by almost an order of magnitude as compared to root growth, suggesting that the main target of NO_2Tyr is not the mechanism of cell elongation but rather other mechanisms involved in cell division.

BY-2 cells (in contrast to rice coleoptiles a model for cycling cells and therefore adequate for experiments regarding cell division) treated for 3 d with NO_2Tyr also displayed growth inhibition, in this experiment measured as a decrease in packed volume cell density (Figure 3.2).

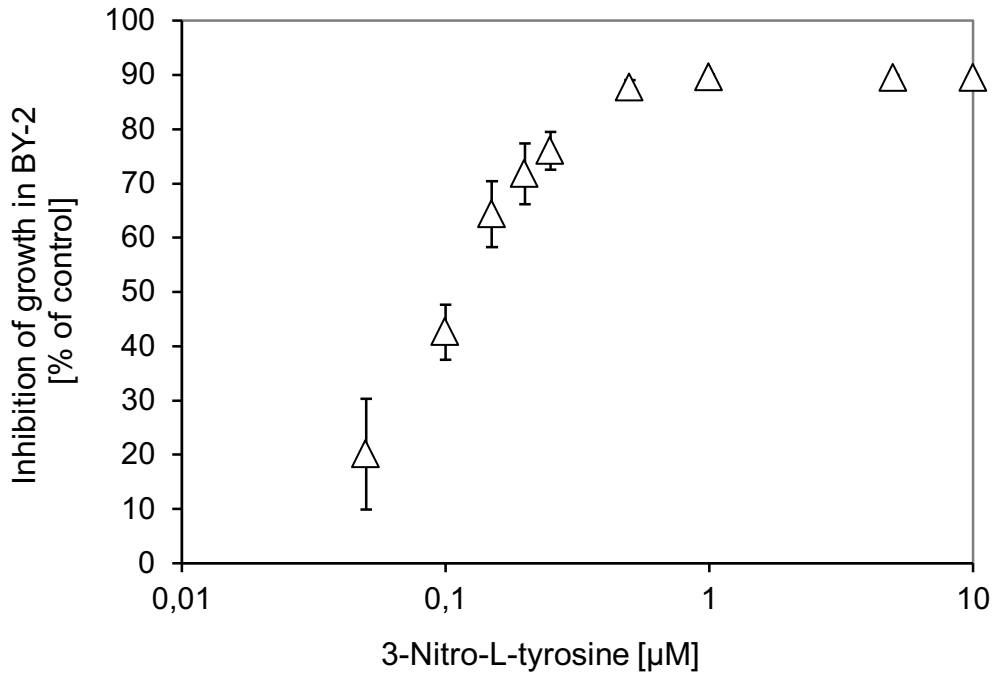

Figure 3.2: Quantification of the inhibitory effects of NO_2Tyr to BY-2 cell culture. Inhibition of growth (given as % of control packed volume) in BY-2 cells (white triangles; n≥4, error bar=SE).

Growth inhibition was observed already starting from 50 nM NO_2Tyr and increased strongly to about 40 % at 0,1 µM NO_2Tyr, reaching saturation at 0,5 µM NO_2Tyr with approximately 90 % inhibition as compared to untreated controls.

As cell division was likely to be a target for NO_2Tyr, mitotic indices of rice root tips and tobacco BY-2 were determined for deeper insight.

Figure 3.3 shows the increase of mitotic inhibition for rice root tips either after 6 d of continuous cultivation (black diamonds) with the accordant concentration of NO_2Tyr or after 6 d of cultivation on water followed by incubation with NO_2Tyr for 1 h only (white diamonds). Interestingly, 1 h incubation produced almost the

same inhibition as continuous treatment for 6 d, indicating rapid uptake and metabolisation or incorporation of NO_2Tyr.

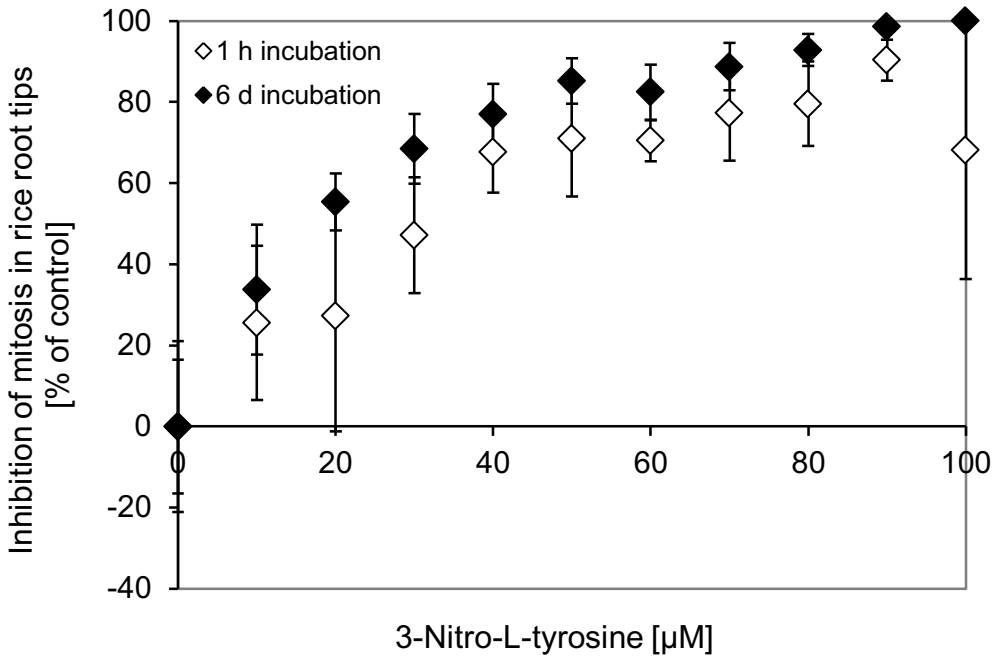

Figure 3.3: Quantification of the inhibitory effects of NO_2Tyr to 6 d old rice seedlings. Inhibition of mitosis (given as % of control) in rice root tips, incubated for 1 h with NO_2Tyr (white diamonds), or incubated 6 d with NO_2Tyr (black diamonds; n=3 independent experiments with 300 cells each, error bar=SE).

Similarly, BY-2 cells treated with NO_2Tyr showed a decline of mitotic index (indicated as inhibition of mitosis, Figure 3.4), whereby the inhibition occurred at much lower concentrations of the applied agent as compared to rice root tips. Higher sensitivity of BY-2 cells to NO_2Tyr (as already observed for the dose-response studies considering rice root growth versus packed volume in BY-2) was thereby confirmed.

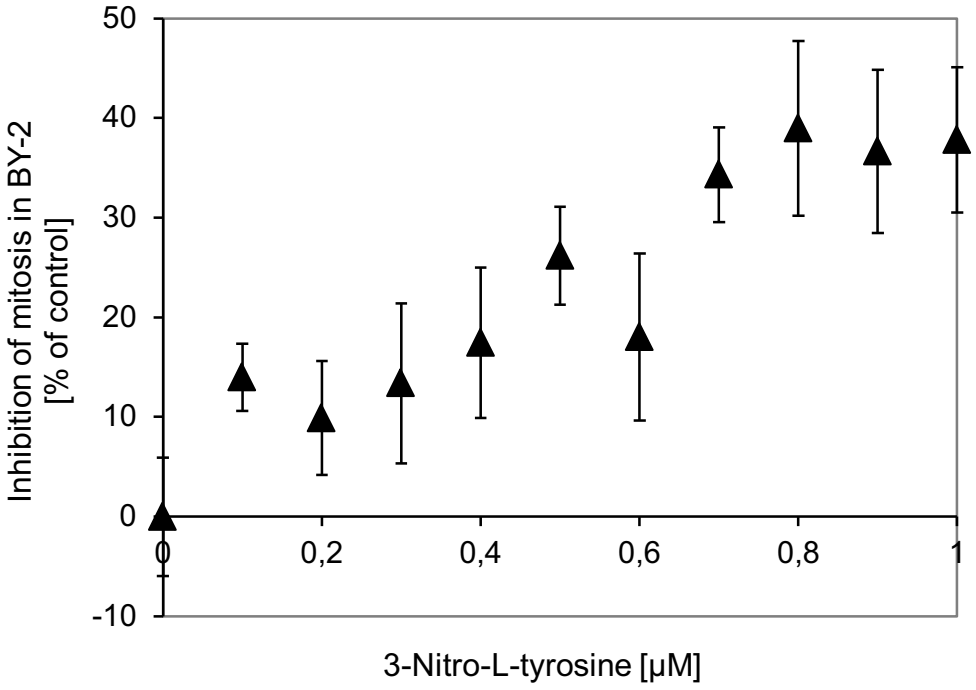

Figure 3.4: Quantification of the inhibitory effects of NO_2Tyr in BY-2 cell culture. Inhibition of mitosis (given as % of control) in BY-2 treated with NO_2Tyr (black triangles; n=7 independent experiments with 300 cells each, error bar=SE).

3.1.2 The inhibition of total growth and mitosis is specific for nitrosylated tyrosine

To test whether mitotic inhibition was specific for the nitrosylated form of tyrosine, dose-response curves were recorded for non-nitrosylated tyrosine.

In Figure 3.5, growth inhibition in rice roots and BY-2 cell culture is shown in a comparison of treatment with NO_2Tyr and tyrosine. Neither for root growth nor for culture growth a significant inhibition by tyrosine could be observed.

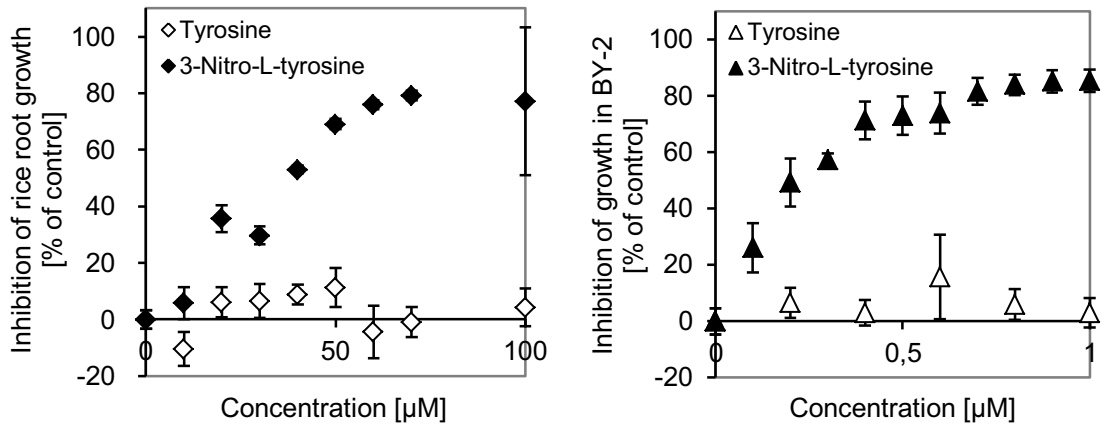

Figure 3.5: Quantification of the inhibitory effects of Tyr and NO_2Tyr to 6 d old rice seedlings (left diagram) and BY-2 cell culture (right diagram). **Left diagram**: Comparison of the inhibition of root growth (given as % of control) either treated with Tyr (white diamonds) or NO_2Tyr (black diamonds; n≥11, error bar=SE). **Right diagram**: Comparison of the inhibition of growth (given as % of packed volume) either treated with Tyr (white triangles) or NO_2Tyr (black triangles; n=4, error bar=SE).

Furthermore, there was no significant inhibition of mitotic indices in rice root tips and tobacco BY-2, even at the highest concentrations where strong inhibition was observed for NO_2Tyr (Figure 3.6). Thus, the inhibition of mitosis is specific for the nitrosylated form of tyrosine.

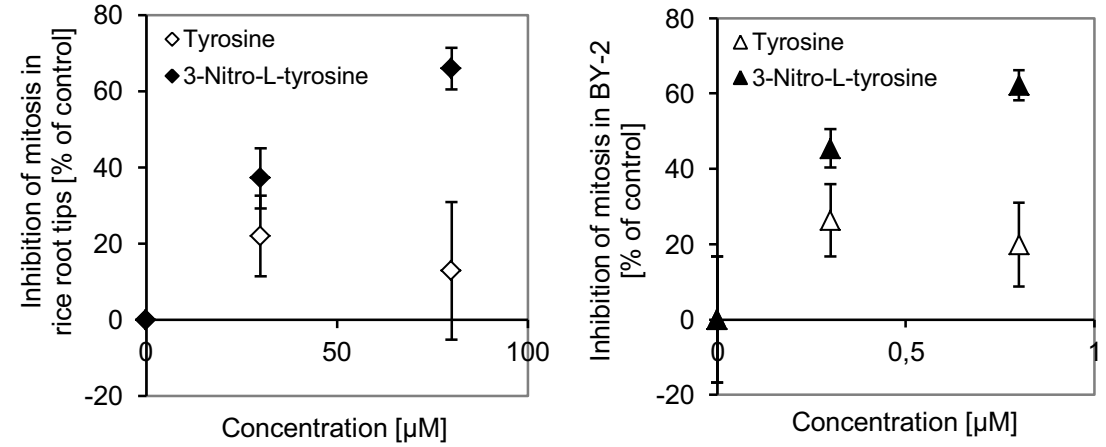

Figure 3.6: Quantification of the inhibitory effects of NO_2Tyr to 6 d old rice seedlings (left diagram) and BY-2 cell culture (right diagram). **Left diagram**: Comparison of the inhibition of mitosis (given in % of control) in rice root tips either treated with Tyr (white diamonds) or NO_2Tyr (black diamonds; n=5 independent experiments with 240 cells each, error bar=SE). **Right diagram**: Comparison of the inhibition of mitosis (given in % of control) in BY-2 cells either treated with Tyr (white triangles) or NO_2Tyr (black triangles; n=5 independent experiments with 260 cells each, error bar=SE).

3.1.3 NO_2Tyr stimulates cell length and affects the formation of cross walls

Cell length in tobacco cells is a sensitive indicator for reduced mitotic activity (Holweg et al., 2003). Therefore, a dose-response relationship in tobacco BY-2 cells was recorded. For this purpose, a 3 d old BY-2 cell culture was treated with NO_2Tyr for another 24 h.

At 2 µM NO_2Tyr an increase of 5 % in cell length could be observed (Figure 3.7). At a concentration of 5 and 10 µM NO_2Tyr an increase in cell length of almost 20 % was observed, indicating a saturation of the effect with 5 µM NO_2Tyr.

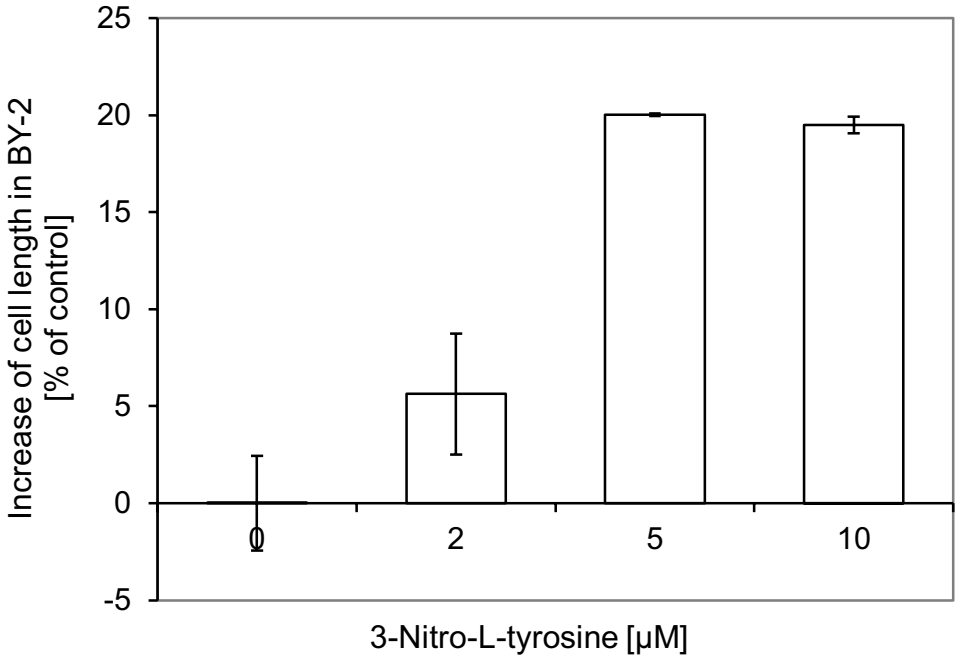

Figure 3.7: Physiological effects of 24 h treatment with NO_2Tyr on 4 d old BY-2 cells (3 d old plus 24 h treatment with NO_2Tyr). Columns display increase of cell length, given in % of control (n=3 independent experiments with 500 cells each, error bar=SE).

To get insight into the cellular events that accompany the observed inhibition of cell division in BY-2 cells, the deposition of cross walls that appeared to be affected upon treatment with NO_2Tyr was investigated. The ratio of the angles between cross wall and side walls was determined as measure for orientation symmetry (see material and methods, chapter 2.4.2, Figure 2.1). This ratio is 1

in case of symmetrical cross walls, but deviates from 1, when the cross wall is laid down asymmetrically. In untreated cells, the cross walls were mostly symmetrical (manifest as a high frequency of ratios between 1,0 and 1,09). With increasing NO_2Tyr concentration, the number of incorrect oriented cross walls with oblique orientation (ratio ≥1.1) increased (Figure 3.8). As for the stimulation of cell length, this effect was saturated from 5 µM NO_2Tyr.

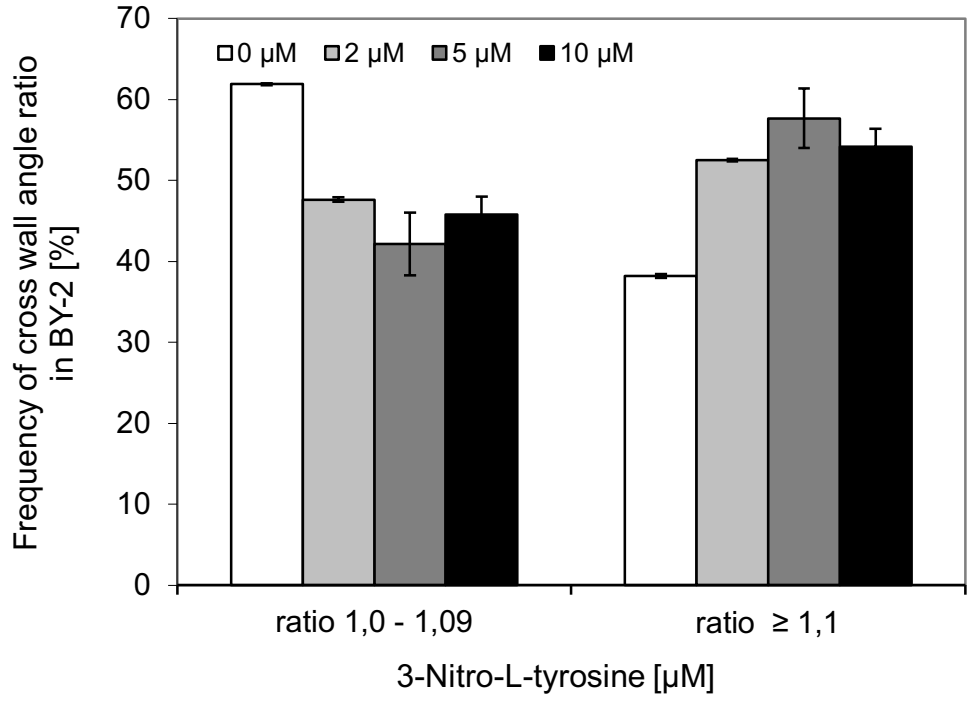

Figure 3.8: Physiological effects of 24 h treatment with NO_2Tyr on 4 d old BY-2 cells (3 d old plus 24 h treatment with NO_2Tyr). Frequency of correct (ratio 1,0 – 1,09) and incorrect (ratio≥1,1) cross walls (n=2 independent experiments with 150 cells each, error bar=SE).

3.1.4 NO_2Tyr increases the sensitivity to oryzalin

Oryzalin inhibits polymerisation of plant MTs by sequestering tubulin heterodimers from their integration into the polymer such that MTs are eliminated dependent on the extent of their particular turnover. To analyse the interaction between oryzalin and NO_2Tyr, dose-response curves over packed volume of BY-2 cells in the absence or in the presence of 0,1 µM NO_2Tyr (Figure 3.9) were performed. The excess inhibition caused by the combination of NO_2Tyr and oryzalin over the inhibition caused by oryzalin alone was not constant, but dependent on the concentration of oryzalin. At lower

concentrations of oryzalin, the effect of NO_2Tyr was more pronounced than at higher concentrations. A comparison of the two curves shows that in presence of NO_2Tyr the dose-response curve was shifted to lower concentrations of oryzalin demonstrating an increased sensitivity to oryzalin in the presence of NO_2Tyr.

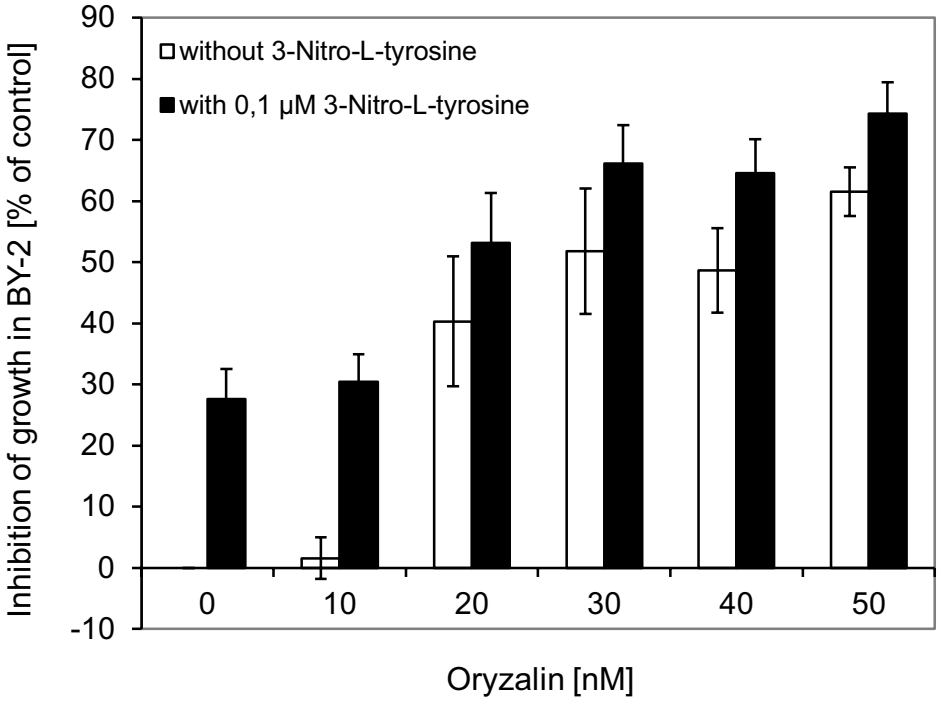

Figure 3.9: Inhibition of growth (given as % of packed volume of control) of BY-2 cell culture. White columns represent growth inhibition with oryzalin only (from 0 to 50 nM), black columns represent growth inhibition with additional 0,1 µM NO_2Tyr (n≥3, error bar=SE).

3.1.5 NO_2Tyr induces a decrease in the proportion of detyr-tub

To detect potential changes in the proportion of tyr-tub versus detyr-tub, the total soluble protein fraction of BY-2 cells was extracted and probed for signals of tyr-tub and detyr -tub after 24 h of treatment with 10 µM NO_2Tyr (Figure 3.10).

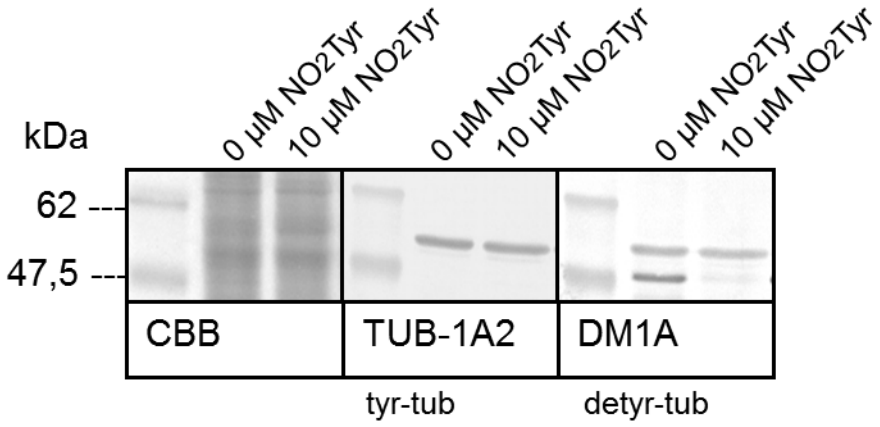

Figure 3.10: Distribution of tyr-tub and detyr-tub in samples derived from total soluble protein extract from 4 d old BY-2 cells, untreated or treated with 10 µM NO_2Tyr for 24 h. Left box represents SDS polyacrylamide gel stained with CBB, showing equal concentration of the applied proteins (left lane protein marker, middle lane untreated cells, right lane cells treated with 10 µM NO_2Tyr). The middle box shows interactions of the antibody TUB-1A2 with tyr-tub in the untreated and treated samples. The right box shows proteins of untreated and treated cells tested with the antibody DM1A against detyr-tub. The upper signal is a cross reaction of the antibody with tyr-tub, the lower signal (only abundant in the untreated sample) corresponds to detyr-tub.

Equal loading of protein samples was verified by staining a replicate gel with Coomassie Brilliant Blue (CBB, Figure 3.10). For detection of tyr-tub, one replicate was probed with the antibody TUB-1A2; for detection of detyr-tub, a second replicate was probed with the antibody DM1A (for detection and specificity see Wiesler et al., 2002). The signal for tyr-tub was the same in untreated as compared to treated samples (Figure 3.10, TUB-1A2). In contrast, the signal for detyr-tub (Figure 3.10, DM1A) differed between untreated and treated samples. The untreated cells displayed a double band, with the upper band corresponding to the band detected by the TUB-1A2 antibody, consistent with previous results (Wiesler et al., 2002). The lower band corresponds to detyr-tub that is characteristically shifted in apparent molecular weight (Wiesler et al., 2002). In samples treated with 10 µM NO_2Tyr, this lower band was hardly detectable, whereas the upper band remained. Thus, the abundance of tyr-tub is not significantly altered by NO_2Tyr, whereas the *bona-fide* signal for detyr-tub is eliminated consistent with an inhibition of tubulin detyrosination.

3.2 Suppression of the detyrosination signal by treatment with parthenolide

In another set of experiments in order to unravel the function of detyrosination, the detyrosination signal is suppressed by inhibition of TTC, the so far undiscovered enzyme which is responsible for detyrosination of α-tubulin. Inhibition of TTC can be accomplished by the sesquiterpene parthenolide.

The experiments in this chapter are a compendium of the results from diploma thesis of N. Schneider and H. Ludwig (Schneider, 2010; Ludwig, 2010) and are mentioned in this work because they complement the results.

3.2.1 Treatment with parthenolide makes the detyr-tub level decline

In order to test whether parthenolide has an effect on plant cells at all, 50 µM of the inhibitor was added to a 4 d old BY-2 cell culture and cultivated for another 24 h. A soluble protein extraction was carried out and proteins were separated by SDS-PAGE. Loading was checked with a CBB stained gel, and Western blot membranes were probed with the antibodies TUB-1A2 (tyr-tub) and DM1A (detyr-tub).

For evaluation of the signals which were produced by antibody reaction, the membranes were analysed as follows: Signals on Western blot membranes were plotted by ImageJ 1,42q; the results could be illustrated in a diagram (Figures 3.11A, B and 3.12A, B). To evaluate signal intensity, the area in square pixels under the accordant peak was calculated and illustrated in a bar diagram (Figures 3.11C and 3.12C).

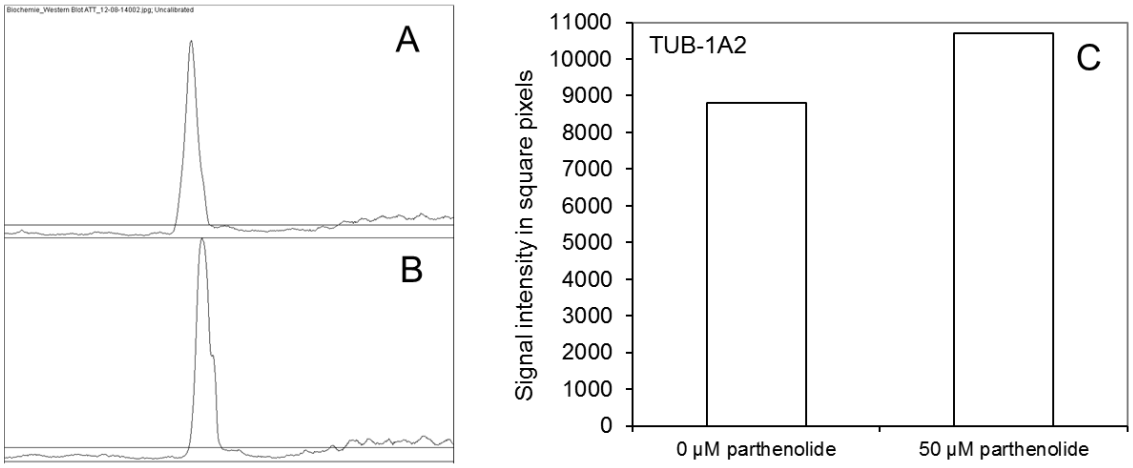

Figure 3.11: Evaluation of the signals for TUB-1A2 antibody (against tyr-tub) of untreated and treated BY-2 on Western blot membranes. **[A, B]** Signal intensity of the bands on Western blot membranes detected by TUB-1A2 (recognises tyr-tub). **[A]** BY-2 untreated. **[B]** BY-2 treated with 50 µM parthenolide. **[C]** Evaluation of the square pixels under the accordant peak (source: Schneider, 2010).

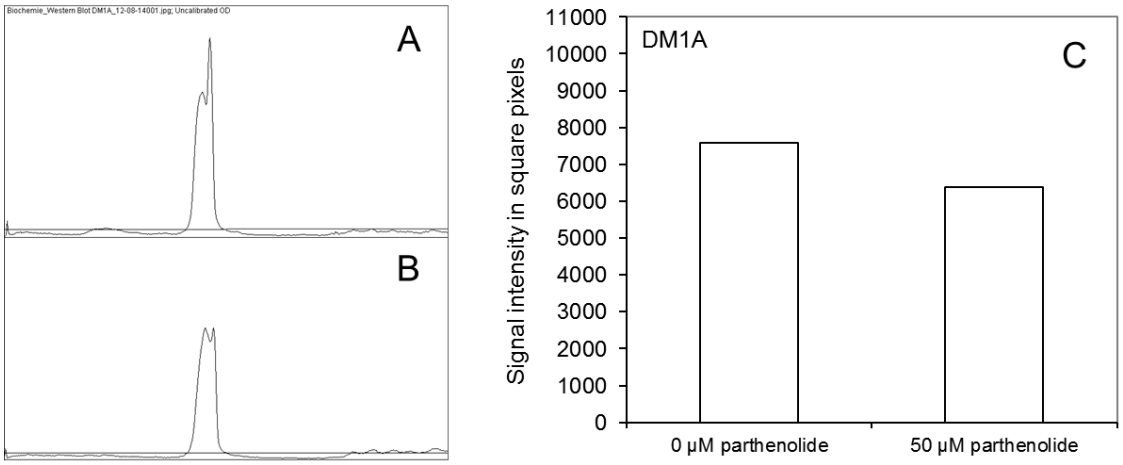

Figure 3.12: Evaluation of the signals for DM1A antibody (against detyr-tub) of untreated and treated BY-2 on Western blot membranes. **[A, B]** Signal intensity of the bands on Western blot membranes detected by TUB-1A2 (recognises tyr-tub). **[A]** BY-2 untreated. **[B]** BY-2 treated with 50 µM parthenolide. **[C]** Evaluation of the square pixels under the accordant peak (source: Schneider, 2010).

Evaluation of untreated samples of BY-2 WT show the natural distribution of tyr-tub and detyr-tub in a 5 d old BY-2 cell culture, in which the abundance of tyr-tub is a little higher than the one of detyr-tub (left columns in Figure 3.11C and 3.12C).

After treatment with parthenolide, the situation changes: the level of tyr-tub in BY-2 increases by ~20 %, whereas the level of detyr-tub decreases by ~15 %, leading to the conclusion that parthenolide has the expected influence on the

tubulin tyrosination cycle of α-tubulin in tobacco BY-2 cells: parthenolide makes the tyr-tub level rise and detyr-tub level decline.

3.2.2 Nuclear migration is affected by parthenolide

During preparation for oncoming mitosis, the nucleus migrates from the cell periphery towards the middle of the cell (for review see Nick, 2008). There the nucleus will induce generation of a preprophase band (PPB; Murata and Wada, 1991) and forecast the future division site; delay in nuclear migration causes delay in cell division. Premitotic nuclear migration was shown to be influenced by MT inhibitors (Katsuta et al., 1990) and by overexpression of a specific kinesin (OsKCH1, Frey et al., 2010); so the possible influence of manipulation of the tyr/detyr distribution (by parthenolide) was examined.

Nuclear positions were determined according to Frey et al. (2010): the ratio of the distance between the centre of the nucleus and the nearby cell wall, and the width of the cell was calculated. A small ratio (~0,1 – 0,2) stands for a nuclear positioning at the cell periphery, a bigger ratio (~0,4 – 0,5) for location in the cell middle. Cells were treated with 10 µM parthenolide at the time of subcultivation and evaluated after 1 d. The graph (Figure 3.13) shows that the whole curve of ratio distribution after treatment with parthenolide (grey columns) is switched towards the smaller ratio (when compared to untreated samples, white columns), meaning that treatment of tobacco BY-2 cells with parthenolide inhibits nuclear migration.

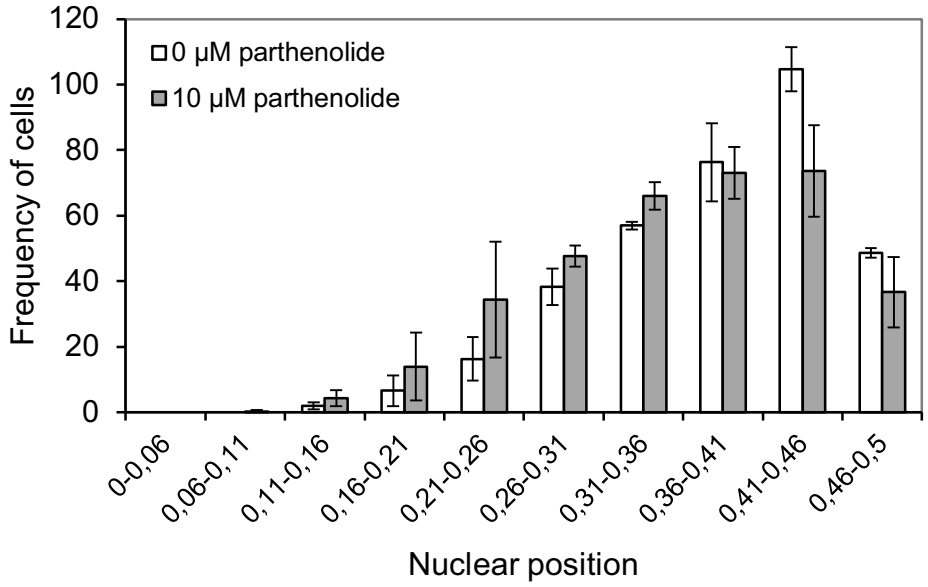

Figure 3.13: Frequency (in a total amount of 350 cells) of nuclear position in BY-2 cells. White columns represent 1 d old untreated BY-2 cells, grey columns represent BY-2 cells treated with 10 µM parthenolide (n=3 independent experiments with 350 cells each, error bar=SE, source: Schneider, 2010).

3.3 Suppression of the detyrosination signal by overexpression of TTL

In this chapter experiments are presented in which the detyrosination signal is shut down by overexpression of TTL, so the level of detyr-tub is kept low by immediate retyrosination by the ligase.

Experiments were accomplished with a BY-2 cell line overexpressing a TTL-RFP fusion construct (by *Agrobacterium* mediated stable transformation); or a TTL-GFP fusion construct (transiently transformed by particle bombardment). In both cases the fluorescent protein is fused to the N-terminus of TTL.

Parts of the results presented in this chapter are the results from diploma thesis of N. Schneider, H. Ludwig and S. Durst (Schneider, 2010; Ludwig, 2010; Durst 2009) and labelled accordingly.

3.3.1 TTL-RFP and TTL-GFP signals in BY-2 cells are ambiguous

In the majority of cases, microscopic analysis of transient and stable transformation of TTL in fusion with GFP and RFP, the observed signals did not convince of a colocalisation with MTs, but rather resembled a diffuse cytoplasmic signal. Figure 3.14A shows transiently transformed BY-2 with TTL in fusion with GFP. The perinuclear region is surrounded by a GFP signal, as well as cytoplasmic strands. The same is true for stable transformation of TTL in fusion with RFP (Figure 3.14B). This cytoplasmic fluorescent signal either stands for unspecific localisation of TTL due to overexpression, or for a specific signal when TTL-GFP and TTL-RFP associate or colocalise with α/β-tubulin heterodimers, which are located in the cytoplasm of a cell, due to their solubility.

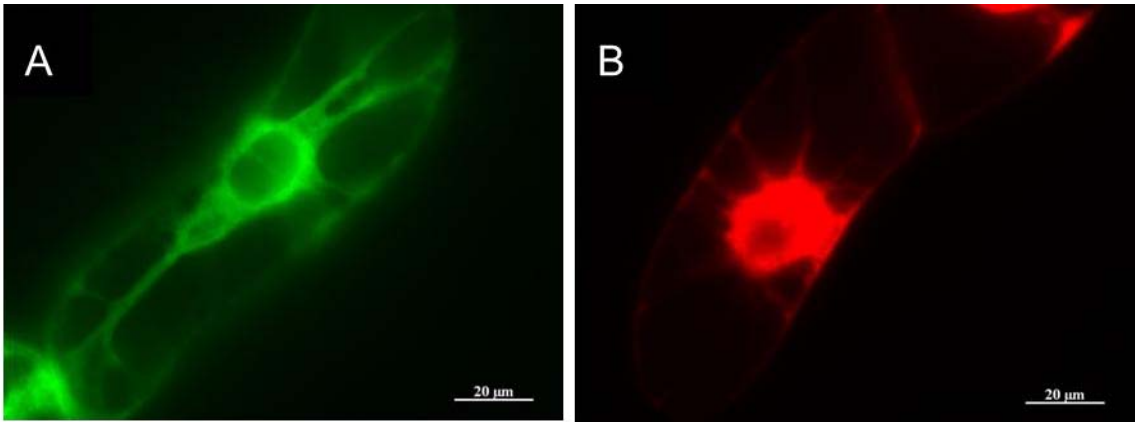

Figure 3.14: Localisation of TTL in transformed BY-2 cell culture. **[A]** Localisation of TTL-GFP in transiently transformed 5 d old BY-2. Area around the nucleus and cytoplasmic strands are labelled with a green signal. **[B]** Localisation of TTL-RFP in stably transformed 3 d old BY-2. Area around the nucleus and cytoplasmic strands are labelled with a red signal (scale bar=20 µm; source: Ludwig, 2010).

Immunostaining of MTs in stably transformed TTL-RFP showed unspecific or not evaluable signals in most experiments, due to the difficulty to achieve both a clear and analysable RFP signal of TTL, and a FITC signal for MTs. However, in some rare cases this challenge could be coped with and showed clear colocalisation of TTL-RFP with interphase cortical MTs (Figure 3.15A), and all mitotic microtubular structures (as an example see PPB Figure 3.15B).

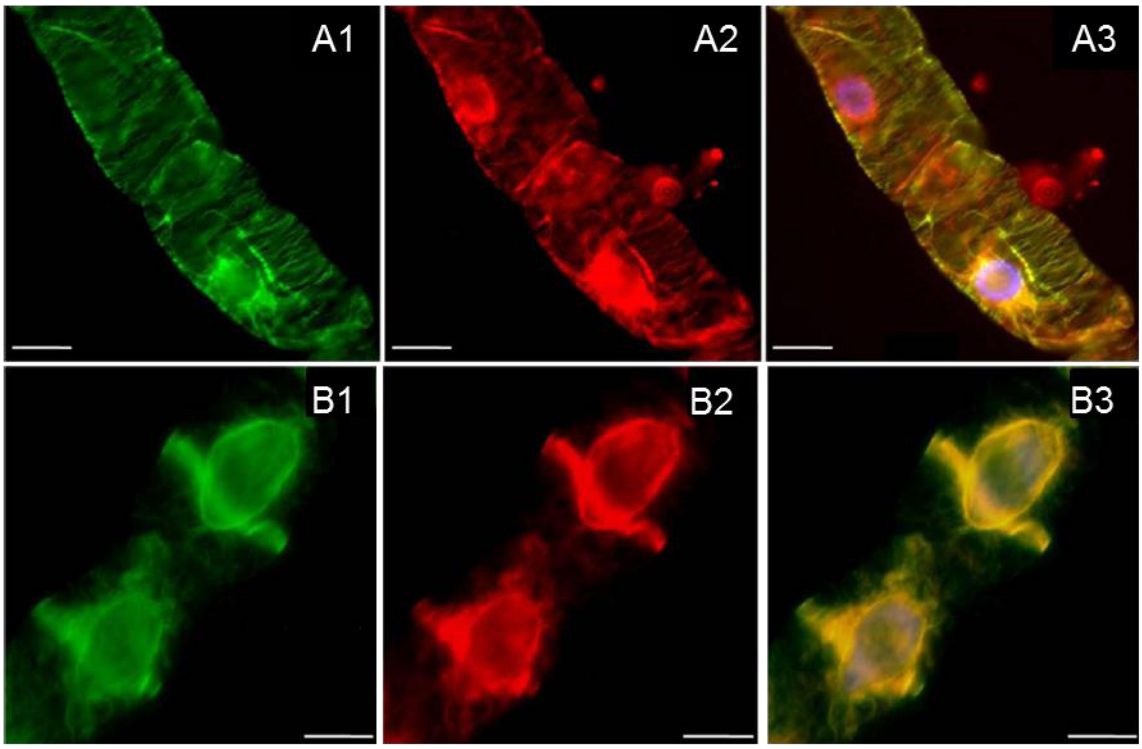

Figure 3.15: Stable expression of TTL-RFP in BY-2 cells, MTs labelled with FITC by immunostaining. **[A]** Elongating interphase cells with a parallel array of cMTs colocalising with TTL-RFP. **[B]** Cells with a PPB, preparing for oncoming mitosis, showing colocalisation of MTs and PPB. **(1)** Green FITC signal, MT staining conducted by immunofluorescence. **(2)** Red signal from stable expression of TTL in fusion with RFP. **(3)** Merge, yellow signal where red and green signals overlay by colocalisation of proteins, blue signal for chromosomes labelled by Hoechst 33258 (scale bar=20 µm; source: Durst, 2009).

3.3.2 Treatment of TTL-RFP with NO_2Tyr presents unexpected results

A proof for interference of NO_2Tyr in the tubulin tyrosination cycle can be given by biochemical analysis of the distribution of tyr-tub and detyr-tub in a protein sample. For this purpose, soluble protein extracts from treated and untreated BY-2 and TTL-RFP were produced and probed with the antibodies TUB-1A2 (against tyr-tub) and DM1A (against detyr-tub; Figure 3.16).

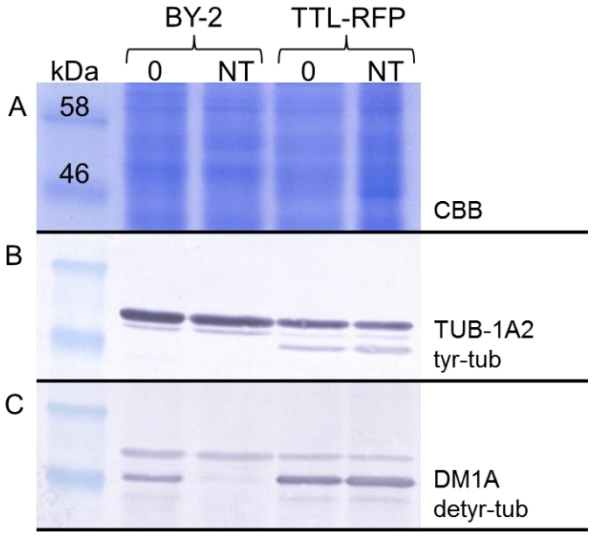

Figure 3.16: Biochemical analysis of BY-2 and TTL-RFP cell lines, untreated or treated with NO_2Tyr (NT). 1st lane: molecular weight marker. 2nd lane: 4 d old BY-2 cells, untreated (control). 3rd lane: 4d old BY-2 cells, treated with 10 µM NO_2Tyr for 24 h. 4th lane: 4 d old TTL-RFP cells, untreated (control). 5th lane: 4d old TTL-RFP cells, treated with 10 µM NO_2Tyr for 24 h. **[A]** CBB gel as a loading control. **[B]** Western blot membrane probed with antibody TUB-1A2 against tyr-tub. **[C]** Western blot membrane probed with antibody DM1A against detyr-tub.

Equal loading of protein samples was verified by staining a replicate gel with CBB (Figure 3.16A). Detection of tyr-tub was performed with the antibody TUB-1A2; detection of detyr-tub with the antibody DM1A.

For untransformed BY-2 cells, the signal for tyr-tub was about the same in both untreated and treated samples (Figure 3.16B), whereas detyr-tub abundance (Figure 3.16C) was almost eliminated, due to inhibition of tubulin detyrosination (see also chapter 3.1.6).

In TTL-RFP, membranes probed with the antibody TUB-1A2 showed no influence of NO_2Tyr on the concentration of tyr-tub (Figure 3.16B), whereas it can be observed that signal intensity for tyr-tub is generally lower in TTL-RFP than in BY-2 (Figure 3.16B). Concerning abundance of detyr-tub, membranes probed with DM1A demonstrated unexpected results: although usage of NO_2Tyr is supposed to create irreversibly tyrosinated α-tubulin and TTL is overexpressed, the abundance of detyr-tub after treatment with NO_2Tyr is apparently unchanged (Figure 3.16C).

3.3.3 Parthenolide enhances detyr-tub abundance in TTL-RFP

To test the influence of the TTC inhibitor parthenolide on TTL-RFP (in comparison to BY-2), the experiment presented in chapter 3.2.1 was arranged with the overexpression cell culture, too: 4 d old cell cultures of BY-2 and TTL-RFP were incubated with 50 µM parthenolide and cultivated for another 24 h. A soluble protein extraction was carried out and proteins were probed with the antibodies TUB-1A2 (tyr-tub) and DM1A (detyr-tub). The signals were evaluated as the area (in square pixels) under the accordant peak (curve chart not shown).

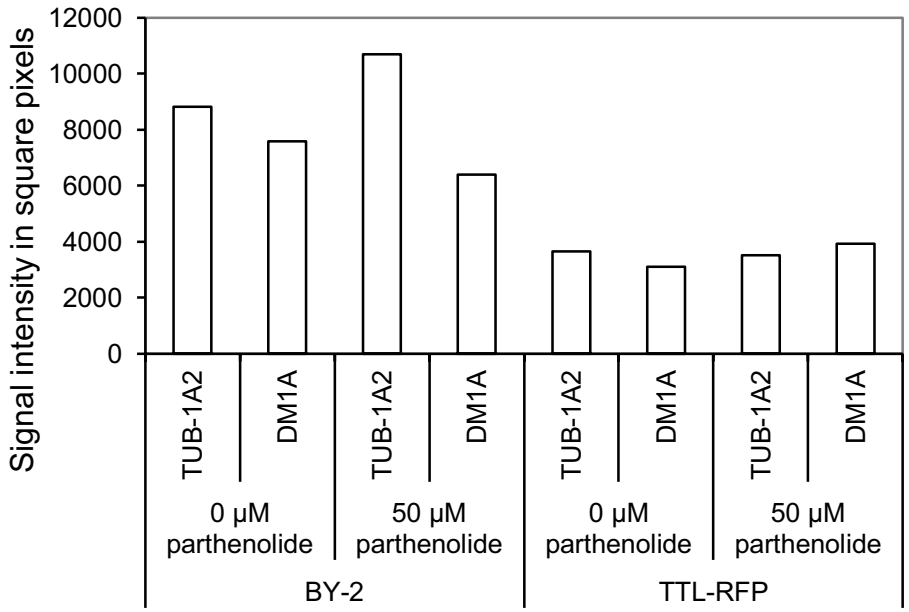

Figure 3.17: Evaluation of the signals for TUB-1A2 and DM1A antibodies of untreated and treated BY-2 and TTL-RFP cells on Western blot membranes. BY-2 cell culture demonstrates increase of TUB-1A2 signal and decrease of DM1A signal after treatment with the TTC inhibitor parthenolide Treatment with parthenolide has almost no effect on signal intensity of the band detected by TUB-1A2, whereas DM1A signal even rises mildly (source: Schneider, 2010).

Comparison of signal evaluation in BY-2 and TTL-RFP is given in Figure 3.17. In contrast to BY-2, where incubation with 50 µM of the TTC inhibitor parthenolide induces an (expected) increase in tyr-tub and decrease in detyr-tub, the presumed ligase TTL doesn't change the abundance of tyr-tub, and detyr-tub concentration even rises. Also remarkable is that the tubulin level itself is much lower in the overexpression lines when compared to the untransformed wild type of BY-2, most noticeable in the case of tyr-tub. As a

final conclusion for biochemical analysis it can be said that parthenolide, a TTC inhibitor induces rising of the detyr-tub level in the overexpression line.

3.3.4 Changes in extracellular pH as a reaction to parthenolide

Measurements of pH changes were arranged as described in Qiao et al. (2010), with some modifications. Cells were preincubated for 120 min until pH stabilisation, then parthenolide was added to the accordant concentration (10 µM) and the pH value was recorded for another 60 min.

MTs are involved in control of ion channels, two models exist to explain ion channel opening: a susceptor model and a perceptor model (Nick, 2008). The difference is that in the first model cMTs sense mechanical stress and initiate opening of an ion channel, whereas in the second model MTs keep the ion channel closed until they are degraded due to mechanical stress, and the channel opens as a consequence of this degradation.

In Figure 3.18, treatment of 3 d old tobacco BY-2 cells and TTL-RFP with parthenolide is shown.

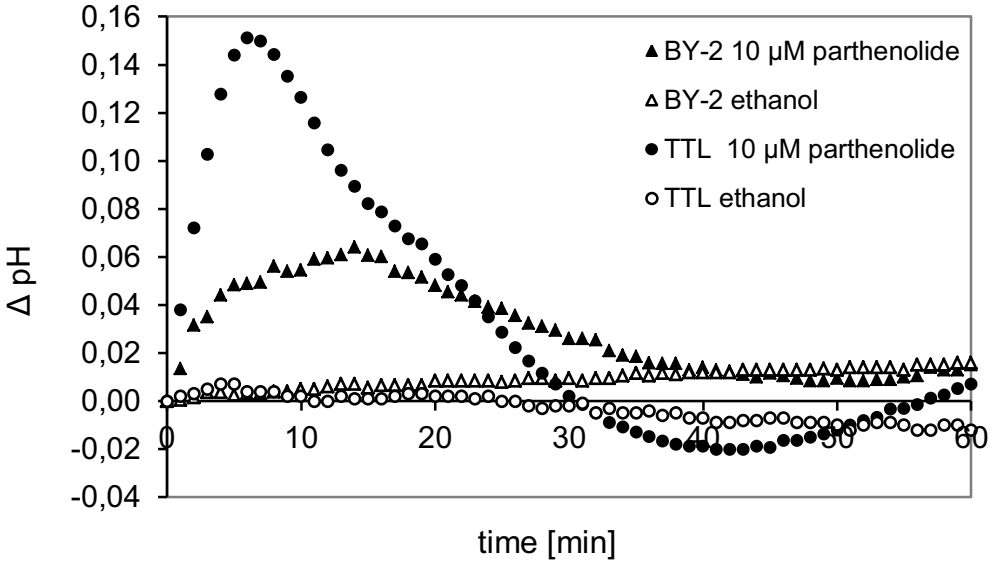

Figure 3.18: Diagram of pH changes over time (60 min) in 3 d old control and treated cell cultures. BY-2 cells treated with 10 µM parthenolide (black triangles) and control BY-2 cells treated with the same amount of the solvent ethanol (white triangles). TTL-RFP cell culture treated with 10 µM parthenolide (black circles) and control TTL-RFP cells treated with the same amount of the solvent ethanol (white circles; n=2; source: Ludwig, 2010).

When BY-2 cell culture is treated with 10 µM parthenolide, the extracellular pH is increased by 0,6 within 15 min, where it reaches a maximum. Adaptation to the original pH does not happen just yet, although it reaches a point after another 25 min where the pH does not change dramatically.

The reaction of TTL-RFP to treatment with the TTC inhibitor is more excessive. The pH change towards alkalinisation after parthenolide addition is more than double when compared to BY-2 and it reaches its maximum two times faster. Also recreation of the original pH happens faster, it even overshoots that level.

To summarise: In matters of extracellular changes of pH, TTL-RFP was more sensitive to treatment with parthenolide than BY-2. Addition of ethanol, the solvent of parthenolide, did not show a comparable reaction.

3.4 Identification and examination of a possible acceptor of the detyrosination signal

The next step in unravelling the function of detyrosination is the identification of a possible acceptor of this signal. For this purpose, microtubule associated proteins (MAPs) were isolated by three methods which will be described in more detail in the following.

The results in this chapter are the achievement of a cooperation with Jana Kobrlová and Kateřina Schwarzerová from the Department of Plant Physiology, Faculty of Science at Charles University in Prague, Czech Republic.

3.4.1 Hsp90 is co-purified with tubulin from cMTs

Cortical MTs (cMTs) are the dominating array in interphasic plant cells and differ fundamentally from mitotic MT arrays with respect to morphology and organisation. To get insight into these molecular differences, we ventured to isolate MT binding proteins from cMTs. To ensure that the cMT preparations were not contaminated by mitotic arrays, three approaches were used. Firstly, cytoskeletal extracts from rice coleoptiles that are void of dividing cells were

generated, such that MTs are exclusively organised in cortical interphasic arrays. From these extracts MAPs were purified either by affinity to the tubulin binding herbicide EPC (Figure 3.19A; Wiesler et al., 2002), or, secondly by taxol-induced MT coassembly (Figure 3.19B; Vantard et al., 1991). Thirdly, cMTs were separated from mitotic arrays in cycling tobacco BY-2 cells by preparation of membrane ghosts (Figure 3.19C; Sonobe and Takahashi, 1994).

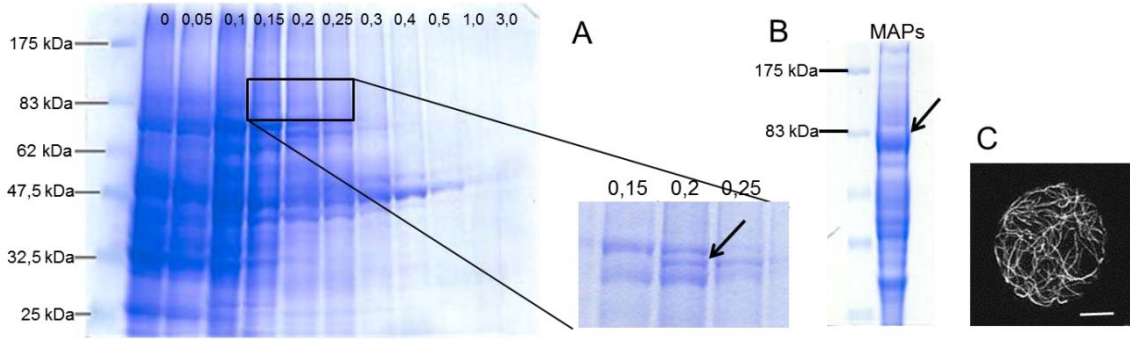

Figure 3.19: Methods of Hsp90 isolation as an interactor of cMTs. **[A]** EPC affinity chromatography with soluble extracts from rice coleoptiles with cMTs only. Proteins were separated by SDS-PAGE and stained by CBB. Arrow in inset shows protein band which was analysed by MALDI-TOF and identified as Hsp90. **[B]** Taxol induced coassembly from rice coleoptiles, protein separation and analysis as described above. Arrow shows protein band which was analysed by MALDI-TOF and again identified as Hsp90. **[C]** MT cosedimentation with proteins solubilised from tobacco BY-2 membrane ghosts. Image shows immunofluorescence visualisation of cMTs on a membrane ghost, scale bar=20 µm.

The proteins solubilised by the non-ionic detergent CHAPS (3-[(3-cholamidopropyl)dimethylammonio]-2-hydroxy-1-propanesulfonate) from these membrane ghosts were then cosedimented with prestabilised neural MTs (Vantard et al., 1994). The proteins copurified with cMTs through these three approaches were separated by SDS-PAGE and identified by MALDI-TOF.

To identify interesting candidates from non-cycling rice cells, proteins identified with the taxol-coassembly approach were compared to proteins identified by the EPC affinity chromatography approach. The proteins detached from taxol-induced MTs included α-tubulin (Swiss-Prot accession Q43605), β-tubulins (Swiss-Prot accessions Q43594, P46265), components of the tubulin folding CCT-chaperone complex (Swiss-Prot accessions Q75HJ3, Q6AV23), Hsp70 chaperonins (Swiss-Prot accessions Q40693, Q84TA1, Q5KQJ9, Q2QZ41), the MT plus-end annealing initiation factor 4A (Swiss-Prot accession Q54AC9), phospholipase D (Swiss-Prot accession Q43007), but also several enzymes

such as sucrose-UDP glucosyltransferase (Swiss-Prot accession Q7G7N0), a putative phenylalanine ammonia lyase (Swiss-Prot accession Q6K1Q8), lipoxygenase L-2 (Swiss-Prot accession P29250), a sucrose synthase (Swiss-Prot accession P31924), and Hsp90 family member Hsp81-1 (Swiss-Prot accession A2YWQ1). From those proteins, sucrose-UDP glucosyltransferase, sucrose synthase, MT-membrane anchor phospholipase D, and Hsp81-1 (subsequently termed as OsHsp90_MT) could be relocated in the tubulin binding fractions from the EPC affinity experiment.

To identify interesting protein candidates from cycling tobacco BY-2 cells, the protein set interacting with both plasma membrane and MTs was compared to the total protein set solubilised from membrane ghosts (Figure 3.19C). Among MT-specific proteins were enzymes such as methionine synthase, but also translation factor EF2, and the *N. tabacum* homologue of *N. benthamiana* Hsp90 (subsequently termed as NtHsp90_MT, Swiss-Prot accession Q14TB1). Thus, three independent approaches searching for proteins associated with cMTs, yielded a member of the Hsp90 family in both the monocot rice and in the dicot tobacco. We therefore focussed on the functional characterisation of these MT-binding Hsp90 proteins.

3.4.2 Microtubule binding Hsp90 harbours a specific KE-rich repeat

Both MT-binding Hsp90 proteins from tobacco and rice harbour the characteristic features of cytoplasmic Hsp90 (Figure 3.20A, Krishna and Gloor, 2001). This includes the highly conserved N-terminal ATP-binding pocket that is important for activation of client proteins (Grenert et al., 1999; Pearl and Prodromou, 2000) and is also a target of the inhibitors geldanamycin (GDA) and radicicol (Prodromou et al., 1997; Stebbins et al., 1997; Sharma et al., 1998; Neckers et al., 1999; Pearl and Prodromou, 2000).

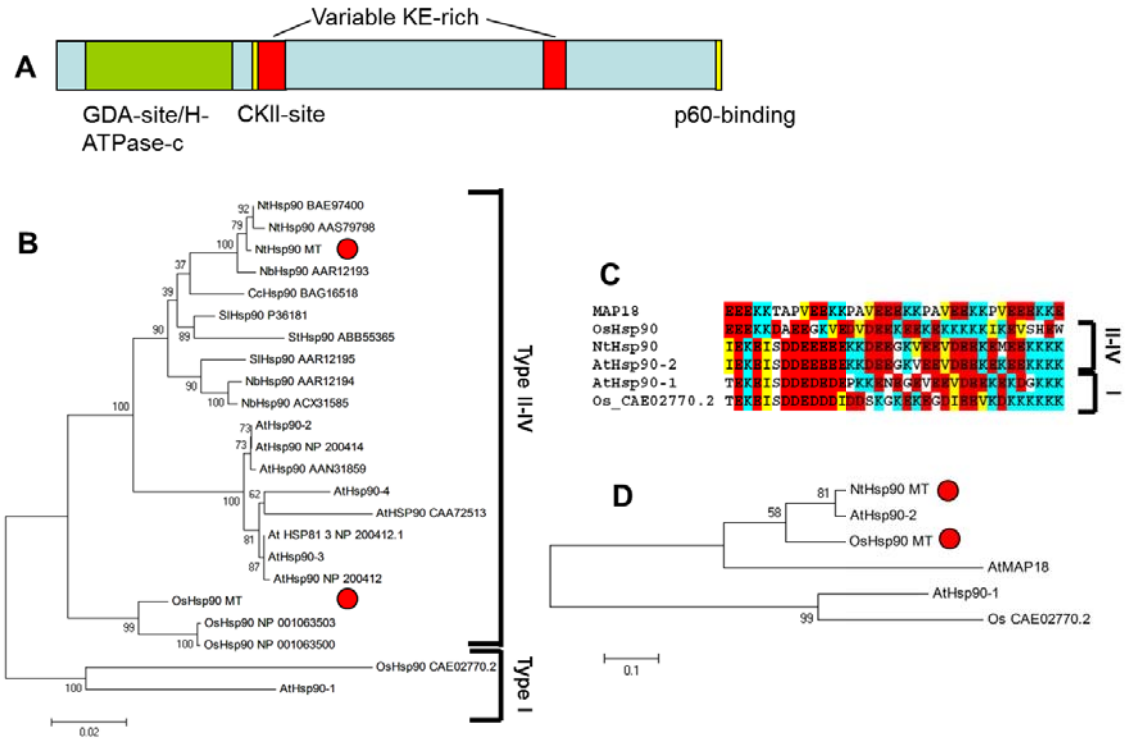

Figure 3.20: Graphical presentation of Hsp90 characteristics. **[A]** Hsp90 domains: N-terminal ATP-binding pocket and GDA binding site (green), CKII (casein-kinase II binding motif KEISDDE, yellow), lysine and glutamic acid rich repeats (KE rich repeats, red), C-terminal binding motif for binding of co-chaperones, e.g. p60 (yellow). **[B]** Phylogeny tree based upon neighbour-joining algorithm, red dots indicate NtHsp90 and OsHsp90, both cluster with type II-IV cytoplasmic Hsp90 proteins. **[C]** KE rich repeats of MAP18; OsHsp90, NtHsp90, and AtHsp90-2 (type II-IV Hsp90); AtHsp90-1 and OsHsp90_CAE02770.2 (type I Hsp90). **[D]** OsHsp90 and NtHsp90 (indicated by red dots) have higher similarity to AtMAP18 than with type I Hsp90.

Further, the cytosolic Hsp90 proteins contain the conserved putative casein-kinase II binding motif KEISDDE, and the C-terminal MEEVD motif mediating the binding of co-chaperones such as p60 (Krishna and Gloor, 2001; Meyer et al., 2003), immunophilins (Young et al., 2001), and the ten conserved sequence blocks diagnostic for cytosolic Hsp90 species (Krishna and Gloor, 2001). Hsp90 are generally highly conserved, and alignments of the two MT-binding Hsp90 proteins with other cytosolic Hsp90 from *Solanaceae*, *Arabidopsis thaliana*, *Vitis vinifera* and rice revealed about 90 % identity (data not shown). When a phylogeny is constructed over these sequences based on a neighbour-joining algorithm (Figure 3.20B), the two MT-binding Hsp90 accessions cluster with type II-IV cytoplasmic Hsp90 proteins following the classification of Krishna and Gloor (2001), and not with the slightly divergent Hsp90 of type I. Differences between these Hsp90 proteins are mainly located in two variable stretches that

are rich in glutamic acid residues (Figure 3.20A), and are thought to mediate rapid interactions with client proteins (Cadepond et al., 1994; Smith, 1993). Both regions contain a charge signature, where positive (lysine, K) and negative (glutamic acid, E) charges follow in several repeats as shown exemplarily for the first region (Figure 3.20C). Similar KE containing repeats have been found to mediate MT-binding in the neural MAP1B, and have been conducted to mediate the binding of tubulin in the plant MAP AtMAP18 (Wang et al., 2007) or adenomatous polyposis coli (APC, a tumor suppressor; Deka et al., 1998; Moseley et al., 2007). In these two KE-rich regions, both MT-binding Hsp90 proteins share around 40 % identity with AtMAP18 (data not shown) and their similarity with AtMAP18 is higher than with type I Hsp90 proteins (Figure 3.20D).

3.4.3 Purified Hsp90 binds directly to polymerised tubulin *in vitro*

To test whether NtHsp90_MT can bind to MTs *per se*, the protein was recombinantly expressed as a fusion with a His-tag in *E. coli* (strain BL21(DE3).RIL, using the pET28 vector). His-tag fusion protein was purified on a Ni-NTA resin column and subsequently analysed *in vitro* for binding to MTs. After incubation with polymerised, taxol stabilised bovine neurotubulin supplemented with bovine serum albumine (BSA) as a negative control of MT-binding activity, proteins were cosedimented through a sucrose cushion. The MT precipitate (P), the sucrose cushion (C), and the supernatant (S) containing soluble α/β-tubulin heterodimers and unbound NtHsp90_MT were separated by SDS-PAGE and visualised by CBB (Figure 3.21).

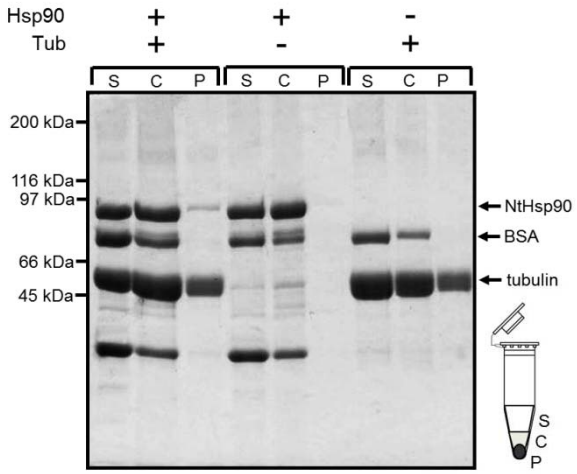

Figure 3.21: Cosedimentation assay of Hsp90 and MTs. Three experimental settings presented: one in the presence of both Hsp90 and MTs (3 lanes on the left), one in the presence of Hsp90 and absence of MTs (3 middle lanes), one in the absence of Hsp90 and presence of MTs (3 lanes on the right). S=supernatant, C=sucrose cushion, P=precipitate, image source: J. Kobrlová.

NtHsp90_MT was precipitated in the presence, but not in the absence of MTs. In contrast, BSA was exclusively found in the soluble fractions (C and S), whether MTs were present or not. These data suggest that NtHsp90_MT cosediments with MTs. A band with 30 kDa apparent molecular weight was observed in those samples, where Hsp90_MT was abundant, and was absent in the lanes without Hsp90_MT indicating that this band originates from cleavage of the degraded recombinant product. As ATP binds to Hsp90 and regulates binding of its client proteins (Pearl and Prodromou, 2000), we wondered, whether similar behaviour could be observed for tobacco Hsp90_MT. To test, whether ATP promotes the MT-binding activity of NtHsp90_MT binding activity, a cosedimentation assay was performed with addition of ATP. However, the presence of ATP had no effect on the MT-binding activity of Hsp90_MT (data not shown).

3.4.4 Hsp90_MT colocalises with MTs *in vivo*

To test binding of Hsp90_MT to MTs *in vivo*, BY-2 cell lines stably overexpressing fusions between GFP and NtHsp90_MT or OsHsp90_MT were established. Localisation of the GFP-tagged Hsp90_MT through the cell cycle was investigated by confocal laser scanning microscopy (CLSM). Structures

resembling the typical microtubular arrays during the respective phase of cell cycle could be observed, for instance, the Hsp90_MT signal was observed in an equatorial band in cells preparing for mitosis (Figure 3.22A), reminding of a PPB. In metaphase cells, the Hsp90_MT signal was found in a spindle-like pattern (Figure 3.22B), and in telophase cells a double-ring emerged that resembled a phragmoplast (Figure 3.22C). The localisation of the GFP fusions of NtHsp90_MT (Figure 3.22) and OsHsp90_MT (data not shown) were indistinguishable. As negative control a tobacco BY-2 cell line stably expressing free GFP (Figure 3.22D - F) was used. In premitotic cells, free GFP localised to the cytoplasm and to the interior of the nucleus (Figure 3.22D), which was in clear contrast to the equatorial band found for GFP-Hsp90_MT (Figure 3.22A). The difference was less evident for metaphase cells (compare Figures 3.22B and 3.22E), which might be linked to the fact that the cytoplasm during that stage agglomerates around the spindle. However, during telophase, localisation of GFP-Hsp90_MT versus free GFP was clearly different. Here, free GFP covered the whole cell centre (Figure 3.22F), whereas GFP-Hsp90_MT revealed a characteristic interdigitated structure and was confined to a narrower zone along the subsequent cell plate (Figure 3.22C).

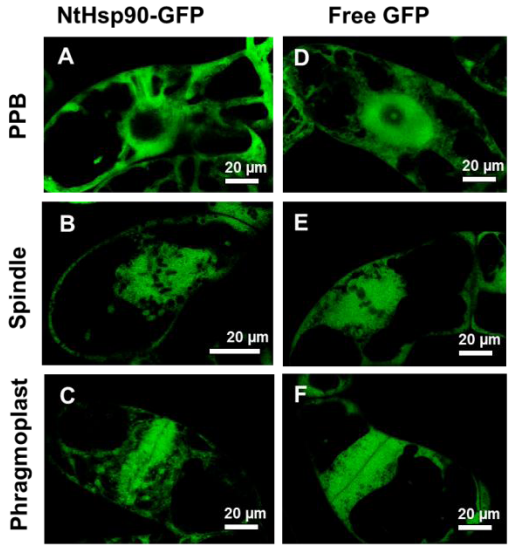

Figure 3.22: Localisation studies of the GFP-signal in NtHsp90_MT (A, B, C), and free GFP as a control (D, E, F). **[A]** Equatorial band of GFP, resembling a PPB-like structure. **[B]** Cell in metaphase with the GFP-signal in a spindle-like structure. **[C]** Telophase cell with GFP signal in a structure resembling a phragmoplast. **[D, E, F]** Free GFP cell line as a control for NtHsp90_MT, in the corresponding stages. Image source (NtHsp90_MT and free GFP) J. Kobrlová, scale bar=20 µm.

To test the presumed localisation of Hsp90_MT to MTs in PPB, spindle and phragmoplast, MTs were immunostained in both GFP-Hsp90_MT overexpressing lines. Hsp90_MT was found to colocalise with MTs in phragmoplast very clearly (Figure 3.23C). In PPB and spindle the colocalisation was less prominent, however, Hsp90_MT clearly accumulated in these structures (Figures 3.23A, B, respectively). In contrast, free GFP neither localised with the PPB (Figure 3.23D), nor with spindle (Figure 3.23E) or phragmoplast (Figure 3.23F). Again, no difference could be detected between NtHsp90_MT and OsHsp90_MT.

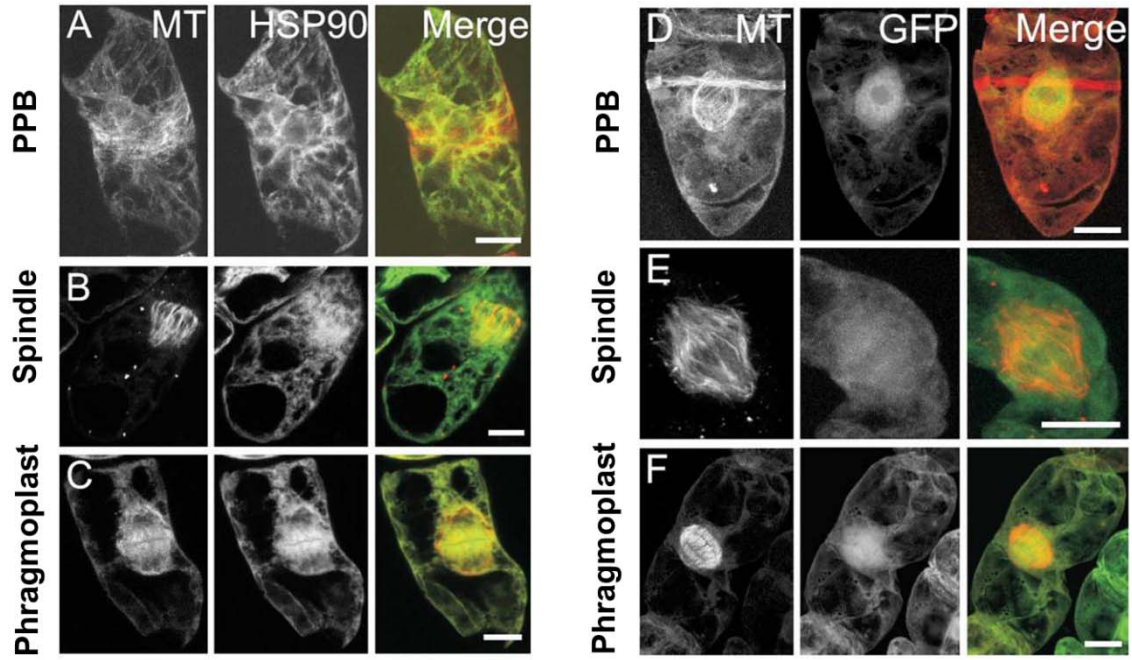

Figure 3.23: Colocalisation studies of MTs (labelled with TRITC by immunofluorescence) and GFP-Hsp90_MT (A, B, C) or free GFP (D, E, F). Left column shows signal for MTs, middle column GFP signal for Hsp90_MT, right column merge of both channels, yellow colour indicates colocalisation. **[A, D]** Cells with a PPB, GFP-Hsp90_MT colocalises with the equatorial band of MTs, whereas in free GFP no colocalisation can be observed. **[B, E]** Metaphase cells; GFP-Hsp90_MT colocalising with TRITC stained MTs, no colocalisation with free GFP. **[C, F]** Cells in telophase, GFP signal from Hsp90_MT colocalising with phragmoplast stained by TRITC, no colocalisation observable for free GFP. Image source (NtHsp90_MT and free GFP) J. Kobrlová, scale bar=20 µm.

From these results it can be concluded that Hsp90_MT is associated with microtubular structures during cell division, most prominently with the phragmoplast.

3.4.5 Geldanamycin affects events requiring MT plasticity

To probe for potential cellular functions of MT-binding Hsp90, the phenotype of GFP-NtHsp90_MT and GFP-OsHsp90_MT overexpressors was carefully analysed. Viability, rates of cell division and cell elongation, division synchrony (Maisch and Nick, 2007) were not significantly different from non-transformed BY-2 cells or from cells overexpressing free GFP (data not shown). The only traceable difference was a mildly increased resistance to antimicrotubular drugs such as oryzalin and EPC (data not shown), indicating a slightly decreased turnover of MTs. But this effect was at the verge of insignificance. Since the phenotype of Hsp90_MT overexpression did not give much insight, Hsp90 function was pharmacologically inhibited by geldanamycin (GDA). GDA binds to the ATP-binding pocket, thus preventing Hsp90 from performing its activity (Prodromou et al. 1997; Stebbins et al., 1997; Pearl and Prodromou, 2000). The response of viability was followed in the two GFP-Hsp90_MT lines, using the line overexpressing free GFP and a non-transformed BY-2 (wild type, WT) as controls. Neither for a concentration of 0,178 µM GDA nor for a tenfold higher concentration of 1,78 µM GDA, any decrease in viability over a period of two days could be observed (data not shown), indicating that these concentrations within the effect-causing range (Queitsch et al., 2002) do not cause unspecific toxicity. This treatment did cause a cellular response, though. Cytoplasmic strands were disrupted (Figure 3.24L), resembling the effect observed for treatment with latrunculin B (Van Gestel et al., 2002). Moreover, mitotic activity was inhibited (data not shown).

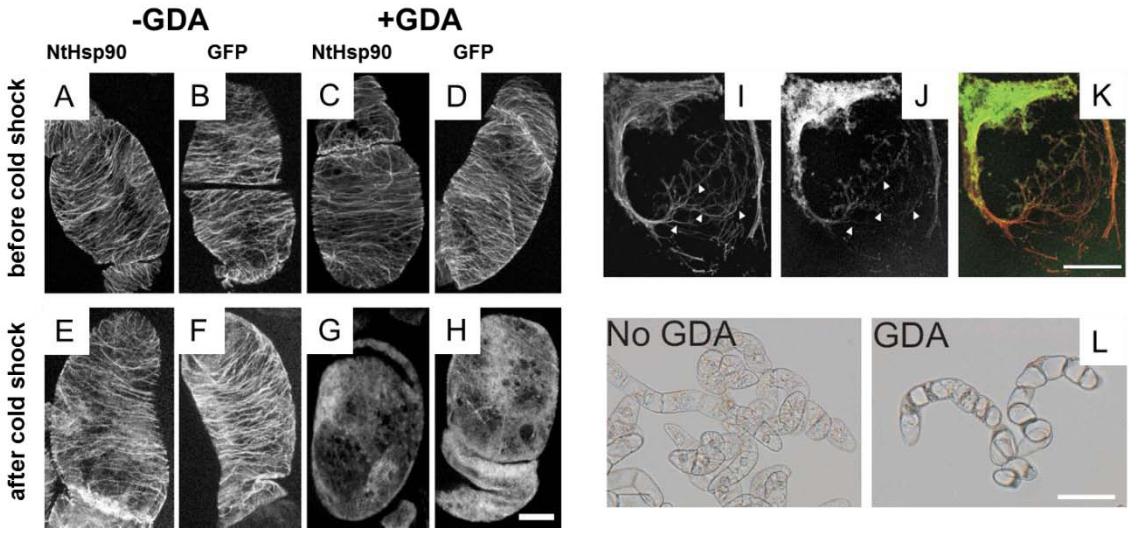

Figure 3.24: [A – H] Effect of 1,78 µM GDA on MT recovery from elimination by cold shock in GFP-NtHsp90_MT, using free GFP as a control. **[A, B]** cMTs in untreated cells of GFP-NtHsp90_MT and free GFP. **[C, D]** cMTs in GDA-treated cells of GFP-NtHsp90_MT and free GFP. **[E, F]** Successful repolymerisation of cMTs after cold shock in untreated cells of GFP-NtHsp90_MT and free GFP. **[G, H]** Impaired repolymerisation of cMTs after cold shock in GDA-treated cells of GFP-NtHsp90_MT and free GFP. **[I – K]** Membrane ghost from GFP-Hsp90_MT with cMTs visualised by immunostaining. **[I]** cMTs visualised by immunostaining **[J]** GFP signal from the overexpressor GFP-Hsp90_MT **[K]** Merge of both channels. **[L]** Differential interference contrast image of untreated (left) and GDA-treated (right) BY-2 cell files. Scale bar=20 µm (A – K), scale bar=100 µm (L), image source: J. Kobrlová.

The higher concentration of GDA (1,78 µM) blocked mitosis already within the first 12 hours of treatment, whereas with the lower concentration (0,178 µM) inhibition was only intermediate and required more time to develop. For this non-saturating concentration, an interesting difference between BY-2 WT and the GFP-Hsp90_MT overexpressor was observed. While GFP-Hsp90_MT was initially more severely inhibited as compared to WT, it could recover mitotic activity from 12 hours after addition of the inhibitor and eventually was able to sustain mitotic activity to a final level that was only slightly reduced when compared to untreated controls at that time point. In other words: the GFP-Hsp90_MT overexpressor, but not the non-transformed BY-2 WT was able to adapt to low concentrations of GDA.

Mitotic indices are linked to the plasticity of microtubular division arrays such as PPB, spindle, and phragmoplast. To probe for MT plasticity in the interphasic cortical array, the influence of GDA on the recovery of cMTs after cold shock was investigated. Cold treatment efficiently eliminates cMTs, which are then dissociated in the nucleus (Schwarzerová et al., 2006). Upon rewarming, a new

cortical array is reorganised from this sequestered tubulin pool within minutes. If Hsp90 is required for microtubular plasticity, inhibition of Hsp90 activity by GDA is expected to become manifest during this microtubular recovery from cold shock.

This experiment is only meaningful when Hsp90_MT is actually localised with cMTs. This was tested by isolating membrane ghosts from GFP-Hsp90_MT overexpressor lines and subsequently visualised cMTs by immunofluorescence. As the inner content of the cell is washed out, the background of cytoplasmic GFP-Hsp90_MT is reduced such that observation of the cortical layer becomes easier. In fact, the GFP signal reporting Hsp90_MT (Figure 3.24J) was observed decorating cMTs (Figure 3.24I). A merge of the two channels (Figure 3.24K) confirms that this association is very tight. Thus, Hsp90_MT binds to cMTs, too.

After this precondition of a potential function of Hsp90_MT for the plasticity of cMTs was demonstrated, the effect of 1,78 µM GDA on microtubular recovery from cold-induced elimination in GFP-NtHsp90_MT was tested, using free GFP as a control (Figure 3.24A - H). In a first control it was checked, whether the GDA treatment affected cMTs *per se*. No difference between untreated (Figure 3.24A, B) versus GDA-treated cells (Figure 3.24C, D) could be observed, when the cells were incubated at the permissive temperature (25°C) for 1 h, which was the time interval used for the cold treatment. To induce MT elimination, the cells were kept at 0 °C for 1 h and then allowed to recover for 5 min at 26 °C before fixation and immunostaining of MTs. Repolymerisation of MTs was clearly impaired in the presence of 1,78 µM GDA (Figure 3.24G, H), whereas in the absence of GDA, MTs re-established successfully (Figure 3.24E, F). In contrast to the mitotic index situation, here GFP-NtHsp90_MT did not behave differently from the line overexpressing free GFP. Despite the impaired recovery, GDA treatment did not affect viability over the subsequent days (data not shown).

3.5 Summary of results

In order to supress the detyr-signal by application of the modified amino acid NO_2Tyr, rice seedlings and tobacco BY-2 cell culture were used as plant model organisms. Treatment of rice seedlings gave first hints that cycling cells are more affected than non-cycling cells, as inhibition of growth was more pronounced in roots than in coleoptiles. Total growth observations in BY-2 showed drastic inhibition of growth, too. These results were confirmed by dose-dependent inhibition of mitosis in both plant models. Additionally, NO_2Tyr caused increased cell elongation in BY-2 cells and oblique cross wall formation. On the protein level, a decrease in detyr-tub abundance in comparison to the natural level in controls could be observed.

Another approach to supress the detyr-signal was by applying the sesquiterpene parthenolide, which is an inhibitor to TTC. Parthenolide confirmed the results obtained by treatment with NO_2Tyr and made the detyr-level decline as well. Additionally, the sesquiterpene caused delay in premitotic nuclear migration.

The overexpressor TTL-RFP showed both localisation of the RFP signal in cytoplasm and colocalisation with microtubular structures during interphase and mitosis (cMTs, PPB, spindle and phragmoplast). Further investigation and treatment with NO_2Tyr and parthenolide showed effects that were not expected from an overexpressor of TTL: NO_2Tyr did not change detyr-tub abundance in treated cells and parthenolide even made it increase. Measurements of the extracellular pH displayed higher sensitivity of the TTL-RFP cell line in comparison to BY-2 WT: extracellular medium featured stronger and quicker alkalinisation, but also quicker recovery of extracellular pH after addition of parthenolide.

The possible acceptor of the detyr-signal Hsp90 was co-purified with tubulin from cMTs by three different approaches and in two model organisms, rice and tobacco. Cosedimentation assay with recombinant Hsp90 showed that Hsp90 directly binds to polymerised tubulin. Microscopic studies showed that

GFP-HSP90_MT localises with structures resembling PPB, mitotic spindle and phragmoplast. Further experiments demonstrated a colocalisation of GFP-Hsp90_MT with cMTs in immunostained membrane ghosts.

4 Discussion

For strategies were chosen to get insight into the function detyrosination of α-tubulin:

- ➔ Suppression of the detyr-signal by treatment with NO_2Tyr (in order to create irreversibly tyrosinated α-tubulin)
- ➔ Suppression of the detyr-signal by treatment with parthenolide (to inhibit the detyrosination-enzyme TTC)
- ➔ Suppression of the detyr-signal by overexpression of TTL (the opponent of TTC)
- ➔ Examination of Hsp90, a MAP (microtubule associated protein) and a possible acceptor of the detyrosination signal

In this chapter, the previously introduced results are discussed with the objective of possible functions of the detyrosination signal.

4.1 Application of NO_2Tyr influences MT-dependent mechanisms

To get insight into the possible function of detyrosination in plants, NO_2Tyr was administered in two plant model organisms, which were rice coleoptiles as an exemplar for non-cycling cells and tobacco BY-2 cell culture for cycling cells. A specific, sensitive, and dose-dependent inhibition of cell division became manifest that was not observed after treatment with non-nitrosylated tyrosine and became detectable from 1 h after treatment. This effect was most pronounced in cycling tobacco BY-2 cells. Here, the inhibition of cell division was accompanied by a stimulation of cell length, and a disorientation of cross wall deposition. NO_2Tyr increased the sensitivity of BY-2 cells to the MT assembly blocker oryzalin and reduced the abundance of detyr-tub, whereas the abundance of tyr-tub was not affected.

Incorporation of NO_2Tyr into the C-terminus of α-tubulin is accomplished by TTL, with NO_2Tyr as alternative substrate for Tyr. However, in contrast to the canonical substrate Tyr, NO_2Tyr cannot be cleaved off by TTC, such that nitrotyrosination of α-tubulin is irreversible (Eiserich et al., 1999; Kalisz et al., 2000).

Figure 3.10 shows changes in the tyrosination-detyrosination arrangement after application of NO_2Tyr. When tobacco BY-2 cells were treated with 10 µM NO_2Tyr, the abundance of tyr-tub (tested with the antibody TUB-1A2) was not affected, suggesting that TTL activity was not affected by NO_2Tyr. In contrast, the abundance of detyr-tub (tested with the antibody DM1A) was strongly reduced. This is evidence for an inhibition of TTC activity by NO_2Tyr and provides an approach to investigate possible functions of detyrosination in plant cells.

The upper band visualised by the TUB-1A2 antibody, is expected to correspond to a mixture of tyrosinated and nitrotyrosinated α-tubulin. To verify this, commercially available antibodies against NO_2Tyr were tested. However, since these antibodies failed to produce specific signals either in extracts from tobacco cell culture or from rice (data not shown), this prediction could not be tested experimentally.

Inhibition of mitosis (Figure 3.4) was accompanied by an increase of cell length in BY-2 cells (Figure 3.7). This stimulation is not unique to NO_2Tyr, but was also found in response to the myosin inhibitor 2,3-butanedione monoxime (Holweg et al., 2003). This antagonism between cell division and cell elongation can be ascribed to cross talk between two auxin-signalling pathways that regulate cell expansion and cell division, respectively (Chen, 2001). These pathways are triggered by two receptors that differ with respect to their ligand affinities and the involvement of G-proteins as signal transducers (Campanoni and Nick, 2005).

Misorientation of the cell plate emerged as one of the most sensitive and specific symptoms for NO_2Tyr activity. In fact, cell plate formation has been

reported to be especially sensitive to disorganisations of the microtubular cytoskeleton. For instance, in response to experimentally induced doubling of the PPB (Murata and Wada, 1991; Yoneda et al., 2005) or in treatment with caffeine (*Tradescantia* stamen hairs: Bonsignore and Hepler, 1985; BY-2 cells: Yasuhara, 2005). In BY-2 cells, caffeine applied prior to the onset of mitosis inhibited the deposition of callose into the cross wall completely (Yasuhara, 2005). This was accompanied by reduced depolymerisation of phragmoplast MTs, supporting a model where disassembly of phragmoplast MTs in combination with MT translocation drives the formation of the cell plate.

Detyrosination of α-tubulin increases as a consequence of increased MT stability (Skoufias and Wilson, 1998), and kinesins have been proposed as targets for the detyrosination signal. In fact, in mammalian cells, kinesin was shown to bind preferentially to detyr-tub (Liao and Gundersen, 1998). In experiments with saturated levels of antibodies against tyr-tub and detyr-tub as competitors for the binding sites of kinesin, it appeared that the antibodies against detyr-tub were more effective in blocking the binding of kinesis to MTs. Additionally, MTs exclusively composed of detyr-tub showed a higher binding of the kinesin head than MTs composed of tyr-tub. In addition, there is evidence that kinesin functions as a cross bridge between MTs and intermediate filaments, giving an explanation for the extension of intermediate filaments onto MTs. The link between detyrosinated MTs and kinesin binding seems to hold for other systems as well. Recently it could be shown that in the filamentous fungus *Aspergillus nidulans*, UncA, a plus-end directed kinesin-3 motor preferentially binds to detyrosinated MTs (Zekert and Fischer, 2009), although other kinesins (kinesin-1 and kinesin-7) did not show such a preferential binding, suggesting that the detyrosination signal is targeted to specific kinesins.

Evidence has accumulated for an important role of kinesins in proper organisation of the phragmoplast. Already almost two decades ago, a kinesin-like 125 kDa protein has been purified from phragmoplasts which were isolated from synchronised BY-2 cells (Yasuhara et al., 1992). When the cell cycle dependent proteolytic degradation of this protein is blocked by the proteasome

inhibitor MG 132, this causes formation of a displaced additional phragmoplast (Oka et al., 2004). In the moss *Physcomitrella patens*, it could be shown that the two kinesins KINID1a and KINID1b (kinesin for interdigitated microtubules 1a and 1b) are necessary for the interdigitation of phragmoplast MTs (Hiwatashi et al., 2008). Double-deletion mutants showed that ~20 % of the phragmoplasts formed incomplete cell plates, which did not reach the plasma membrane.

We therefore arrive at the following working hypothesis for the inhibitory effect of NO_2Tyr on plant mitosis: NO_2Tyr is incorporated into α-tubulin by a plant homologue of TTL and reduces or inhibits the activity of a TTC, which results in (irreversible) tyrosinated α-tubulin. The target of the detyrosination signal might be specific kinesins, which play important roles in phragmoplast organisation and vesicle transport to the growing cell plate. As consequence of impaired α-tubulin detyrosination, the binding of these kinesins is impaired, disturbing phragmoplast function and cell plate formation manifest as oblique cross walls and delayed exit from mitosis. This will lead to pleiotropic secondary effects, such as reduced root growth as a consequence of reduced meristematic activity or elevated cell elongation in BY-2 cells.

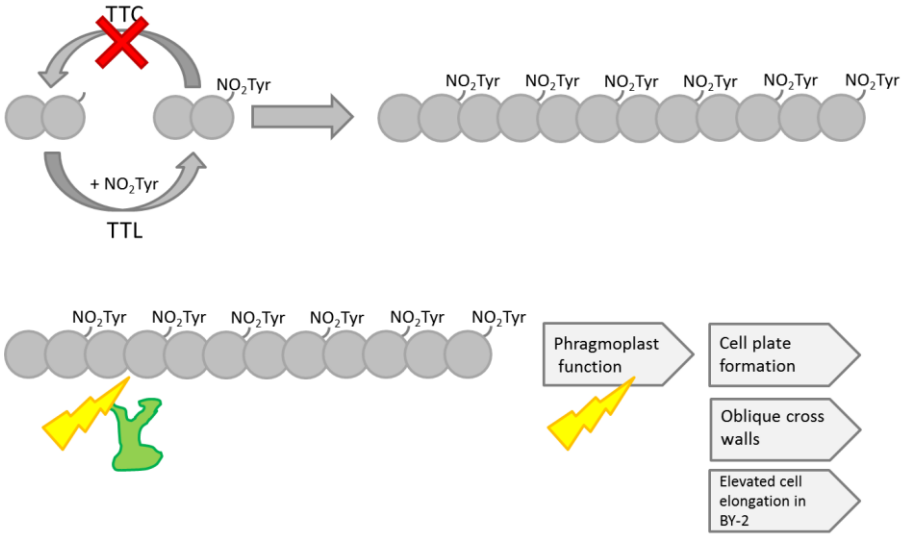

Figure 4.1: Scheme of the presumed effect of NO_2Tyr on plant mitosis. **Upper row:** By application of NO_2Tyr, (irreversibly) nitrotyrosinated tubulin is generated and incorporated into protofilaments. **Lower row:** One nitrotyrosinated protofilament shown exemplarily for a MT. Interaction with kinesin motor (green), presumed acceptor of the detyrosination signal, is impaired (flash) by suppression of the detyrosination signal. This impaired interaction results in proper function of the phragmoplast and several secondary effects.

4.2 TTC functionality is required for smooth mitotic process

In this approach it was tested whether parthenolide, an inhibitor of TTC, could interfere in the tyr/detyr distribution in BY-2 cells in a similar way like NO_2Tyr does. This was expected to be so, as both approaches were supposed to hinder TTC function, NO_2Tyr by altering the substrate, and parthenolide by inhibition of TTC.

The first question to be answered was whether parthenolide would be useable in plant systems, too. For this purpose, untransformed BY-2 WT cells were either treated with the TTC inhibitor or left untreated as a control; protein extracts were produced, and separated by SDS-PAGE. Western blot membranes were then probed with the antibodies TUB-1A2 (for detection of tyr-tub) or DM1A (for detection of detyr-tub). The results presented in Figures 3.11 and 3.12 demonstrate a shift of tyr/detyr distribution in BY-2 WT towards the tyrosinated form of α-tubulin. This result shows that parthenolide can be used as an inhibitor of TTC activity in a plant model system (tobacco BY-2), in which the tyrosination level rises at the expense of detyrosination.

Correct location of the nucleus is one of the important prerequisites for oncoming mitosis; delay in nuclear migration and positioning causes delay in cell division. Katsuta and colleagues (Katsuta et al., 1990) could demonstrate that MTs are necessary for nuclear migration in premitotic tobacco BY-2 cells (by application of MT drugs such as propyzamide and cytochalasin D). By application of parthenolide, the microtubular cytoskeleton is altered in its posttranslational modification; MTs display a higher percentage of tyr-tub. As a consequence of a higher tyrosination level, premitotic nuclear migration is delayed.

The facts point towards a model in which highly specific proteins which distinguish between tyr-tub and detyr-tub participate in the mechanism of premitotic nuclear movement. Such possible interactors are kinesins, motor proteins which were already demonstrated to be able to distinguish between these subpopulations of α-tubulin. Recently OsKCH1 (kinesin with calponin-

homology domain from *Oryza sativa*, belonging to the minus-end directed kinesis-14 subfamiliy; Frey et al., 2010) was shown to be involved in premitotic nuclear migration. In yeast, filamentous fungi and animal cells, nuclear movement was shown to require dynein as a component (Yamamoto and Hiraoka, 2003; Morris, 2003). As higher plants lack dynein, minus-end driven kinesins are likely to take the functional part of these motors. Whether OsKCH1 is such a minus-end driven motor protein which can distinguish between tyr-tub and detyr-tub is not yet solved but represents a highly interesting task.

4.3 TTL – a presumed ligase with carboxypeptidase activity?

Another approach to suppress the detyrosination signal was overexpression of the enzyme which is responsible for retyrosination of detyr-tub: TTL (identified by database research, Swiss-Prot accession Q10QY4).

Transient and stable overexpression of TTL-GFP or TTL-RFP, respectively, showed localisation of the fluorescence signal in cytoplasm and colocalisation with all microtubular arrays: cMTs in interphasic cells, PPB, spindle, and phragmoplast in mitotic cells.

Protein biochemical analysis displayed no decline in detyr-tub abundance in TTL-RFP after treatment with NO_2Tyr; in contrast to untransformed BY-2 WT, in which treatment with NO_2Tyr made the quantity of detyr-tub almost disappear.

Usage of TTC inhibitor parthenolide on TTL-RFP caused rising of the detyr-tub level, whereas tyr-tub level was almost unchanged, again in contrast to BY-2 WT; here treatment with parthenolide made the tyr-tub concentration increase, together with a decrease of the detyr-tub level.

Measurements of extracellular pH displayed higher sensitivity of TTL-RFP to parthenolide in comparison to BY-2 WT, manifested as stronger alkalinisation of extracellular pH, but also faster recovery of the pH.

Microscopic analysis of stable (TTL-RFP) and transiently (TTL-GFP) transformed tobacco BY-2 cells mainly showed cytoplasmic distribution of the fluorescent proteins, both for TTL-RFP and TTL-GFP (see Figure 3.14). In contrast to this, immunofluorescence studies of TTL-RFP (with FITC-stained MTs) clearly showed colocalisation of TTL-RFP and MTs, both in interphasic and mitotic cells (exemplarily shown for cMTs and PPB in Figure 3.15).

TTL is the enzyme which carries out retyrosination of free tubulin dimers (Beltramo et al., 1987; MacRae, 1997; Idriss, 2000), therefore the localisation of TTL-RFP and TTL-GFP is expected to be in cytoplasm, where soluble α/β-tubulin heterodimers are located. Consequently, colocalisation of the RFP signal with MTs is more surprising than the cytoplasmic signal. How can TTL-RFP be located both in the cytoplasm and on MTs, although affinity of TTL to assembled tubulin is doubtful?

Two explanations are possible: One is that TTL is capable of the reverse reaction of tyrosination, which is detyrosination: TTL normally retyrosinates detyr-tub when some preconditions are fulfilled, which are the existence of the C-terminal recognition sequence Gly-Glu-Glu (MacRae, 1997) and the presence of ATP. Once ATP is completely substituted by high concentrations of ADP and phosphate, TTL is capable of the reverse reaction (Rüdiger et al., 1994). However, this reaction was very inefficient, so that the catalytic function of TTL in the reverse reaction doesn't seem to play a role.

The other explanation is that TTL is not a ligase but the indefinite carboxypeptidase. This possibility will be discussed in the following.

Treatment of BY-2 WT with NO_2Tyr and parthenolide showed similar and, to some degree, expected results (see Figures 3.10, 3.16, 3.17): application of both drugs caused a decline in the abundance of detyr-tub (NO_2Tyr even made the signal for detyr-tub almost disappear), due to inhibition of TTC; NO_2Tyr by altering the substrate, parthenolide by inactivating TTC.

To explain the unexpected results one should make clear at first what results were the expected ones. Would TTL be a ligase, the presumed effect of an overexpression would be a shift in tyr/detyr distribution towards tyr-tub. Treatment of the overexpressor with TTC drugs should even enhance this effect (e.g. parthenolide, Figure 4.2B). However, the TTL overexpressor reacted in contrast to the speculations: After application of NO_2Tyr, the level of tyr-tub did not change obviously, whereas detyr-tub abundance also stayed the same. Usage of parthenolide even increased detyr-tub concentration. These results are not compatible with the conviction that TTL-RFP is overexpressing a ligase, on the contrary, if TTL was a carboxypeptidase, afore mentioned findings would be more reasonable. To explain the presumed process, the following model is suggested in Figure 4.2.

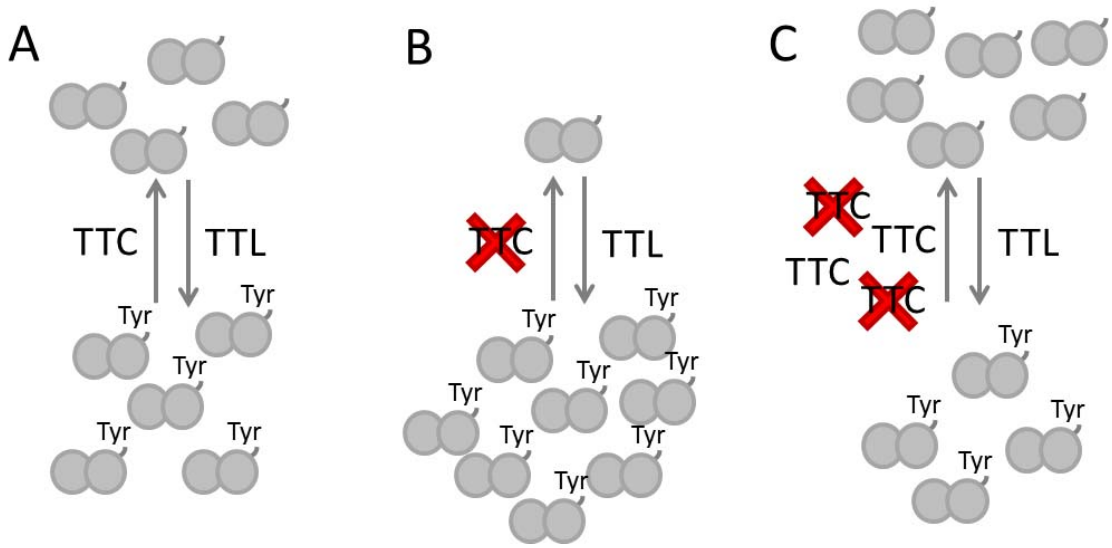

Figure 4.2: Schematic model for TTL-RFP being an overexpressed TTC. **[A]** Natural distribution of tyr-tub and detyr-tub with slightly higher level of tyr-tub. **[B]** Model for TTL-RFP being a ligase, and TTC is inhibited by parthenolide (or NO_2Tyr, respectively). The expected result would be decrease in detyr-tub and an increase in tyr-tub level. **[C]** Probable explanation for elevated detyr-tub level in a putative TTC overexpression line. As TTC level is higher due to overexpression, only a percentage of TTC is blocked by the inhibitor. Still, TTC level is higher than in WT, resulting in a compensation of the inhibitory effects.

In both experiments one property of TTL-RFP was that the general quantity of α-tubulin was lower than in BY-2 WT, although the same amount of proteins was accomplished to the SDS-gels (see Figure 3.16A). Low tubulin level in TTL-RFP could be a reaction of the cells to affected tubulin in general

(independent of unnatural high concentrations of tyr-tub or detyr-tub) and the only way to get rid of the proteins is their degradation.

Another way to show a reaction of plant cells to a chemical or molecule is measurement of external pH changes (demonstrated for elicitors by Qiao et al., 2010). This is possible for microtubular drugs as well, because MTs are involved in control of ion channels (Nick 2008).

As can be observed in Figure 3.18, parthenolide induced a stronger and quicker alkalinisation of the extracellular medium in TTL-RFP when compared to BY-2, indicating a higher sensitivity to the TTC inhibitor. Furthermore, TTL-RFP could also restore the initial pH faster, in 30 min the original pH was reached.

The experiment shows two things: First, that inhibition of TTC with parthenolide and therefore the tyr/detyr distribution has an effect on ion channels controlled by MTs. Secondly, the findings support the idea that TTL-RFP has carboxypeptidase function: the higher sensitivity (faster and stronger alkalinisation) is due to the increased number of TTC in the cells; the more TTC is abundant, the stronger is the effect of the inhibitor, the higher maximum observed in the overexpressor also points in this direction.

4.4 Hsp90 - observations in plant cells

Despite the fact that Hsp90 was reported repeatedly to interact with MTs in animal cells (Fostinis et al., 1992; Czar et al., 1996; Williams and Nelsen, 1997; Giustiniani et al., 2009), little is known about its localisation and the function of its MT-binding activity in plant cells. Moreover, so far, it was not known, whether the binding of Hsp90 to MTs is direct or whether it is mediated by unknown linker proteins.

We identified plant Hsp90s_MT by three independent approaches through co-purification with tubulin from cMTs. Later, we could demonstrate in vitro using recombinant NtHsp90_MT that Hsp90s_MT bind to polymerised tubulin directly without a requirement for linker proteins. Moreover, *in vivo*, Hsp90s_MT were

shown to associate with microtubular structures during cell division, most prominently with the phragmoplast. In addition, Hsp90_MT decorates cMTs. Pharmacological inhibition of Hsp90 by geldanamycin (GDA), produced a cellular phenotype (disruption of cytoplasmic strands) and decreased the mitotic index. The Hsp90_MT overexpressor was shown to be more resistant to non-saturating GDA concentrations as compared to BY-2 WT cells. However, the most prominent effect of Hsp90 inhibition by GDA was observed during cMT recovery after cold treatment. We show that GDA impairs the re-establishment of cortical microtubular network after its disruption during cold stress.

In the last decades, Hsp90 was shown several times to associate with MTs among other proteins. In these studies, Hsp90 was considered as a component of functional network or oligomeric molecular complex. Similar to previous experiments (Freudenreich and Nick, 1998), in our study plant Hsp90 was copurified with both polymerised MTs and with soluble tubulin heterodimers. However, since cytosolic extracts were used, these approaches do not reveal whether the interaction of Hsp90 with tubulin is direct or mediated by other proteins. Similarly, evidence based on immunofluorescence for a colocalisation of plant Hsp90 with MTs, reported by Fostinis et al. (1992), Czar et al. (1996), and Petrášek et al. (1998), cannot discriminate between direct and indirect MT-binding of Hsp90. A further problem of antibody-based approaches is the highly probable cross-reaction with different members of the Hsp90 gene family. By the identification of specific plant Hsp90 associated with MTs, which we termed as NtHsp90_MT and OsHsp90_MT we were able, for the first time, to analyse MT-binding on the background of molecular identity. Using GFP fusions of these specific gene products we could observe colocalisation with MTs *in situ*. The association was shown for MTs during cell division, predominantly for phragmoplast, as well as for cMTs in membrane ghosts. Moreover, we could show cosedimentation recombinant tobacco Hsp90_MT with polymerised MTs *in vitro* in absence of other cytosolic proteins. This provides the first evidence that the interaction is not mediated by third proteins. Since the addition of ATP did not cause any changes in the binding of Hsp90 to MTs in *in vitro*

cosedimentation assay, the process is either ATP-independent, as suggested previously (Jakob et al., 1995).

Even studies of animal Hsp90 so far were founded on experiments based on cellular extracts and antibodies that did not discriminate between different specific Hsp90s. The homologues of Hsp90 were observed to associate with MTs in cilia and cortex of *Tetrahymena* cells (Williams and Nelsen, 1997). In human cells, Hsp90 was recruited preferentially on MTs containing acetylated tubulin (Giustiniani et al., 2009). As a part of heterocomplex with client proteins and immunophilin, Hsp90 is linked to dynein, the motor protein for retrograde movement along MTs towards nucleus (Pratt et al., 2004; Harrell et al., 2004, Galigniana et al., 2004). Further, Hsp90 was reported to localise in *Drosophila* centrosomes (Lange et al., 2000), and to be involved in γ-tubulin ring assembly (Glover, 2005). Regarding these multiple MT targeted functions of animal Hsp90, the Hsp90 interactions with plant MTs reported in our study, are likely to be accompanied by additional functions as well.

We isolated the rice homologue of Hsp90_MT by its binding to dimers containing detyr-tub, which draws an interesting analogy to the results of Giustiniani et al. (2009), where Hsp90 was found to be preferentially recruited on MTs consisting of acetylated tubulin and to stimulate the signalling role of its clients Akt/PKB and p53. The tyrosination/detyrosination of tubulin influence binding of different MAP groups to MTs (Hammond et al., 2008; Cai, 2010), for instance, kinesin-1 as a motor protein preferentially binds to detyrosinated MTs (Reed et al., 2006). Therefore, Hsp90_MT may mediate the recruitment of other proteins on PPB, spindle, phragmoplast and cMTs in plants. However, the fact that the Hsp90_MT signal on cMTs was manifest in membrane ghosts, but was obscured in living cells, indicates that the association plant Hsp90_MT with MTs is transient and of short duration. Such short and transient associations of highly dynamic heterocomplexes mediated by Hsp90 was in fact detected in mammalian cells (Pratt et al., 1999).

To uncover the function of Hsp90_MT binding to plant MTs, we searched for a phenotype in lines that overexpressed GFP-Hsp90_MT. However, we failed to observe any striking phenotype, with exception of a slight decrease in turnover of MTs deduced from a small reduction in sensitivity to the tubulin sequestering drug oryzalin. Therefore, we used the Hsp90 inhibitor geldanamycin (GDA) that binds to the ATP-binding pocket of Hsp90, thus preventing the subsequent activation of Hsp90 client proteins (Prodromou et al. 1997; Grenert et al., 1999) to identify MT-driven functions of Hsp90. We focused on events where MTs exhibit their plasticity, i.e. where the whole microtubular network undergoes extensive remodelling. The reconstitution of cMTs after their cold-induced depolymerisation (Pokorná et al., 2004; Schwarzerová et al., 2006) represents such a situation. Since Hsp90_MT in fusion with GFP was found to decorate immunolabelled cMTs in membrane ghosts, recovery of cMTs after cold treatment appeared to be a promising candidate. In fact, we found that GDA-treated cells were not able to restore MTs, in clear contrast to control cells. At room temperature, the same concentration of GDA had no effects on MTs, indicating that Hsp90 is not required for MT organisation *per se*, but becomes limiting under conditions of rapid remodelling. This conclusion is also supported by our finding that Hsp90 is concentrated on phragmoplast MTs, where high MT growth and assembly is required.

A similar role of Hsp90 in MT plasticity has also been reported for Drosophila, where Hsp90 was reported as a core centrosomal component (Lange et al., 2000). Salt-stripped *Drosophila* centrosomes failed to re-establish MT-nucleating activity after GDA treatment (de Carcer et al., 2001). In animal cells, MT nucleation requires additional Hsp90-interacting centrosomal proteins, such as Polo kinase in *Drosophila* (de Carcer, 2004; Glover, 2005) and Hsp90 is required to recruit Msps, a homologue of XMAP215/chTOG in *Drosophila*, and cyclin B to centrosome in *Drosophila* and human cells (Basto et al., 2007). It is therefore likely that also in acentrosomal plant nucleation sites, Hsp90 is acting in concert with other MT nucleating proteins. It would be interesting to investigate the role of Hsp90 in acentrosomal plants with their dispersed nucleation centres and characterisation of its possible interacting proteins in

these structures because molecular differences with centriolar nucleation might be identified.

The role of Hsp90_MT in MT remodelling might also contribute to the role of Hsp90 as morphogenetic capacitator described for *Arabidopsis thaliana* Queitsch et al. (2002). Since reorientations of cMTs precede and control the axis of cell expansion via the orientation of cellulose synthesis (Paredez et al., 2006), Hsp90_MT are expected, under environmental constraints, to act as limiting factors for plant morphogenesis. Therefore, the link between phenotypic capacity and Hsp90_MT might be rewarding. In addition, potential dependence of some of the numerous Hsp90 client and interacting proteins (for review see Wegele et al., 2004) on Hsp90_MT mediated interaction with MTs in plants should be investigated.

Functional assignment is straightforward in cases, where a protein performs a unique task, such as catalysing a step in a metabolic pathway. Proteins that are ubiquitous and interact with a large number of partners are analytically more difficult, because loss- and gain-of-function assays will produce pleiotropic effects. This often leads to the impression that these proteins will not perform any specific functions. However, it might be that these, at first sight not very attractive, proteins are crucial for developmental and evolutionary plasticity. These proteins, by their multiple interactions are pacemakers for new interaction networks (Uhrig, 2006) and can fulfil, in addition to their primary function several “moonlighting” tasks that, in a different functional context can evolve into a new main function (Kurakin, 2005). Our central finding that Hsp90_MT as relatively ubiquitous protein will exert specific effects under conditions of environmental constraints (microtubular recovery from cold stress) would be consistent with a central role as phenotypic capacitator (Queitsch et al. 2002).

4.5 Conclusion

Almost all eukaryotic α-tubulins undergo various posttranslational modifications, which are considered to be mechanisms to distinguish between different subpopulations of the protein. The tubulin tyrosination cycle is one of the best investigated ones and is unique for α-tubulin. This work investigated the biological function of detyrosination in the plant models rice and tobacco by four approaches:

Suppression of the detyr-signal was accomplished by treatment with NO_2Tyr, or parthenolide, by overexpression of TTL and by investigation of Hsp90, which was identified in a fraction together with detyr-tub.

By treatment with NO_2Tyr, (irreversibly nitro-) tyrosinated α-tubulin was created and the tyr/detyr-tub distribution was altered in a way that cells have a deficiency in detyr-tub, which could be shown by Western blot analysis. Furthermore, NO_2Tyr had several effects on rice and tobacco cells, all of them indicating that mainly cell division is affected by the modified amino acid, suggesting a model in which proper cell division requires a detyrosination signal for accurate interaction with the probable acceptors of this signal: kinesins.

Treatment with parthenolide was expected to have similar effects on BY-2 cells, as it supresses the detyrosination signal as well, not by altering the substrate of TTC but by direct inhibition of the protein. The results obtained for NO_2Tyr were confirmed by parthenolide: tyr/detyr distribution was modified in a similar way, detyr-tub abundance was even elevated when compared to untreated cells. Nuclear migration, which is tightly related to cell division, as correct nuclear positioning is a prerequisite for mitosis, was slowed down by parthenolide.

These two drugs were also used for experiments with a TTL overexpressor, again in order to supress the detyrosination signal. Besides colocalisation with MTs in immunofluorescence studies, the TTL overexpressor demonstrated effects that could most likely be explained if TTL was not a ligase but the so far unknown TTC.

Analysis of a possible interaction partner with detyrosinated MTs (Hsp90, which was identified by three different approaches in two model organisms), showed that Hsp90 directly bound to MTs *in vitro* (demonstrated by cosedimentation with polymerised tubulin), and that it colocalised with cortical MTs *in vivo* (in colocalisation studies with membrane ghosts). Overexpressing lines of GFP-Hsp90 showed localisation in structures resembling PPB, spindle and phragmoplast. Additionally, by application of the Hsp90 inhibitor GDA, Hsp90 displayed participation in the re-establishment of cMTs after their disruption by cold shock.

4.6 Outlook

In this work it could be demonstrated that incorporation of NO_2Tyr into plant α-tubulin has some highly specific effects, such as inhibition of cell division, accompanied by stimulation of cell elongation and oblique cell plate formation. Additionally, it could be shown that cells grown with NO_2Tyr were influenced in terms of the amount of detyrosinated α-tubulin so that hardly any detyr-tub could be detected. Besides these findings there are still open questions in the field of the tubulin tyrosination cycle. One issue is whether the insertion of NO_2Tyr into (plant) α-tubulin is a reversible process or not. To answer this, one might use carboxypeptidase A and test *in vitro* whether decarboxylation of tubulin is impaired when it is purified from cells that have been treated with NO_2Tyr. However, carboxypeptidase A cleaves a fairly broad range of unspecific substrates, whereas the TTC is specific for tubulin, making it difficult to transfer the results from one experiment to the other. Additionally, the search for a NO_2Tyr antibody which produces a specific signal in plant protein extracts (to show incorporation of NO_2Tyr in α-tubulin) or in immunofluorescence studies (to observe the signal distribution and colocalisation with different microtubular arrays) should proceed.

When it comes to premitotic nuclear positioning and a possible acceptor for the detyr-signal, further investigation of kinesins (and OsKCH1 in particular) could provide interesting insight into the function of detyrosination and the discussion

about a possible acceptor of this signal. As a possible acceptor for the detyr-signal, Hsp90 came into play. Although specificity of Hsp90 towards detyr-tub is still open, further experiments could be of assistance. As separation of tyr-tub and detyr-tub is possible by EPC affinity chromatography, it would be interesting to find out whether there is a difference in cosedimentation behaviour between samples with tyr-tub or detyr-tub.

Considering the experiments with the overexpression line TTL-RFP, the formerly presumed ligase, one of the most important issues for the future is to purify recombinant “TTL”. In this approach, separation of tyr-tub from detyr-tub by EPC affinity chromatography and treatment of “TTL” with the respective subpopulation of tubulin could give insight into the enzymatic reaction “TTL” catalyses. Furthermore, two additional candidates for TTL could be identified in *Oryza sativa* by database search, investigation and characterisation of these two is still missing.

5 Appendix

5.1 Sequence information

5.1.1 Amino acid sequence of OsHsp90 (Swiss-Prot accession number A2YWQ1)

```
        10         20         30         40         50         60
MASETETFAF QAEINQLLSL IINTFYSNKE IFLRELISNS SDALDKIRFE SLTDKSKLDA

        70         80         90        100        110        120
QPELFIHIVP DKASNTLSII DSGIGMTKSD LVNNLGTIAR SGTKEFMEAL AAGADVSMIG

       130        140        150        160        170        180
QFGVGFYSAY LVAERVVVTT KHNDDEQYVW ESQAGGSFTV TRDTSGEQLG RGTKITLYLK

       190        200        210        220        230        240
DDQLEYLEER RLKDLIKKHS EFISYPISLW TEKTTEKEIS DDEDEEEKKD AEEGKVEDVD

       250        260        270        280        290        300
EEKEEKEKKK KKIKEVSHEW SLVNKQKPIW MRKPEEITKE EYAAFYKSLT NDWEEHLAVK

       310        320        330        340        350        360
HFSVEGQLEF KAVLFVPKRA PFDLFDTRKK LNNIKLYVRR VFIMDNCEEL IPEWLSFVKG

       370        380        390        400        410        420
IVDSEDLPLN ISREMLQQNK ILKVIRKNLV KKCVELFFEI AENKEDYNKF YEAFSKNLKL

       430        440        450        460        470        480
GIHEDSTNRN KIAELLRYHS TKSGDELTSL KDYVTRMKEG QNDIYYITGE SKKAVENSPF

       490        500        510        520        530        540
LEKLKKKGYE VLYMVDAIDE YAVGQLKEFE GKKLVSATKE GLKLDESEDE KKRKEELKEK

       550        560        570        580        590        600
FEGLCKVIKE VLGDKVEKVV VSDRVVDSPC CLVTGEYGWT ANMERIMKAQ ALRDSSMAGY

       610        620        630        640        650        660
MSSKKTMEIN PENAIMEELR KRADADKNDK SVKDLVLLLF ETALLTSGFS LDDPNTFGSR

       670        680        690
IHRMLKLGLS IDEDETAEAD TDMPPLEDDA GESKMEEVD
```

5.1.2 Amino acid sequence of NtHsp90 (Swiss-Prot accession number Q14TB1)

```
        10         20         30         40         50         60
MADTETFAFQ AEINQLLSLI INTFYSNKEI FLRELISNSS DALDKIRFES LTDKSKLDAQ

        70         80         90        100        110        120
PELFIHIIPD KTNNSLTIID SGIGMTKADL VNNLGTIARS GTKEFMEALA AGADVSMIGQ

       130        140        150        160        170        180
FGVGFYSAYL VAEKVIVTTK HNDDEQYVWE SQAGGSFTVT RDTSGENLGR GTKITLFLKE

       190        200        210        220        230        240
DQLEYLEERR LKDLIKKHSE FISYPISLWV EKTIEKEISD DEEEEEKKDE EGKVEEVDEE

       250        260        270        280        290        300
KEMEEKKKKK VKEVSNEWSL VNKQKPIWMR KPDEITKEEY AAFYKSLTND WEEHMAVKHF

       310        320        330        340        350        360
SVEGQLEFKA ILFVPKRAPF DLFDTRKKPN NIKLYVRRVF IMDNCEELIP EYLSFVKGIV

       370        380        390        400        410        420
DSEDLPLNIS REMLQQNKIL KVIRKNLVKK CVELFFEIAE NKEDYNKFYE AFSKNLKLGI

       430        440        450        460        470        480
HEDSQNRSKF AELLRYHSTK SGDEMTSLKD YVTRMKEGQN DIYYITGESK KAVENSPFLE

       490        500        510        520        530        540
KLKKKGYEVL YMVDAIDEYS IGQLKEFEGK KLVSATKEGL KLDESEDEKK KQEELKEKFE

       550        560        570        580        590        600
GLCKVIKDVL GDKVEKVVVS DRVVDSPCCL VTGEYGWTAN MERIMKAQAL RDSSMAGYMS

       610        620        630        640        650        660
SKKTMEINPE NAIMEELRKR ADADKNDKSV KDLVLLLFET ALLTSGFSLE EPNTFGNRIH

       670        680        690
RMLKLGLSID DDSGDADVDM PALEDPEADA EGSKMEEVD
```

5.1.3 Amino acid sequence of TTL (Swiss-Prot accession number Q10QY4)

```
        10         20         30         40         50         60
MSPAAASPDD RIRSYEDFAR VHAYLLAASG IPPSLHQRLY RKLADEVFDG GEAFSVEPCE

        70         80         90        100        110        120
GGRQRRLVLA AEWTLGRESD VFLVDHAWSF RLSDALKQLR EVPGLAERMA ALMCVDLDER

       130        140        150        160        170        180
TELEEADEQD NGNGGSLESA LEVVEKERTR IQEKGSDFAA WLELEELGID DDMLIALDLS

       190        200        210        220        230        240
SKFPNMVALN LWGNKLQDPE KIMKGIGECR RLKALWLNEN PALKEGVDKV ILDGLPELEI

       250        260        270        280        290        300
YNSHFTRKAG EWALGFCGDI IGADNPCSSA ESIPLENIAS LDLSDRCIHK LPVVFSPRKL

       310        320        330        340        350        360
SSLLSLNIRG NPLDQMSSDD LLKLISGFTQ LQELEVDIPG SLGNSAISIL ECLPNLSLLN

       370        380        390        400        410        420
GINVASIIES GKHIIDSALK PRLPEWSPQE SLPERVIGAM WLYLMTYRLA DEEKIDETPV

       430        440        450        460        470        480
WYVMDELGSA MRHSDDANFR IAPFLFMPDG KLASAISYTI LWPVHDVHTG EECTRDFLFG

       490        500        510        520        530        540
VGEDKQRSAR LTAWFHTPEN YFIQEFRKYK EQLQSSSICP SRKVTPVTKS IRPSDGHALR

       550        560        570        580        590        600
VFTDIPQVEE FLTRPEFVLT SDPKEADIIW VSMQVDSELK NALGLTDQQY TNQFPFEACL

       610        620        630        640        650        660
VMKHHLAETI HKAWGSPEWL QPTYNLETHL SPLIGDYCVR KRDGMDNLWI MKPWNMARTI

       670        680        690        700        710        720
DTTVTGDLSA IIRLMETGPK ICQKYIECPA LFQGRKFDLR YIVFVRSICP LEIFLSDVFW

       730        740        750        760        770        780
VRLANNQYTL EKTSFFEYET HFTVMNYIGR MNHMNTPEFV KEFEKEHQVK WLEIHGRIRD

       790        800        810        820        830        840
MIRCVFESAT AVHPEMQNPF SRAIYGVDVM LDNKFNPKIL EVTYCPDCTR ACKYDTQALV

       850        860        870
GSQGVIRGTE FFNTVFGCLF LDELKDVSPL
```

6 References

Agueli C, Geraci F, Giudice G, Chimenti L, Cascino D, Sconzo G. (2001) A constitutive 70 kDa heat-shock protein is localized on the fibres of spindles and asters at metaphase in an ATP-dependent manner: a new chaperone role is proposed. Biochemical Journal **360**, 413-419.

Alberts B, Bray D, Hopkin K, Johnson A, Lewis J, Raff M, Roberts K, Walter P. (2005) Lehrbuch der Molekularen Zellbiologie. 3. Auflage, WILEY-VCH Verlag GmbH & Co. KGaA.

Banerjee A. (2002) Coordination of Posttranslational Modifications of Bovine Brain α-Tubulin. Journal of Biological Chemistry **227**, 46140-46144.

Barra HS, Rodriguez JA, Arce CA, Caputto R. (1973) A soluble preparation from rat brain that incorporates into its own proteins [^{14}C]Arginine by a ribonuclease-sensitive system and [^{14}C]Tyrosine by a ribonuclease-insensitive system. Journal of Neurochemistry **20**, 97-108.

Basto R, Gergely F, Draviam VM, Ohkura H, Liley K, Raff JW. (2007) Hsp90 is required to localise cyclin B and Msps/ch-TOG to the mitotic spindle in *Drosophila* and humans. Journal of Cell Science **120**, 1278-1287.

Beckman JS, Koppenol WH. 1996. Nitric oxide, superoxide, and peroxynitrite: the good, the bad, and the ugly. American Journal of Physiology **271**, 1424-1437.

Beltramo DM, Arce CA, Barra HS. (1987) Tubulin, but Not Microtubules, Is the Substrate for Tubulin:Tyrosine Ligase in Mature Avian Erythrocytes. Journal of Biological Chemistry **262**, 15673-15677.

Bensadoun A, Weinstein D. (1976) Assay of Proteins in the Presence of Interfering Materials. Analytical Biochemistry **70**, 241-250.

Bisig CG, Purro SA, Contin MA, Barra HS, Arce CA. 2002. Incorporation of 3-nitrotyrosine into the C-terminus of α-tubulin is reversible and not detrimental to deviding cells. European Journal of Biochemistry **269**, 5037-5045.

Bonsignore CL, Hepler PK. (1985) Caffeine Inhibition of Cytokinesis: Dynamics of Cell Plate Formation-Deformation *in vivo.* Protoplasma **129,** 28-35.

Breitling F, Little M. (1986) Quantitative measurement of the catastrophe rate of dynamic microtubules. Epitope locations of YOL1/34, DM1A and DM1B. Journal of Molecular Biology **189**, 367-370.

Cadepond F, Jibard N, Binart N, Schweizergroyer G, Segardmaurel I, Baulieu EE. (1994) Selective deletions in the 90 kDa heat-shock protein (hsp90) impede heterooligomeric complex-formation with the glucocorticosteroid receptor (GR) or hormone-binding by GR. Journal of Steroid Biochemistry and Molecular Biology **48**, 361-367.

Cai G. (2010) Assembly and disassembly of plant microtubules: tubulin modifications and binding to MAPs. Journal of Experimental Botany **61**, 623-625.

Campanoni P, Blasius B, Nick P. (2003) Auxin transport synchronizes the pattern of cell division in a tobacco cell line. Plant Physiology **133**, 1251-1260.

Campanoni P, Nick P. (2005) Auxin-Dependent Cell Division and Cell Elongation. 1-Naphthaleneacetic Acid and 2,4-Dichlorophenoxyacetic Acid Activate Different Pathways. Plant Physiology **137,** 939-948.

de Carcer G. (2004) Heat shock protein 90 regulates the metaphase-anaphase transition in a polo-like kinase-dependent manner. Cancer Research **64**, 5106-5112.

de Carcer G, Avides MD, Lallena MJ, Glover DM, Gonzalez C. (2001) Requirement of Hsp90 for centrosomal function reflects its regulation of Polo kinase stability. EMBO Journal **20**, 2878-2884.

Chan J, Calder G, Fox S, Lloyd C. (2007) Cortical microtubule arrays undergo rotary movements in Arabidopsis hypocotyl epidermal cells. Nature Cell Biology **9**, 171-175.

Chang W, Webster DR, Salam AA, Gruber D, Prasad A, Eiserich JP, Bulinski JC. (2002) Alteration of the C-terminal Amino Acid of Tubulin Specifically Inhibits Myogenic Differentiation. Journal of Biological Chemistry **277**, 30690-30698.

Chen JG. (2001) Dual Auxin Signaling Pathway Control Cell Elongation and Division. Journal of Plant Growth Regulation **20,** 255-264.

Chrétien D, Fuller SD, Karsenti E. (1995) Structure of Growing Microtubule Ends: Two-Dimensional Sheets Close Into Tubes at Variable Rates. Journal of Cell Biology **129**, 1311-1328.

Chuong SDX, Good AG, Taylor GJ, Freeman MC, Moorhead GBD, Muench DG. (2004) Large-scale Identification of Tubulin-binding Proteins Provides Insight on Subcellular Trafficking, Metabolic Channeling, and Signaling in Plant Cells. Molecular & Cellular Proteomics **3**, 970-983.

Corpas FJ, del Rio LA, Barroso JB. (2007) Need for biomarkers of nitrosative stress in plants. Trends in Plant Science **12**, 436-438.

Cross RA. (2010) Kinesin-14: the roots of reversal. BMC Biology **8**, 107.

Cuatrecasas P. (1970) Protein purification by affinity chromatography: derivatization of agarose and polyacrylamide beads. Journal of Biological Chemistry **245**, 3059-3065.

Czar MJ, Welsh MJ, Pratt WB. (1996) Immunofluorescence localization of the 90-kDa heat-shock protein to cytoskeleton. European Journal of Cell Biology **70**, 322-330.

Deka J, Kuhlmann J, Muller O. (1998) A domain within the tumor suppressor protein APC shows very similar biochemical properties as the microtubule-associated protein tau. European Journal of Biochemistry **253**, 591-597.

Durst S. (2009) Funktionelle Analyse einer mutmaßlichen Tubulinyl-Tyrosin-Ligase aus Reis. Diploma thesis. Universität Karlsruhe, Institut für Botanik I.

Eiserich JP, Estévez AG, Bamberg TV, Ye YZ, Chumley PH, Beckman JS, Freeman BA. (1999) Microtubule dysfunction by posttranslational nitrotyrosination of α-tubulin: A nitric oxide-dependent mechanism of cellular injury. Proceedings of the National Academy of Sciences **96,** 6365-6370.

Ersfeld K, Wehland J, Plessmann U, Dodemont H, Gerke V, Weber K. (1993) Characterization of the Tubulin-Tyrosin Ligase. Journal of Cell Biology **120**, 725-732.

Fonrose X, Ausseil F, Soleilhac E, Masson V, David B, Pouny I, Cintrat J-C, Rousseau B, Barette C, Massiot G, Lafanechère L. (2007) Parthenolide Inhibits Tubulin Carboxypeptidase Activity. Cancer Research **67**, 3371-3378.

Fostinis Y, Theodoropoulos PA, Gravanis A, Stournaras C. (1992) Heat shock protein HSP90 and its association with the cytoskeleton – a morphological study. Biochemistry and Cell Biology-Biochimie Et Biologie Cellulaire **70**, 779-786.

Frey N, Klotz J, Nick P. (2010) A kinesin with calponin-homology domain is involved in premitotic nuclear migration. Journal of Experimental Botany **61**, 3423-3437.

Galigniana MD, Harrell JM, O'Hagen HM, Ljungman M, Pratt WB. (2004) Hsp90-binding immunophilins link p53 to dynein during p53 transport to the nucleus. Journal of Biological Chemistry **279**, 22483-22489.

Gill BS, Appels R, Botha-Oberholster A-M, Buell CR, Bennetzen JL, Chalhoub B, Chumley F, Dvoršák J, Iwanaga M, Keller B, Li W, McCombie WR, Ogihara Y, Quetier F, Sasaki T. (2004) A Workshop Report on Wheat Genome Sequencing: International Genome Research on Wheat Consortium. Genetics **168**, 1087-1096.

Giustiniani J, Daire V, Cantaloube I, Durand G, Pous C, Perdiz D, Baillet A. (2009) Tubulin acetylation favors Hsp90 recruitment to microtubules and stimulates the signaling function of the Hsp90 clients Akt/PKB and p53. Cellular Signalling, **21**, 529-539.

Glover DM. (2005) Polo kinase and progression through M phase in *Drosophila*: a perspective from the spindle poles. Oncogene **24**, 230-237.

Goddard RH, Wick SM, Silflow CD, Snustad DP. (1994) Microtubule Components of the Plant Cell Cytoskeleton. Plant Physiology **104**, 1-6.

Gooljarsingh LT, Fernandes C, Yan K, Zhang H, Grooms M, Johanson K, Sinnamon RH, Kirkpatrick RB, Kerrigan J, Lewis T, Arnone M, King AJ, Lai Z, Copeland RA, Tummino PJ. (2006) A biochemical rationale for the anticancer effects of Hsp90 inhibitors: Slow, tight binding inhibition by geldanamycin and its analogues. Proceedings of the National Academy of Sciences **103**, 7625-7630.

Grenert JP, Johnson BD, Toft DO. (1999) The importance of ATP binding and hydrolysis by hsp90 in formation and function of protein heterocomplexes. Journal of Biological Chemistry **274**, 17525-17533.

Hammond JW, Cai D, Verhey KJ. (2008) Tubulin modifications and their cellular functions. Current Opinion in Cell Biology **20**, 71-76.

Harrell JM, Murphy PJM, Morishima Y, Chen HF, Mansfield JF, Galigniana MD, Pratt WB. (2004) Evidence for glucocorticoid receptor transport on microtubules by dynein. Journal of Biological Chemistry **279**, 54647-54654.

Hepler PK, Vidali L, Cheung AY. (2001) Polarized cell growth in higher plants. Annual Review of Cell and Developmental Biology **17**, 159-187.

Higaki T, Sano T, Hasezawa S. (2007) Actin microfilament dynamics and actin side-binding proteins in plants. Current Opinion in Plant Biology **10**, 549-556.

Himmelspach R, Wymer CL, Lloyd CW, Nick P. (1999) Gravity-induced reorientation of cortical microtubules observed *in vivo*. The Plant Journal **18**, 449-453.

Hiwatashi Y, Obara M, Sato Y, Fujita T, Murata T, Hasebe M. (2008) Kinesins Are Indispensable for Interdigitation of Phragmoplast Microtubules in the Moss *Physcomitrella patens.* Plant Cell **20,** 3094-3106.

Holmes KC, Popp D, Gebhard W, Kabsch W. (1990) Atomic model of the actin filament. Nature **347**, 44-49.

Holweg C, Honsel A, Nick P. (2003) A myosin inhibitor impairs auxin-induced cell division. Protoplasma **222,** 193-204.

Hussey PJ, Ketelaar T, Deeks MJ. (2006) Control of the Actin Cytoskeleton in Plant Cell Growth. Annual Review of Plant Biology **57**, 109-25.

Idriss HT. (2000) Phosphorylation of Tubulin Tyrosine Ligase: A Potential Mechanism for Regulation of α-Tubulin Tyrosination. Cell Motility and the Cytoskeleton **46**, 1-5.

Idriss HT. (2004) Defining a physiological role for the tubulin tyrosination cycle. European Journal of General Medicine **1**, 1-2.

Infante AS, Stein MS, Zhai Y, Borisy GG, Gundersen GG. (2000) Detyrosinated (Glu) microtubules are stabilized by an ATP-sensitive plus-end cap. Journal of Cell Science **113**, 3907-3919.

Jakob U, Lilie H, Meyer I, Buchner J. (1995) Transient interaction of hsp90 with early unfolding intermediates of citrate synthase - implications for heat-shock *in vivo*. Journal of Biological Chemistry **270**, 7288-7294.

Jovanovic AM, Durst S, Nick P. (2010) Plant cell division is specifically affected by nitrotyrosine. Journal of Experimental Botany **61**, 901-909.

Kalisz HM, Erck C, Plessmann U, Wehland J. (2000) Incorporation of nitrotyrosine into α-tubulin by recombinant mammalian tubulin-tyrosine ligase. Biochimica et Biophysica Acta **1481,** 131-138.

Katsuta J, Hashiguchi Y, Shibaoka H. (1990) The role of the cytoskeleton in positioning of the nucleus in premitotic tobacco BY-2 cells. Journal of Cell Science **95**, 413-422.

Kreis TE. (1987) Microtubules containing detyrosinated tubulin are less dynamic. The EMBO Journal **6**, 2597-2606.

Krishna P, Gloor G. (2001) The Hsp90 family of proteins in *Arabidopsis thaliana*. Cell Stress & Chaperones **6**, 238-246.

Kurakin A. (2005) Self-organization versus Watchmaker: stochastic dynamics of cellular organization. Biological Chemistry **386**, 247-254.

Laemmli UK. (1970) Cleavage of structural proteins during the assembly of the head of bacteriophage T4. Nature **227**, 680-685.

Lange BMH, Bachi A, Wilm M, Gonzalez C. (2000) Hsp90 is a core centrosomal component and is required at different stages of the centrosome cycle in *Drosophila* and vertebrates. EMBO Journal **19**, 1252-1262.

Ledbetter MC, Porter KR. (1963) A “microtubule“ in plant cell fine structure. Journal of Cell Biology **19**, 239-250.

Liang P, MacRae TH. (1997) Molecular chaperones and the cytoskeleton. Journal of Cell Science **110**, 1431-1440.

Liao G, Gundersen GG. (1998) Kinesin Is a Candidate for Cross-bridging Microtubules and Intermediate Filaments. Journal of Biological Chemistry **273**, 9797-9803.

Ludwig H. (2010) Funktionelle Analyse einer mutmaßlichen Tubulinyl-Tyrosin-Ligase aus Reis. Diploma thesis. Universität Karlsruhe, Institut für Botanik I.

MacRae TH. (1997) Tubulin post-translational modifications. European Journal of Biochemistry **244**, 265-278.

Maisch J, Nick P. (2007) Actin is involved in auxin-dependent patterning. Plant Physiology **143**, 1695-1704.

Meyer P, Prodromou C, Hu B, Vaughan C, Roe SM, Panaretou B, Piper PW, Pearl LH. (2003) Structural and functional analysis of the middle segment of Hsp90: Implications for ATP hydrolysis and client protein and cochaperone interactions. Molecular Cell **11**, 647-658.

Mizuno K, Sek F, Perkin J, Wick S, Duniec J, Gunning B. (1985) Monoclonal Antibodies Specific to Plant Tubulin. Protoplasma **129**, 100-108.

Morejohn LC. (1994) Microtubule Binding Proteins Are Not Necessarily Microtubule-Associated Proteins. The Plant Cell **6**, 1696-1699.

Morris NR. (2003) Nuclear positioning: the means is at the ends. Current Opinion in Cell Biology **15**, 54-59.

Moseley JB, Bartolini F, Okada K, Wen Y, Gundersen GG, Goode BL. (2007) Regulated binding of adenomatous polyposis coli protein to actin. Journal of Biological Chemistry **282**, 12661-12668.

Murata T, Wada M. (1991) Effects of centrifugation on preprophase-band formation in *Adiantum* protonemata. Planta **183,** 391-398.

Nagata T, Kumagai F. (1999) Plant cell biology through the window of the highly synchronized tobacco BY-2 cell line. Methods in Cell Science **21**, 123-127.

Nagata T, Nemoto Y, Hasezawa S. (1992) Tobacco BY 2 cell line as the 'HeLa' cells in the cell biology of higher plants. International Review of Cytology **132**, 1-30.

Nebenführ A, Frohlick JA, Staehelin LA. (2000) Redistribution of Golgi Stacks and Other Organells during Mitosis and Cytokinesis in Plant Cells. Plant Physiology **124**, 135-151.

Neckers L, Schulte TW, Mimnaugh E. (1999) Geldanamycin as a potential anti-cancer agent: Its molecular target and biochemical activity. Investigational New Drugs **17**, 361-373.

Neill SJ, Desikan R, Hancock JT. (2003) Nitric oxide signalling in plants. New Phytologist **159**, 11-35.

Nick P. (1998) Signaling to the Microtubular Cytoskeleton in Plants. International Review of Cytology **184**, 33-80.

Nick P. (2008) Plant microtubules – Development and Flexibility. Springer Verlag Berlin Heidelberg.

Nick P, Heuing A, Ehmann B. (2000) Plant chaperonins: a role in microtubule-dependent wall formation? Protoplasma **211**, 234-244.

Nick P, Lambert A-M, Vantard M. (1995) A microtubule-associated protein in maize is expressed during phytochrome-induced cell elongation. The Plant Journal **8**, 835-844.

Nick P, Yatou O, Furuya M, Lambert A-M. (1994) Auxin-dependent microtubule responses and seedling development are affected in a rice mutant resistant to EPC. The Plant Journal **6**, 651-663.

Nocarova E, Fischer L. (2009) Cloning of transgenic tobacco BY-2 cells; an efficient method to analyse and reduce high natural heterogeneity of transgene expression. BMC Plant Biology **9**.

Oka M, Yanagawa Y, Asada T, Yoneda A, Hasezawa S, Sato T, Nakagawa H. *(*2004) Inhibition of Proteasome by MG-132 Treatment Causes Extra Phragmoplast Formation and Cortical Microtubule Disorganization during M/G1 Transition in Synchronized Tobacco Cells. Plant Cell Physiology **45,** 1623-1632.

Opperman C, Lommel SA, Sosinski B, Burke M, Lakey N, He L, Brierley R, Salstead A, Gadani F, Hayes A. (2003) The Tobacco Genome Initiative. Plant & Animal Genomes XI Conference. P32.

Palevitz, B.A. (1987) Actin in the Preprophase Band of *Allium cepa*. Journal of Cell Biology **104**, 1515-1519.

Paredez AR, Somerville CR, Erhardt DW. Visualization of Cellulose Synthase Demonstrates Functional Association with Microtubules. Science **312**, 1491-1495.

Pearl LH, Prodromou C. (2000) Structure and *in vivo* function of Hsp90. Current Opinion in Structural Biology **10**, 46-51.

Petrasek J, Freudenreich A, Heuing A, Opatrny Z, Nick P. (1998) Heat-shock protein 90 is associated with microtubules in tobacco cells. Protoplasma **202**, 161-174.

Pickett-Heaps JD, Northcote DH. (1966) Organisation of microtubules and the endoplasmatic reticulum during mitosis and cytokinesis in wheat meristems. Journal of Cell Science **1**, 109-120.

Planchet E, Kaiser WM. (2006) Nitric Oxide Production in Plants. Plant Signaling & Behavior **1**, 46-51.

Pokorná J, Schwarzerová K, Zelenkova S, Petrásek J, Janotova I, Capkova V, Opatrny Z. (2004) Sites of actin filament initiation and reorganization in cold-treated tobacco cells. Plant Cell and Environment **27**, 641-653.

Pratt WB, Galigniana MD, Harrell JM, DeFranco DB. (2004) Role of hsp90 and the hsp90-binding immunophilins in signalling protein movement. Cellular Signalling **16**, 857-872.

Pratt WB, Silverstein AM, Galigniana MD. (1999) A model for the cytoplasmic trafficking of signalling proteins involving the hsp90-binding immunophilins and p50(cdc37). Cellular Signalling **11**, 839-851.

Prodromou C, Roe SM, Obrien R, Ladbury JE, Piper PW, Pearl LH. (1997) Identification and structural characterization of the ATP/ADP-binding site in the Hsp90 molecular chaperone. Cell **90**, 65-75.

Qiao F, Chang X, Nick P. (2010) The cytoskeleton enhances gene expression in the response to the harpin elicitor in grapevine. Journal of Experimental Botany **10**, 1-11.

Queitsch C, Sangster TA, Lindquist S. (2002) Hsp90 as a capacitor of phenotypic variation. Nature **417**, 618-624.

Reed NA, Cai DW, Blasius TL, Jih GT, Meyhofer E, Gaertig J, Verhey KJ. (2006) Microtubule acetylation promotes kinesin-1 binding and transport. Current Biology **16**, 2166-2172.

Rüdiger M, Wehland J, Weber K. (1994) The carboxy-terminal peptide of detyrosinated α tubulin provides a minimal system to study the substrate specificity of tubulin-tyrosine ligase. European Journal of Biochemistry **220**, 309-320.

Sambrook J, Russell DW. (2001). Molecular cloning: a laboratory manual. Cold Spring Harbor Laboratory Press.

Samsonov A, Yu JZ, Rasenick M, Popov SV. (2004) Tau interaction with microtubules in vivo. Journal of Cell Science **117**, 6129-6141.

Sasaki T, Sederoff RR. (2003) Genome studies and molecular genetics / The rice genome and comparative genomics of higher plants. Current Opinion in Plant Biology **6**, 97-100.

Schneider N. (2010) Funktionelle Analyse einer mutmaßlichen Tyrosinyl-Tubulin-Ligase aus Reis. Diploma thesis. Universität Karlsruhe, Institut für Botanik I.

Schoof H, Karlowski WM. (2003) Comparison of rice and Arabidopsis annotation. Current Opinion in Plant Biology **6**, 106-112.

Schwarzerová K, Petrasek J, Panigrahi KCS, Zelenkova S, Opatrny Z, Nick P. (2006) Intranuclear accumulation of plant tubulin in response to low temperature. Protoplasma **227**, 185-196.

Sept D, Baker NA, McCammon JA. (2003) The physical basis of microtubule structure and stability. Protein Science **12**, 2257-2261.

Sharma SV, Agatsuma T, Nakano H. (1998) Targeting of the protein chaperone, HSP90, by the transformation suppressing agent, radicicol. Oncogene **16**, 2639-2645.

Shaw S, Kamyar R, Ehrhardt DW. (2003) Sustained Microtubule Treadmilling in *Arabidopsis* Cortical Arrays. Science **300**, 1715-1718.

Skoufias DA, Wilson L. (1998) Assembly and Colchicine Binding Characteristics of Tubulin with Maximally Tyrosinated and Detyrosinated α-Tubulins. Archives of Biochemistry and Biophysics **351**, 115-122.

Smith DF. (1993) Dynamics of heat-shock protein 90-progesterone receptor-binding and the disactivation loop model for steroid receptor complexes. Molecular Endocrinology **7**, 1418-1429.

Sonobe S. Takahashi S. (1994) Association of microtubules with the plasma-membrane of tobacco BY-2 cells *in vitro*. Plant and Cell Physiology **35**, 451-460.

Stebbins CE, Russo AA, Schneider C, Rosen N, Hartl FU, Pavletich NP. (1997) Crystal structure of an Hsp90-geldanamycin complex: Targeting of a protein chaperone by an antitumor agent. Cell **89**, 239-250.

Taiz L, Zeiger E. (2000) Physiologie der Pflanzen. Spektrum Akademischer Verlag GmbH Heidelberg, Berlin.

Uhrig JF. (2006) Protein interaction networks in plants. Planta (2006) **224**, 771-781.

Van Gestel K, Kohler RH, Verbelen JP. (2002) Plant mitochondria move on F-actin, but their positioning in the cortical cytoplasm depends on both F-actin and microtubules. Journal of Experimental Botany **53**, 659-667.

Vantard M, Peter C, Fellous A, Schellenbaum P, Lambert A-M. (1994) Characterization of a 100-kDa heat-stable microtubule-associated protein from higher plants. European Journal of Biochemistry **220**, 847-853.

Vantard M, Schellenbaum P, Fellous A, Lambert A-M. (1991) Characterization of Microtubule Associated Proteins, One of Which is Immunologically Related to Tau. Biochemistry **30**, 9334-9340.

Wang X, Zhu L, Liu BQ, Wang C, Jin LF, Zhao Q, Yuan M. (2007) *Arabidopsis* MICROTUBULE-ASSOCIATED PROTEIN18 functions in directional cell growth by destabilizing cortical microtubules. Plant Cell **19**, 877-889.

Wasteneys GO. (2002) Microtubule organization in the green kingdom: chaos or self-order? Journal of Cell Science **115**, 1345-1354.

Webster DR, Wehland J, Weber K, Borisy GG. (1990) Detyrosination of Alpha Tubulin Does Not Stabilize Microtubules In Vivo. Journal of Cell Biology **111**, 113-122.

Wegele H, Muller L, Buchner J. (2004) Hsp70 and Hsp90 - a relay team for protein folding. Ergebnisse der Physiologie, biologischen Chemie und experimentellen Pharmakologie **151**, 1-44.

Westermann S, Weber K. (2003) Post-translational modifications regulate microtubule function. Nature Reviews Molecular Cell Biology **4**, 938-947.

Wiesler B, Wang Q-Y, Nick P. (2002) The stability of cortical microtubules depend on their orientation. The Plant Journal **32**, 1023-1032.

Williams NE, Nelsen EM. (1997) HSP70 and HSP90 homologs are associated with tubulin in hetero-oligomeric complexes, cilia and the cortex of Tetrahymena. Journal of Cell Science **110**, 1665-1672.

Wilson L, Panda D, Jordan MA. (1999) Modulation of Microtubule Dynamics by Drugs: A Paradigm for the Actions of Cellular Regulators. Cell Structure and Function **24**, 329-335.

Yamamoto A, Hiraoka Y. (2003) Cytoplasmic dynein in fungi: insights from nuclear migration. Journal of Cell Science **116**, 4501-4512.

Yasuhara H. (2005) Caffeine Inhibits Callose Deposition in the Cell Plate and the Depolymerization of Microtubules in the Central Region of the Phragmoplast. Plant Cell Physiology **46,** 1083-1092.

Yasuhara H, Sonobe S, Shibaoka H. (1992) ATP-Sensitive Binding to Microtubules of Polypeptides Extracted from Isolated Phragmoplasts of Tobacco BY-2 Cells. Plant Cell Physiology **33,** 601-608.

Yoneda A, Akatsuka M, Hoshino H, Kumagai F, Hasezawa S. (2005) Decision of Spindle Poles and Division Plane by Double Preprophase Bands in a BY-2 Cell Line Expressing GFP-Tubulin. Plant Cell Physiology **46,** 531-538.

Young JC, Moarefi I, Hartl FU. (2001) Hsp90: a specialized but essential protein-folding tool. Journal of Cell Biology **154**, 267-273.

Yuan Q, Quackenbush J, Sultana R, Pertea M, Salzberg SL, Buell CR. (2001) Rice Bioinformatics. Analysis of Rice Sequence Data and Leveraging the Data to Other Plant Species. Plant Physiology **125**, 1166-1174.

Zekert N, Fischer R. (2009) The *Aspergillus nidulans* Kinesin-3 UncA Motor Moves Vesicles along a Subpopulation of Microtubules. Molecular Biology of the Cell **20,** 673-684.

Zou J, Liu A, Chen X, Zhou X, Gao G, Wang W, Zang X. (2009) Expression analysis of nine rice heat shock protein genes under abiotic stresses and ABA treatment. Journal of Plant Physiology **166**, 851-861.

Internet sources:

http://blast.ncbi.nlm.nih.gov/Blast.cgi

http://expasy.org/sprot

http://ghr.nlm.nih.gov

http://rice.plantbiology.msu.edu

http://www.expasy.org

http://www.invitrogen.com

http://www.jcvi.org

http://www.uniprot.or

Parts of this work can be found in the following publications:

Jovanovic, A.M., Durst, S., Nick, P. (2010) Plant cell division is specifically affected by nitrotyrosine. Journal of Experimental Botany, **61**, 901-909.

Krtková, J., Zimmermann, A.M., Schwarzerová, K., Nick, P. (2010) Hsp90 Modulates the Plasticity of Plant Microtubules, in revision.